Elucidation of the Specificity of *Sinorhizobium meliloti* Chemoreceptors for Host Derived Attractants

Benjamin Allen Webb

Dissertation submitted to the faculty of the Virginia Polytechnic Institute and State University in partial fulfillment of the requirements for the degree of

Doctor of Philosophy

in

Biological Sciences

Birgit E. Scharf, Chair
Richard F. Helm
Florian D. Schubot
Dorothea Tholl
Mark A. Williams

August 12th, 2016
Blacksburg, VA

Keywords: alfalfa, chemotaxis, ligand, methyl accepting chemotaxis protein, symbiosis

Elucidation of the Specificity of *S. meliloti* Chemoreceptors for Host Derived Attractants

Benjamin A. Webb

ABSTRACT

The bacterium *Sinorhizobium* (*Ensifer*) *meliloti* is a member of the *Rhizobiaceae* family and can enter a mutualistic, diazotrophic relationship with most plants of the genera *Medicago, Melilotus*, and *Trigonella*. *Medicago sativa* (alfalfa) is an agriculturally important legume that hosts *S. meliloti* and allows the bacterium to invade the plant root and begin fixing nitrogen. Prior to invasion, *S. meliloti* exists as a free living bacterium and must navigate through the soil to find alfalfa, using chemical signals secreted by the root. Alfalfa is the 4th most cultivated crop in the United States, therefore, identification of plant host signals that lure *S. meliloti*, and identification of the bacterium's chemoreceptors that perceive the signals can aid in propagating the symbiosis more efficiently, thus leading to greater crop yields. Investigations here focus on discovering alfalfa derived attractant signals and matching them to their respective chemoreceptors in *S. meliloti*. We have determined the chemotactic potency of alfalfa seed exudate and characterized and quantified two classes of attractant compounds exuded by germinating alfalfa seeds, namely, amino acids and quaternary ammonium compounds (QACs). At all points possible, we have compared alfalfa with the closely related non-host, spotted medic (*Medicago arabica*). The chemotactic potency of alfalfa seed exudate is the same as spotted medic seed exudate, however, the attractant compositions are chemically different. The amount of each proteinogenic amino acid (AA) exuded by spotted medic is slightly greater than the amounts exuded by alfalfa. In addition,

the five QACs studied are exuded in various amounts between the two *Medicago* species. In comparison, the total amount of proteinogenic AAs exuded be alfalfa and spotted medic are 2.01 μg/seed and 1.94 μg/seed respectively, and the total amount of QACs exuded are 249 ng/seed and 221 ng/seed respectively. By performing a chemotaxis assay with synthetic AA mixtures mimicking the amounts exuded from the medics, it was found that the AA mixtures contribute to 23% and 37% of the responses to alfalfa and spotted medic exudates, respectively. The chemoreceptor McpU was found to be the most important chemoreceptor of the eight for chemotaxis to the whole exudates and the AA mixtures. Furthermore, McpU is shown to mediate chemotaxis to 19 of 20 AAs excluding aspartate. McpU directly interacts with 18 AAs and indirectly mediates chemotaxis to glutamate. Through single amino acid residue substitutions, it is determined that McpU directly binds to amino acids in the annotated region called the Cache_1 domain, likely utilizing residues D155 and D182 to interact with the amino group of AA ligands. In all, McpU is a direct sensor for AAs except for the acidic AAs aspartate and glutamate. Work is presented to show that the QACs betonicine, choline, glycine betaine, stachydrine, and trigonelline are potent attractants for *S. meliloti*, McpX is the most important chemoreceptor for chemotaxis to these QACs, and we demonstrate the binding strength of McpX to the QACs with dissociation constants ranging from low millimolar to low nanomolar, thus making McpX the first observed bacterial MCP that mediates chemotaxis to QACs. Overall, we match medic derived AAs with McpU and QACs with McpX. These results can aid in optimizing chemotaxis to the host derived attractants in order to propagate the symbiosis more efficiently resulting in greater crop yields.

Chapter 2 characterizes the function of the *S. meliloti* Methyl accepting Chemotaxis Protein U (McpU) as receptor for the attractant, proline. A reduction in chemotaxis to proline is observed

in an McpU deletion strain, but the defect is restored in an *mcpU* complemented strain. Single amino acid substitution mutant strains were created, each harboring a mutant *mcpU* gene. The behavioral experiments with the mutants display a reduction in chemotaxis to proline when aspartate 155 and aspartate 182 are changed to glutamates. The periplasmic region of wild type McpU was purified and demonstrated to directly bind proline with a dissociation constant (K_d) of 104 μM. The variant McpU proteins show a reduction in binding affinity confirming McpU as a direct proline sensor.

Chapter 3, describes the development of a high-throughput technique that is able to observe chemotaxis responses in ten separate chemotaxis chambers all at once. This procedure also allows for real time observations at intervals of two minutes for however long the experiment is scheduled. Using this new method it was found that McpU and the Internal Chemotaxis Protein A (IcpA) are the most involved with chemotaxis to seed exudates followed by McpV, W, X, and Y. The amounts of each proteinogenic amino acid (AA) in host and non-host seed exudates are quantified, which reveals that similar amounts are exuded from each species. It is shown that McpU is the most important receptor for chemotaxis toward synthetic mixtures that mimic the amounts seen in the exudates.

Chapter 4 further investigates the role of McpU in sensing amino acids using the high-throughput technique developed in Chapter 3. It is shown that McpU is important for chemotaxis to all individual proteinogenic amino acids except the acidic AA, aspartate. *In vitro* binding experiments confirm that McpU directly interacts with all AAs except the acidic AAs aspartate and glutamate. Binding parameters are determined for aspartate, glutamate, phenylalanine and proline.

In Chapter 5, five quaternary ammonium compounds (QACs) are quantified from the host and non-host seed exudates, which reveals distinctive QAC profiles. *S. meliloti* is found to display strong chemotaxis to all QACs, which is further shown to be mediated mostly by McpX. McpX is then established as a direct binder to all QACs as well as proline, with dissociation constants ranging from nanomolar to millimolar.

These studies have increased our knowledge of how chemoreceptors sense attractants, and they have contributed to the bank of known attractant molecules for bacteria. Our new understandings of chemotaxis and how it relates to the *Sinorhizobium*-alfalfa model can allow for manipulations of the system to enhance chemotaxis to the host, thus propagating the symbiosis more efficiently, ultimately leading to greater crop yields.

Elucidation of the Specificity of *S. meliloti* Chemoreceptors for Host Derived Attractants

Benjamin A. Webb

GENERAL AUDIENCE ABSTRACT

The bacterial species known as *Sinorhizobium meliloti* exists in the soil as a free living bacterium. The microbe can also form a symbiotic relationship with alfalfa, where it invades the plant root and fixes atmospheric nitrogen into a form that is utilizable by the plant. This relationship results in an increase in plant biomass and productivity. As a free-living organism, *S. meliloti* must navigate through the soil to find the root, and does so using chemical attractants secreted by the alfalfa seeds and roots. Here we identify several attractant molecules that are exuded by the germinating seeds of alfalfa. We then match the attractant molecules to the particular *S. meliloti* chemoreceptors that sense them. Alfalfa-derived amino acids are sensed by the chemoreceptor named McpU, and alfalfa derived betaines are sensed by McpX. The identification of these attractants and the chemoreceptors that perceive them can aid in propagating the symbiosis more efficiently, thus leading to greater crop yields.

ACKNOWLEDGEMENTS

This could not have been done without the people I've interacted with and gotten advice from along the way. Though you may not be mentioned here, know that I thank you for all that you have done for me. I hope that I have been able to help you as well.

I would like to thank Birgit Scharf for being the best advisor she could possibly be. When I resisted, you pushed me to not be afraid. When I was down, you motivated me to get up. When I had a spark of an idea, you blew on it and made it a flame. When I needed you, you were always there. I could not have done this without you. Your bottomless pit of understanding and care is wholly appreciated. Thank you for being so open, honest, wise, and for helping me to grow and succeed in many aspects of life. You will continue to inspire me to do the best that I can. Thank you, Dr. Scharf ☺

I would like to thank my committee members (in alphabetical order) Richard Helm, Florian Schubot, Dorothea Tholl, and Mark Williams. I have had nothing but productive and enlightening experiences with you all. We made one heck of a committee. Thank you for your support and guidance along this journey.

Hardik Zatakia… my friend, with a polar opposite personality, yet we get along so well… whether it was working together in the lab, planning surprises, or doing things that we knew we shouldn't be doing, I have always enjoyed sharing time with you. I hope that our paths cross again.

Katie Broadway, your hard work ethic amazes me to this day. When I think I've seen you bend over backwards as far as you can go, you just keep going. You are a source of inspiration for me. Thank you for being a great confidant. I know I can tell you anything. May we continue to help each other out.

Karl Compton, I've yet to see someone grasp an idea as quick as you do and then *run* with it. It has been joyful watching you grow from an undergraduate researcher to a full-fledged graduate student. I see a good deal of myself in you. Thank you for being a reflection of myself. Teaching you, in effect has taught me about me. You are a good person with whole lot of potential and I am extremely happy to have worked with you.

Rafael Castñeda-Saldaña, your constant enthusiasm and positive attitude is a beacon of happiness that I gravitate towards. Thank you for being you and brightening my day, every day. You are always willing to put others before yourself no matter what. Thank you for everything you have done for me. You have taught me that giving is worth more than receiving. You are truly appreciated.

Timofey Arapov, without your help I would not have as many great papers as we do. Thank you for having the patience to work with me and for taking the time to teach me. Also, thank you for helping me to see my flaws, now help me fix them and I will help you fix yours.

Angelica Thapa, even before the day we met, I was already super excited to meet you and to get to know you (The Scharf lab members bore-witness to this). I will always cherish the times

we spent together in the scope room. I don't think I've ever laughed as hard as I have with you. To this day, you support me in all that I do. Thank you.

Doris Taylor, I'm glad that I got to work with such a talented person and I get excited just thinking of all the amazing things that you will do in life as well as all the joy and kindness that you will bring to those in your life. Thank you for making every day exciting and fruitful.

To the many Scharf lab members of now and then, each one of you has had a great impression upon me. Whatever the specific effect you made, know that I appreciate you and the time that we interacted. The Scharf lab is a unique place that can't quite be fully explained. A simple acknowledgement would not do it justice. But to note, this place builds comradery, friendships, understanding, and progress, and it couldn't happen without all of you. Thank you.

To the inhabitants of LS1, thank you for your help and resources, surely much of my experiments depended upon some rare chemical, or an ancient instrument, or a good piece of advice that I eventually found in your lab. Thank you, Jody Jervis for encouraging me and boosting my confidence. Thank you Annette Fluri for taking chat breaks with me. Thank you Manisha for our late night talks. To the members of TPS, thank you for being a source of knowledge, resources, and friendship. To Horace G. Fralin, thanks for the Douwe Egberts, indeed most of this work was fueled by your generosity.

A huge thanks goes out to Sean Mury. You introduced me to the world of microbes and created an excellent lab environment that allowed my interest in microbiology grow exponentially.

You saw what my naïve mind needed and you delivered as I soaked up every little morsel of knowledge you laid down. You continue to lead me to new things that peak my curiosity and you motivate me to delve into the nitty gritty and find things I never knew existed. Thank you for helping me to become a more engaged and knowledgeable human being.

Mom, thank you for letting me steer my life, though I appreciate the minor corrections here and there. Also, thank you SO much for the surprise food deliveries to the lab. Those made my day.

I want to thank one of my best friends, Cara Cheshire for always being there for me and for showing me new perspectives of life. Thank you for motivating me in the mornings with coffee and breakfast. You have helped me get through some tough times. I don't know if I would still be around if we had not found each other. Speaking of finding one another, I owe Earl Sheehan a lot for introducing us. Thank you Earl for taking the time and effort to cut through my malarkey and tell me how it really is. You have been a constant source of truth and wisdom for me, which has allowed me to break through many mental barriers and explore this exciting world and its exiting people. Had I not met Birgit Scharf, I would not have met Earl, and I would not have met Cara, and life may have taken a different and less exciting turn.

This chain-link pattern of cause and effect has led me to realize that I can't stop the gratitude here, and while I would love so much to acknowledge all, there is not enough space in this document, but know that I do thank all that is in between, so for now you'll have to pardon my brevity as I skip to way way back… I'd like to thank the beginning of all time and things for setting into motion what would become of this amazing and harmonious universe.

Contents

List of Figures

List of Tables

Chapter 1 - Introduction

The bacterium *Sinorhizobium* (*Ensifer*) *meliloti* is a member of the *Rhizobiaceae* family, which is composed of bacteria known for their ability to enter a particular type of symbiosis with plants of the *Fabaceae* family. During this symbiosis the bacteria fix nitrogen for the plant causing a drastic increase in plant biomass and in return the plant supplies the rhizobia with nutrients and a safe haven from fierce competition in the rhizosphere. Prior to symbiosis, *S. meliloti*, exists as a free living bacterium in the bulk soil, rhizosphere, and spermosphere (plant root and seed associated soils). The microbe is proficient in chemotaxis, and actively seeks out the symbiotic relationship with particular genera of legumes, including, *Medicago*, *Melilotus*, and *Trigonella*.

Medicago sativa (alfalfa) is the fourth most cultivated crop in the United States, and biomass accumulation is highly dependent upon symbiosis with particular rhizobial species. This symbiosis is arguably the most important in agriculture since it dissolves the need to use synthetic nitrogen fertilizers, thus saving approximately ten billion dollars annually (1) as well as preventing harmful effects on the environment, such as eutrophication of water bodies and increased acidity, salinity, and erosion of soils.

Alfalfa can form this mutual relationship with two different species of the *Sinorhizobium* genus (2, 3), however, the mostly occurs with *S. meliloti* (4-6). There are many steps along the way that go towards crafting this specific symbiosis, of which, these phases, behaviors, and mechanisms are detailed below.

Symbiosis

Legume root nodules provide rhizobia with nutrients and protection from predation while the rhizobial cells provide the legumes with metabolizable nitrogen. This relationship begins when a rhizobial cell makes contact with a root hair near the tip (Fig. 1.1). The root hair curls over onto itself, in effect, trapping a rhizobial cell. At this junction, a root cell invaginates where the bacterial cell is trapped thus taking up the bacterial cell into the root. This invagination continues inward through several layers of root cells creating an infection thread. During this time, the rhizobial cell growth and division occurs and then the cells are forced into the cytoplasm of a root cell forming a membrane-bound symbiosome called a nodule (1, 7, 8). The rhizobial cells further multiply until the plant recognizes a sufficient number of them. The plant signals the rhizobia to cease growth and differentiate into bacteroids in order to become nitrogen fixing entities. Energy for bacteroid metabolism and nitrogen fixation is supplied by the plant mostly in the form of organic acids (9). To increase the odds of symbiosis with a particular rhizobium strain, seeds are coated prior to planting with a *S. meliloti* species that has a high symbiotic efficiency. When nodulation is successful, many inoculum strains demonstrate greater proficiency in symbiosis than the indigenous populations of rhizobium (10).

Chemotaxis

In order for this symbiosis to occur, Rhizobia must seek out a host legume. Legume seeds and roots exude specific and non-specific attractants for Rhizobia and other soil symbionts. The exudates are primarily composed of a vast array of carbon compounds, and to a lesser extent, ions and water (11). Most of these components are exuded into the rhizosphere and/or spermosphere. Polar compounds tend to diffuse away forming a density gradient while non-polar compounds tend

to localize at the area of exudation. *S. meliloti* senses attractants in this gradient with chemoreceptors named **M**ethyl accepting **C**hemotaxis **P**roteins (MCPs) primarily located in a cluster at each cell pole (12). The chemoreceptors signal cytoplasmic factors that control the rotational speed of flagella and therefore the cell's orientation in space, thus allowing the cell to swim up the gradient toward the roots (12, 13). The general scheme for *S. meliloti* chemotaxis in a gradient is diagrammed in Figure 1.2. Repellents shorten the runs allowing the cell to reorient in a random fashion and begin running in new direction, while attractant molecules induce longer runs. In all, the combination of these runs results in a random yet biased movement towards the source of attract and/or away from repellent.

The factors that play a role in chemotaxis of *S. meliloti* toward a host plant are:

1. Signal Transduction
2. Sensory Adaptation
3. Chemoreception
4. Plant/Microbe Signal Exchange
5. Root and Seed Exudation

Signal Transduction

Chemotaxis signal transduction in E. coli

Signal transduction occurs when an extracellular signal is transformed into an intracellular signal that elicits a cellular response. The signal transduction process of bacterial chemotaxis has been best studied in *E. coli.* An extracellular signal sensed by an MCP is transferred through a

two-component regulatory system consisting of the auto-histidine kinase CheA and the response regulator CheY, which ultimately interacts with the motors of the left-handed peritrichous flagella (Fig. 1.3). The protein interaction domain of the MCP strongly associates with CheA with help of the adaptor protein CheW. It is suggested that an attractant signal causes the protein interaction domain to flare outward, in essence switching off CheA autokinase kinase activity. The deactivation of CheA results in no deactivating signal to the flagellar motors, therefore, the flagella continue to rotate in a **c**ounter **c**lock**w**ise (CCW) fashion, thus keeping the flagellar bundle together. As a result, the cell continues swimming straight forward (14, 15). In the absence of an attractant or sensing of a repellent, the protein interaction domain of the MCP would swing back into its original place, and CheA autophosphorylates at a conserved histidine residue. This phosphate is passed to a conserved aspartate residue on the response regulator, CheY. CheY-P diffuses through the cytoplasm, interacts with a flagellar motor and signals it to rotate in the opposite direction (CW), which results in a tumble. Signal termination is mediated by the phosphatase, CheZ, which removes the phosphate from CheY. This signal transduction pathway in *E. coli* has been the major paradigm for how bacteria perform chemotaxis on the molecular level.

Chemotaxis signal transduction in S. meliloti

There are several studies on chemotaxis signal transduction in *S. meliloti* and since there is structural homology with the well-studied *E. coli* paradigm for chemotaxis, many inferences about *S. meliloti* chemotaxis can be made. *S. meliloti* uses a signal transduction pathway to control the rotational speed of its peritrichous right-handed flagella. The flagella of *S. meliloti* only rotate Clockwise (CW), and when all peritrichous flagella rotate in sync the cell swims, but when the

rotation of one or more flagella slows down, the bundle comes apart and the cell tumbles. When an extracellular signal binds to the periplasmic sensing domain of an MCP this causes a change in the protein's cytoplasmic conformation; this in turn creates an intracellular signal. Much of this signal transduction pathway used for chemotaxis has been characterized in *S. meliloti* and is shown in Figure 1.4. The major differences from the *E. coli* paradigm are flagellar rotation and the method of signal termination. The phosphate of CheA-P is passed to a conserved aspartate residue on the response regulator, CheY2. CheY2-P diffuses through the cytoplasm to regulate the flagellar motor by slowing down the clockwise rotation of the flagellum. The asynchronous change of rotational speed of one or more flagella causes the flagella bundle to fall apart (38). Signal termination is accomplished through retrophosphorylation of CheA by CheY2-P. The phosphate is then transferred to a second response regulator known as CheY1, which acts as a phosphate sink (16). CheS aids in dephosphorylation of CheY1-P, thereby draining the phosphate sink (17). This signal transduction pathway differs from the *E. coli* paragdigm in several ways and it is likely due to large differences in their environments.

Sensory Adaptation

An essential part of chemotaxis is the ability to compare past stimuli with current stimuli. Methylation of chemoreceptors provides the cell with a primitive "memory" that allows it to compare the current concentration of ligand to the recent past, thus allowing movement in a beneficial direction (18). Sensory adaptation is carried out by the methyl transferase, CheR and the methyl esterase, CheB.

Attractant stimuli increase the rate at which CheR methylates the conserved glutamate residues on the kinase signaling domain of an MCP, which "dampens" the attractant signal and

increases the chemoreceptor's ability to enhance CheA autophosphorylation activity. More specifically, the methylation reduces the net negative charge on the four-helix bundles of the MCP CheA signaling domain and this induces a more condensed conformation, thus hiding the specific residues that deactivate CheA autophosphorylation activity (19, 20). Further methylation induces a reversal of the piston-like movement of the transmembrane helices that had originally thrust downward, in turn releasing the ligand (21). Figure 1.5 demonstrates how *E. coli* adapts to chemotactic stimuli. Briefly, when an attractant is added to motile *E. coli* cells, CheA activity drops immediately and from that point, CheA activity slowly recovers due to methylation of the chemoreceptors. CheB, the methyl esterase, acts in contrary to CheR by removing the methyl groups from the glutamate residues. CheB is activated through phosphorylation by increasing CheA-P levels. Demethylation results in inhibition of CheA activity by increasing the net negative charge on the kinase control region to favor a less condensed signaling domain. Counteraction of CheR/CheB activity returns CheA activity to its pre-stimulus value, thus allowing the cell to resample the environment and compare the present concentration of stimuli with the past concentration (18, 20).

Chemoreception

Chemoreception allows motile bacteria to be aware of the immediate chemical environment and to move through the environment accordingly using chemotaxis. Many chemicals typical of legume root and seed exudates have shown to govern the movement of *S. meliloti* such as amino acids, sugars, C4 carboxylic acids, and flavonoids (22-25). Many of these chemicals enter the periplasm and interact with Methyl accepting Chemotaxis Proteins (MCPs).

MCPs are responsible for transducing a signal from an attractant and/or repellent molecule into an internal signal to elicit a flagellar motor mediated swimming response.

The mechanism of chemoreception and signal transduction by MCPs has been well documented for the aspartate receptor (Tar) in *Escherichia coli* (19) and is demonstrated in Figure 1.6. Prior to chemoreception, the single MCP proteins form homodimers, which then form trimers of dimers that are anchored in the cytoplasmic membrane forming array of closely associated trimer-dimers (26). A ligand may interact with one or more of the Periplasmic Regions (PR) in a trimer dimer. In the case of Tar, the aspartate ligand is thought to bind in-between the two four-helix bundles causing a conformational change that forces one or more transmembrane helices downward in the direction of the cytoplasm in a piston-like movement (27). Indeed, this downward movement is likely the mode of PR signaling for most MCPs. The four-helix bundle conformation of Tar allows it to directly bind and sense a relatively small number of molecules including alanine, asparagine, aspartate, cysteine, glutamate, glycine, methionine, and serine (attractants), cobalt and nickel (repellents) and indirectly sense maltose through the aid of a periplasmic binding protein called "maltose binding protein."(28-31). *E. coli* also harbors a gene encoding for the serine receptor (Tsr). The PRs of Tsr and Tar share a large sequence identity and Tsr also forms a 4-helix bundle; however, there are key differences in the amino acid residues of the binding pocket of Tsr (32) that change its ligand binding profile so that it only senses alanine, asparagine, cysteine, glycine, and serine, albeit with different binding affinities (28). The overlap in ligand specificity between Tar and Tsr is due to their structural homology.

Another well studied example of chemoreception in bacterial chemotaxis comes from studies exploring the function of chemoreceptors with tandem Per-Arnt-Sim (PAS) domains that comprise most of the PR. The PAS fold was named after the first proteins in which it was

discovered, i.e. the **P**eriod circadian protein, **A**ryl hydrocarbon receptor nuclear translocator protein, and **S**ingle-minded protein (33-35).

Tandem PAS domains are found in many bacterial and archaeal chemoreceptors and like Tar and Tsr, they are predicted and/or shown to sense amino acids (36). The PR of the MCP known as Tlp3 in *Campylobacter jejuni* has tandem PAS domains and directly binds twelve different ligands, four of which are amino acids (arg, asp, ile, and lys) (37). The PR of the *Bacillus subtilis* chemoreceptor McpC is predicted to have tandem PAS domains and it directly senses eleven of the twenty proteinogenic amino acids (AA) in the membrane distal PAS domain. The PR was also shown to indirectly sense four AAs in the membrane proximal PAS domain (38). The MCP known as PctA in *Pseudomonas putida* directly senses 19 of the 20 proteinogenic AAs where aspartate was the only AA that did not bind (39). The *Vibrio cholera* chemoreceptor Mlp24 also has a PR composed of tandem PAS domains, which mediates chemotaxis to at least eleven of the proteinogenic AAs and directly binds at least four of them. Interestingly, an *mlp24* deletion strain does not produce cholera toxin in a mouse model, implying that chemotaxis to AAs via Mlp24 is necessary for the pathogenicity of *Vibrio cholera* (40). These chemoreceptors harboring tandem PAS domains are structurally very different from Tar and Tsr, and they have a broader ligand profile and likely bind to molecules beyond the proteinogenic AAs. The mechanism of direct AA binding in the distal PAS domain is thought to involve five highly conserved residues. The protein Tlp3 from *C. jejuni* utilizes residues Lys149, Trp151, Tyr167, Asp169 and Asp196, which only bind to the backbone of an AA ligand. Structural flexibility of this domain allows it to "open" in order to allow for entry of AAs with variable lengths and moieties (36). This expansion provides the ability of the aforementioned MCPs to directly bind chemically different AAs, e.g. arginine (the side chain is positively charged and relatively long) and alanine (the side chain is hydrophobic

and relatively short). The variation in ligand profiles amongst these MCPs can be explained by the side chains of the AA residues that protrude into the binding pocket from the opposite side of the binding pocket. For example, in the protein Tlp3, the residues Val126, Leu128, Leu144 and Val171 are short and hydrophobic and allow for binding of large hydrophobic AA ligands, whereas in McpC, these residues are substituted with larger, polar side chains (Tyr121, Gln123, Tyr133 and Ser161) and allow for binding of AAs with polar and relatively small side chains. A mechanism of binding the ligand isoleucine in the distal PAS domain of Tlp3 has been animated with the help of crystallographic structures of the bound protein and the apo-protein. The conformational changes observed in the animation has been used as a model for how chemoreceptors with a tandem PAS domain structure transmit an attractant signal (32). Briefly, the binding of an AA in the membrane distal PAS domain causes a conformational change inducing the proximal PAS domain to undergo a conformational change as well, which finally causes the downward piston-like movement of the transmembrane helix (Fig. 1.7) (36).

It is currently accepted that in most transmembrane MCPs, the downward piston-like movement is sensed by the cytoplasmic HAMP domain. The HAMP domain is a common motif seen in **h**istidine kinases, **a**denylyl cyclases, **m**ethyl-accepting chemotaxis proteins, and **p**hosphatases (41). The domain has a conserved helix-turn-helix fold. Its role is to perform the actual signal conversion. The downward piston-like movement forces the HAMP domain to expand (14). This expansion changes the conformation of the kinase control region of the MCP, which puts stress on the glycine hinge at the flexible bundle domain. The stress is thought to cause the protein interaction domain to flare outward and deactivate CheA autokinase activity (15, 42, 43).

The genome of *S. meliloti* has eight genes encoding MCPs and one gene that codes for a transducer-like protein known as **I**nternal **C**hemotaxis **P**rotein **A** (IcpA). The nine chemoreceptors are sequentially named McpS – Z plus IcpA. Together, *S. meliloti* uses eight of the nine chemoreceptors to sense attractants and/or repellents molecules in the rhizosphere (44) (expression of *mcpS* has never been observed). Attractant and/or repellent signal sensing for the six transmembrane MCPs is based on chemoreception in the periplasm. A domain organization of the MCPs can be seen in Figure 1.8, which draws light on how they function to transmit signals. The chemoreceptors (except McpY and IcpA) have two transmembrane domains. The region between them is the PR and is looped into the periplasm where it is exposed to the extracellular milieu and can interact with potential attractants/repellents. The PR of each chemoreceptor varies in length and amino acid sequence, although there is some conserved homology for those PRs that contain defined sub-domains, such as the Cache_1 domain of McpU, and McpX. The mechanism of chemoreception has yet to be defined for McpY and IcpA for the following key reasons; McpY has no transmembrane domains and is a cytosolic protein; IcpA has no transmembrane domains and lacks a methyl accepting domain, thus is thought to be exempt from adaptation by CheR and CheB (44). Despite not having transmembrane domains, McpY and IcpA still associate with the chemoreceptor cluster at the cell poles (12). It is hypothesized that these two chemoreceptors sense compounds that have been internalized (12) or could be used as energy level sensors by somehow sensing the energy flux in the cell.

Of the compounds tested by Meier et al., 2007, McpU, McpW, McpX, and IcpA are observed on swim plates to be most important for mediating chemotaxis to the organic acids citrate, fumarate, malate, succinate, and the sugars fructose, galactose, maltose, mannitol, and sucrose. McpU, McpW, McpY, and IcpA are the most important receptors for mediating chemotaxis

towards the five amino acids glutamate, glutamine, histidine, lysine, and proline. McpU was shown to be the strongest sensor for histidine, lysine, and proline. McpV appeared to only mediate chemotaxis towards the select amino acids and did not appear to be vital for chemotaxis towards the organic acids and sugars tested above. The chemoreceptors of *S. meliloti* seem to sense more than one ligand and one ligand seems to be detected by more than one receptor (44) creating an overlap in ligand perception by the MCPs.

Most motile bacteria are able to respond to low concentrations of attractant or repellent. This high signal sensitivity is thought to be due to clustering of MCP trimer dimers at the cell pole which would create a packing pattern necessary for the docking of the CheA/CheW sensor histidine kinase at the base of the MCPs. In this model, binding of a ligand could have several effects. 1: The binding of a ligand to one receptor could influence a signaling response from adjacent, unbound receptors. 2: If the ligand is big enough, it could bind to multiple receptors at once. 3: One ligand could bind to multiple receptors in a short period of time (45). For example, the K_d for aspartate binding to the *E. coli* MCP Tar is approximately 1μM, and the half-life of an individual aspartate-bound receptor is about one millisecond. Once an aspartate molecule enters a sensory domain array it will tend to bind numerous times to numerous different receptors (19). This model allows for a highly sensitive signal response.

Attractants from Root and Seed Exudates

As a seed germinates or as a root penetrates the soil, chemicals are released into the soil. The composition of seed/root exudate among plant species is unique, and even different physiological states of a single plant species create varying root exudate profiles. In addition, individual seeds of the same species can produce slightly distinctive exudate profiles (46-51).

Generally, seed and root exudates share many common chemotactically active compounds, such as, sugars, amino acids, and organic acids, (52). Most plant species also exude their own unique profile of secondary metabolites that include phenolic acids, terpenoids, alkaloids, and others. Considering the broad variation and diversity of exudate molecules across plant hosts, characterization of these molecular signals and their impact on bacterial chemotaxis are an important step in the management of the mutualism to benefit alfalfa growth.

Amino acids are attractants for many bacteria and archaea (28, 53, 54) and are known to be exuded by seedlings and roots, which can have selective effects on rhizosphere residents. For example, the high proportion of glycine in cowpea seed exudate has an inhibitory effect on particular Rhizobium species (49). L-proline is commonly exuded by plant roots and is also a strong attractant for *S. meliloti* (44, 55). The amino acids exuded by most plant roots are a mix of L and D enantiomers (43). Uptake and conversion of d-amino acids in Arabidopsis thaliana. Amino Acids 40: 553–563. Prokaryotes and fungi use D-AA to construct portions of their cell walls. They are even found in animal tissues where they aid in cellular signaling, however the role they play in plants is still uncertain (43). Gas Chromatography Mass Spectrometry (GC-MS) studies on the D-amino acid profiles of selected plants have shown differences in the amounts found. Interestingly, D-proline has been found in alfalfa seedlings but not in soybean seedlings (46). The differences in exudate compounds could easily result in attraction to one rhizosphere, while being repelled by another. Evidence supporting this hypothesis, is outlined by Currier and Strobel where they observed the *S. meliloti* 102F66 strain to exhibit positive chemotaxis (attracted) to alfalfa root exudate, but displayed negative chemotaxis (repelled) to the root exudate of the non-host cicer milk vetch (56). The uniqueness of a plant's exudate profile could play a role in discrimination of rhizosphere inhabitants.

Quaternary ammonium compounds (QACs) have also been shown to be exuded by plant seeds and roots (57). These molecules have an ammonium cation that bears no hydrogen atom. This class of compounds includes betaines, which additionally, have a negatively charged moitie, thus making the betaines zwitterionic. Examples of betaines include betonicine (hydroxyproline betaine), glycine betaine, stachydrine (proline betaine), homostachydrine (pipecolic acid betaine), and trigonelline. This class also includes compounds like choline, which is a precursor of glycine betaine, which lacks the carboxylate group and therfore is simply a QAC and not a betaine. QACs can be found in organisms across the domains of life and can serve as osmoprotectants, nutrient sources, and cell-to-cell signals (58-62). The aforementioned roles are observed in *S. meliloti* (63-66) as well. Chemotaxis to QACs has been shown for a few marine microbes and the archaeon *Halobacterium salinarum,* however, these studies did not elucidate an MCP that directly interacts with them (53, 67).

Legume selection for rhizobia is also thought to be mediated by exudation of antibiotics. L-canavanine is an arginine analog exuded by the seeds of the *Glycyrrhiza* genera (licorice legumes), which have been shown to select for one of their rhizobial symbionts, *Mesorhizobium tianshanense*. *M. tianshanense* is resistant to L-canavanine because licorice seed exudate induces expression of an exporter protein belonging to the LysE (lysine exporter) family of translocators known as MsiA (68). Most rhizobia including *S. meliloti* have MsiA homologues, which are essential for canavanine resistance (69, 70). L-canavanine has been shown to elicit positive chemotaxis from *Bradyrhizobium japonicum* even though it does not induce nodule formation with the licorice legumes. *S. meliloti* strain LMG6133 is a symbiont of particular *Glycyrrhiza* sp., yet it does not induce as many nodules as *M. tianshanense* and is therefore considered to be a relatively weak competitor (71). Interestingly, L-canavanine is also exuded by alfalfa seeds (72) and elicits

a chemotactic response (Webb and Scharf, unpublished). Host and non-host specific antimetabolites, such as canavanine are of interest since they have a selective nature for particular rhizobia and may be attractants for *S. meliloti*.

There are molecules that are common between legume seed and root exudates including Nod factor inducing flavonoids, however, for the most part, their chemical profiles are different (73-76). On the species level, the seed exudate chemical profile is generally the same from seed to seed, but the chemical profiles of the roots change drastically. The chemicals exuded from roots are subject to change based on soil type, moisture, temperature, time of day, life cycle, plant health, other symbioses, and even the exudation rates change (50, 52, 77-82). In addition, the exudate profiles vary at different locations on the roots (83). Therefore, knowing the attractants exuded from roots could be beneficial to developing chemotactically enhanced strains, as long as exudation of particular root attractants always coincide with sections of root that are able to form nodules. Furthermore, early nodulation of the young seedling strongly inhibits subsequent nodulation in newer regions of the alfalfa root (84, 85). All together, these factors make it difficult to discover root derived attractants that would be useful in developing strains with enhanced chemotaxis to the host, especially if those attractants were only exuded from section of root that do not form nodules. Since early establishment of a rhizobium population is crucial for nodulation by a seed inoculum strain (51, 86-88) becoming familiar with the attractants from the seed exudate could aid in propagating earlier establishment of *S. meliloti* through chemotaxis. However, nodulation continues through the lifespan of alfalfa at particular sections of new roots.

Signal Exchange

Plant growth is at the mercy of metabolizable nitrogen availability. Approximately 78% of the Earth's atmosphere is nitrogen in the form of N_2 but this species of nitrogen cannot be used by plants. Plants rely on reduced nitrogen that is taken up by their roots. Leguminous plants have the upper hand when it comes to utilizing reduced nitrogen because their roots can form nodules that harbor nitrogen fixing bacteria (specifically Rhizobia), thus allowing the plants to proliferate in soils with a low content of reduced nitrogen. How are legumes able to corral enough nitrogen fixing bacteria? In 1904, Hiltner described the "Rhizosphere effect" in which a multitude of microorganisms are attracted to nutrients exuded by the plant roots and that this occurs in the vicinity of plant roots (89). Miller et al., 2007 showed that chemotaxis towards attractants originating from legume roots promotes nodulation by directing rhizobia to the proper infection site (90). Furthermore, it has been shown that *S. meliloti* displays chemotaxis towards root exudates of leguminous plants (23, 24, 91-94). These exudates are primarily composed of a vast array of carbon compounds including sugars, amino acids, organic acids, and phenolic acids, such as isoflavonoids and flavonoids. The isoflavonoids and flavonoids (Fig 1.9) are considered to be among the main signal components involved in specific host-microbe relationships (11, 95). Isoflavonoids are unique to legumes; specifically, the isoflavonoids daidzein and genistein, which are exuded by the soybean plant *Glycine max*. These two isoflavonoids and have been shown to attract the soybean symbiont, *B. japonicum* and induce expression of the bacterium's nodulation genes. On the other hand, daidzein and genistein *inhibit* nodulation gene expression in *S. meliloti* (96) and have no effect on chemotaxis. Instead, *S. meliloti* has been shown to display a weak positive chemotaxis towards the alfalfa derived flavone luteolin, which also acts to induce transcription of nodulation genes (22). It is these chemical specificities that allow Rhizobia to distinguish between their host and non-host legumes (80).

Legumes must also be able to recognize the difference between their rhizobial symbionts and non-symbionts. The secreted flavonoids are detected by rhizobia through transcriptional activators of nodulation (*nod*) genes, interestingly, some QACs have been shown to activate *nod* genes as well (97). Most of these *nod* genes encode enzymes that synthesize species specific chemical signals (98). These chemical signals are distinctive lipo-chitooligosaccharides known as Nod factors (8, 48). Nod factors are secreted by the bacterium into the rhizosphere to be perceived by receptors on the legume root (99). Nod factors can be thought of as a "password" into the plant root, thus allowing a select species of rhizobia to be taken up by the plant root to form nodules. This communication between legume and rhizobia is diagrammed in Figure 1.10**.**

Exposure of *S. meliloti* to whole root exudate induces transcription of the *nod* genes (100, 101). It is known that alfalfa root exudate contains several *nod* inducing flavonoids, namely luteolin, chrysoeriol, 7,4'-dihydroxyflavone, 7,4'-dihydroxyflavonone, and 4,4'-dihydroxy-2'-methoxychalcone (24), some of which bind to and activate the NodD proteins of *S. meliloti* (22, 102). The genome of *S. meliloti* encodes three *nodD* polypeptides, *nodD1*, *nodD2*, and *nodD3*, which are constitutively expressed and localized in the cytoplasmic membrane (103). These proteins are the transcriptional activators of the other *nod* genes needed for the catalyzation of *S. meliloti* Nod factors.

Objectives of this work

In our current time and place in human civilization, growth and demand has put a stress on the amenities available on Earth. It is becoming more apparent that learning how to conserve and maximize resources will be a major necessity in order to prolong human comfort and increase longevity of our species. The rhizobia-legume mutualism is an invaluable model to learn from, for

it embodies the most efficient process for the production of utilizable nitrogen for plants. This natural process saves approximately $10 billion annually in the United States (1), which otherwise would be invested in the production of synthetic nitrogen fertilizers. Alfalfa (*Medicago sativa*) is the fourth most cultivated crop in the United States and is a major source of animal feed, which in turn feeds a growing population. However, these benefits could be greater. The average potential crop yield of this symbiosis between alfalfa and *S. meliloti* is estimated to be 450 kg ha^{-1} $year^{-1}$ (104), however, in the United States this value hovers around 200 kg ha-1 year-1 (105). Currently, indigenous rhizobia with weaker symbiotic efficiency and or weaker nitrogen fixation abilities mostly outcompete the inoculum strains for nodule residence (a little over 50% of nodules), thus reducing crop yields (6, 106-112). As well, most plant families lack the ability to form such a beneficial mutualism. In this dissertation I aim to 1) define host derived attractants, 2) determine the *S. meliloti* MCPs that sense the attractants, and how. Our new understandings of how the *Sinorhizobium meliloti-Medicago sativa* symbiosis is propagated through chemotaxis could help to outcompete indigenous strains and increase crop yields in a resource conserving manner. Also, our acquired knowledge can aid in non-legume/rhizobia studies that seek to establish a similar mutualism that would open the doors for non-leguminous plant families to take advantage of a natural nitrogen source. Chemotaxis is an important aspect of the relationship between the *S. meliloti* and alfalfa, which helps establish the mutualism and is the focus of this work.

Chapter 2 characterizes the effect of an *S. meliloti* strain lacking *mcpU* on its ability to perform chemotaxis to host seed exudate compared to the wild type. The alfalfa derived attractant, proline is quantified in the seed exudate and the molecular mechanism for how McpU is able to sense proline is evaluated. In Chapter 3, a high throughput chemotaxis method is developed in order to investigate the roles of individual chemoreceptors for mediating chemotaxis toward host

and non-host seed exudates. By assaying single chemoreceptor deletion strains, hierarchies for importance in exudate chemotaxis are uncovered for the MCPs. Furthermore, all proteinogenic amino acids of the alfalfa (host) and spotted medic (non-host) exudates are quantified and the chemotactic contribution of the AAs in exudate is assessed. Additionally, regarding AA chemotaxis, another hierarchy of importance is uncovered for the MCPs regarding. Chapter 4 delves into the relationship between McpU and the individual AAs exuded from seed exudates. The importance of McpU for chemotaxis to each discrete AA is shown. Using previous knowledge from Chapter 2, an investigation of how McpU senses all these AAs is conducted and a correlation is made between AA moieties and direct sensing abilities by McpU. In Chapter 5, a class of molecules called quaternary ammonium compounds (QACs) is quantified from the host and non-host exudates. It is shown how these QACs are attractants for *S. meliloti* and further parses apart the MCPs involved in QAC chemotaxis. McpX is shown to be the most important receptor for QAC chemotaxis and binding studies confirm McpX as a novel bacterial MCP for QAC sensing.

All together these studies improve our understanding of chemotaxis by *S. meliloti* and how it finds its host, alfalfa. Of the attractants identified, the MCPs responsible for sensing them are determined. These results further our understanding of how the symbiosis between rhizobia and legumes is propagated and using this information can aid in optimization of chemotaxis toward the host, ultimately leading to increased nodulation by the intende d *S. meliloti* inoculum strain and thus greater crop yields.

REFERENCES

1. **van Rhijn P, Vanderleyden J.** 1995. The Rhizobium-plant symbiosis. Microbiol Rev **59:**124-142.
2. **Rome S, Fernandez MP, Brunel B, Normand P, CleyetMarel JC.** 1996. *Sinorhizobium medicae sp nov*, isolated from annual *Medicago spp*. Int J Syst Bacteriol **46:**972-980.
3. **Jordan DC.** 1984. Family III. *Rhizobiaceae* Conn 1938, 321AL. *In* Bergey's manual of systematic bacteriology. EDs. N R Krieg and J G Holt.**:**234-242.
4. **Garau G, Reeve WG, Brau L, Deiana P, Yates RJ, James D, Tiwari R, O'Hara GW, Howieson JG.** 2005. The symbiotic requirements of different *Medicago spp*. suggest the evolution of *Sinorhizobium meliloti* and *S. Medicae* with hosts differentially adapted to soil pH. Plant and Soil **276:**263-277.
5. **Cheng Y, Watkin ELJ, O'Hara GW, Howieson JG.** 2002. *Medicago sativa* and *Medicago murex* differ in the nodulation response to soil acidity. Plant and Soil **238:**31-39.
6. **Torres Tejerizo G, Del Papa MF, Soria-Diaz ME, Draghi W, Lozano M, Giusti Mde L, Manyani H, Megias M, Gil Serrano A, Puhler A, Niehaus K, Lagares A, Pistorio M.** 2011. The nodulation of alfalfa by the acid-tolerant Rhizobium sp. strain LPU83 does not require sulfated forms of lipochitooligosaccharide nodulation signals. J Bacteriol **193:**30-39.
7. **Pueppke SG.** 1996. The genetic and biochemical basis for nodulation of legumes by rhizobia. Crit. Rev. in Biotech. **16:**1-51.
8. **Wang D, Yang SM, Tang F, Zhu HY.** 2012. Symbiosis specificity in the legume - rhizobial mutualism. Cell Microbiol **14:**334-342.
9. **Fournier J, Timmers AC, Sieberer BJ, Jauneau A, Chabaud M, Barker DG.** 2008. Mechanism of infection thread elongation in root hairs of *Medicago truncatula* and dynamic interplay with associated rhizobial colonization. Plant physiology **148:**1985-1995.
10. **Catroux G, Hartmann A, Revellin C.** 2001. Trends in rhizobial inoculant production and use. Plant and Soil **230:**21-30.
11. **Nannipieri P.** 2007. The Rhizosphere. Biochemistry and Organic Substances at the Soil-Plant Interface, p. 23,24, May 11, 2007 ed. CRC Press, Florence, Italy.
12. **Meier VM, Scharf BE.** 2009. Cellular localization of predicted transmembrane and soluble chemoreceptors in *Sinorhizobium meliloti*. J Bacteriol **191:**5724-5733.
13. **Attmannspacher U, Scharf B, Schmitt R.** 2005. Control of speed modulation (chemokinesis) in the unidirectional rotary motor of *Sinorhizobium meliloti*. J Mol Micro **56:**708-718.
14. **Khursigara CM, Wu X, Zhang P, Lefman J, Subramaniam S.** 2008. Role of HAMP domains in chemotaxis signaling by bacterial chemoreceptors. Proc. Natl Acad Sci USA **105:**16555-16560.
15. **Parkinson JS.** 2007. Ancient chemoreceptors retain their flexibility. Proc Natl Acad Sci USA **104:**2559-2560.
16. **Scharf B, Schmitt R.** 2002. Sensory transduction to the flagellar motor of *Sinorhizobium meliloti*. J Mol Microbiol Biotechnol **4:**183-186.
17. **Dogra G, Purschke FG, Wagner V, Haslbeck M, Kriehuber T, Hughes JG, Van Tassell ML, Gilbert C, Niemeyer M, Ray WK, Helm RF, Scharf BE.** 2012. *Sinorhizobium meliloti* CheA complexed with CheS exhibits enhanced binding to CheY1, resulting in accelerated CheY1 dephosphorylation. J Bacteriol **194:**1075-1087.

18. **Vladimirov N, Sourjik V.** 2009. Chemotaxis: how bacteria use memory. Biol Chem **390:**1097-1104.
19. **Baker MD, Wolanin PM, Stock JB.** 2006. Signal transduction in bacterial chemotaxis. Bioessays **28:**9-22.
20. **Borkovich KA, Alex LA, Simon MI.** 1992. Attenuation of sensory receptor signaling by covalent modification. Proc Natl Acad Sci USA **89:**6756-6760.
21. **Hazelbauer GL, Lai WC.** 2010. Bacterial chemoreceptors: providing enhanced features to two-component signaling. Curr Opin Microbiol **13:**124-132.
22. **Peters NK, Frost JW, Long SR.** 1986. A plant flavone, luteolin, induces expression of *Rhizobium meliloti* nodulation genes. Science **233:**977-980.
23. **Caetano-Anolles G, Crist-Estes DK, Bauer WD.** 1988. Chemotaxis of *Rhizobium meliloti* to the plant flavone luteolin requires functional nodulation genes. J Bacteriol **170:**3164-3169.
24. **Dharmatilake AJ, Bauer WD.** 1992. Chemotaxis of *Rhizobium meliloti* towards nodulation gene-inducing compounds from alfalfa roots. Appl Environ Microbiol **58:**1153-1158.
25. **Gulash M, Ames P, Larosiliere RC, Bergman K.** 1984. Rhizobia are attracted to localized sites on legume roots. Appl Environ Microbiol **48:**149-152.
26. **Hazelbauer GL, Falke JJ, Parkinson JS.** 2008. Bacterial chemoreceptors: high-performance signaling in networked arrays. Trends Biochem Sci **33:**9-19.
27. **Falke JJ, Hazelbauer GL.** 2001. Transmembrane signaling in bacterial chemoreceptors. Trends Biochem Sci **26:**257-265.
28. **Yang Y, A MP, Hofler C, Poschet G, Wirtz M, Hell R, Sourjik V.** 2015. Relation between chemotaxis and consumption of amino acids in bacteria. J Mol Microbiol.
29. **Neumann S, Hansen CH, Wingreen NS, Sourjik V.** 2010. Differences in signalling by directly and indirectly binding ligands in bacterial chemotaxis. Embo J **29:**3484-3495.
30. **Englert DL, Adase CA, Jayaraman A, Manson MD.** 2010. Repellent taxis in response to nickel ion requires neither Ni2+ transport nor the periplasmic NikA binding protein (vol 192, pg 2633, 2010). J Bacteriol **192:**4259-4259.
31. **Zhang YH, Gardina PJ, Kuebler AS, Kang HS, Christopher JA, Manson MD.** 1999. Model of maltose-binding protein/chemoreceptor complex supports intrasubunit signaling mechanism. Proc Natl Acad Sci USA **96:**939-944.
32. **Jeffery CJ, Koshland DE.** 1993. 3-Dimensional structural model of the serine receptor ligand-binding domain. Protein Sci **2:**559-566.
33. **Ponting CP, Aravind L.** 1997. PAS: a multifunctional domain family comes to light. Curr Biol **7:**R674-R677.
34. **Hefti MH, Francoijs KJ, de Vries SC, Dixon R, Vervoort J.** 2004. The PAS fold - A redefinition of the PAS domain based upon structural prediction. Eur J Biochem **271:**1198-1208.
35. **Henry JT, Crosson S.** 2011. Ligand-binding PAS domains in a genomic, cellular, and structural context. Ann Rev of Microbiol Vol 65 **65:**261-286.
36. **Liu YC, Machuca MA, Beckham SA, Gunzburg MJ, Roujeinikova A.** 2015. Structural basis for amino-acid recognition and transmembrane signalling by tandem Per-Arnt-Sim (tandem PAS) chemoreceptor sensory domains. Acta Crystallogr D **71:**2127-2136.

37. **Rahman H, King RM, Shewell LK, Semchenko EA, Hartley-Tassell LE, Wilson JC, Day CJ, Korolik V.** 2014. Characterisation of a multi-ligand binding chemoreceptor CcmL (Tlp3) of *Campylobacter jejuni*. Plos Pathog **10**.
38. **Glekas GD, Mulhern BJ, Kroc A, Duelfer KA, Lei V, Rao CV, Ordal GW.** 2012. The *Bacillus subtilis* chemoreceptor McpC senses multiple ligands using two discrete mechanisms. J Biol Chem **287**.
39. **Reyes-Darias JA, Yang YL, Sourjik V, Krell T.** 2015. Correlation between signal input and output in PctA and PctB amino acid chemoreceptor of *Pseudomonas aeruginosa*. J Mol Microbiol **96:**513-525.
40. **Nishiyama S, Suzuki D, Itoh Y, Suzuki K, Tajima H, Hyakutake A, Homma M, Butler-Wu SM, Camilli A, Kawagishi I.** 2012. Mlp24 (McpX) of *Vibrio cholerae* implicated in pathogenicity functions as a chemoreceptor for multiple amino acids. Infect Immun **80:**3170-3178.
41. **Hulko M, Berndt F, Gruber M, Linder JU, Truffault V, Schultz A, Martin J, Schultz JE, Lupas AN, Coles M.** 2006. The HAMP domain structure implies helix rotation in transmembrane signaling. Cell **126:**929-940.
42. **Alexander RP, Zhulin IB.** 2007. Evolutionary genomics reveals conserved structural determinants of signaling and adaptation in microbial chemoreceptors. Proc Natl Acad Sci USA **104:**2885-2890.
43. **Gordes D, Kolukisaoglu U, Thurow K.** 2011. Uptake and conversion of D-amino acids in *Arabidopsis thaliana*. Amino Acids **40:**553-563.
44. **Meier VM, Muschler P, Scharf BE.** 2007. Functional analysis of nine putative chemoreceptor proteins in *Sinorhizobium meliloti*. J Bacteriol **189:**1816-1826.
45. **Wadhams GH, Armitage JP.** 2004. Making sense of it all: bacterial chemotaxis. Nat Rev Mol Cell Biol **5:**1024-1037.
46. **Bruckner H, Westhauser T.** 2003. Chromatographic determination of L- and D-amino acids in plants. Amino Acids **24:**43-55.
47. **Landgraf R, Schaarschmidt S, Hause B.** 2012. Repeated leaf wounding alters the colonization of *Medicago truncatula* roots by beneficial and pathogenic microorganisms. Plant Cell Environ.
48. **Somers E, Vanderleyden J, Srinivasan M.** 2004. Rhizosphere bacterial signalling: A love parade beneath our feet. Crit Rev Microbiol **30:**205-240.
49. **Odunfa VSA.** 1979. Free amino acids in the seed and root exudates in relation to the nitrogen requirements of rhizosphere soil Fusaria. Plant and Soil **52:**491-499.
50. **Marin JA AP, Carrasco A, Arbeloa A.** 2009. Determination of proline concentration, an abiotic stress marker, in root exudates of excised root cultures of fruit tree rootstocks under salt stress, Jerba (Tunisie).
51. **Nelson EB.** 2004. Microbial dynamics and interactions in the spermosphere. Annu Rev Phytopathol **42:**271-309.
52. **Vancura V, Stanek M.** 1975. Root exudates of plants .5. Kinetics of exudates from bean roots as related to presence of reserve compounds in cotyledons. Plant and Soil **43:**547-559.
53. **Kokoeva MV, Storch KF, Klein C, Oesterhelt D.** 2002. A novel mode of sensory transduction in archaea: binding protein-mediated chemotaxis towards osmoprotectants and amino acids. Embo J **21:**2312-2322.
54. **Storch KF, Rudolph J, Oesterhelt D.** 1999. Car: a cytoplasmic sensor responsible for arginine chemotaxis in the archaeon *Halobacterium salinarum*. Embo J **18:**1146-1158.

55. **Greck M, Platzer J, Sourjik V, Schmitt R.** 1995. Analysis of a chemotaxis operon in *Rhizobium meliloti*. J Mol Microbiol **15:**989-1000.
56. **Currier WW, Strobel GA.** 1976. Chemotaxis of *Rhizobium Spp* to plant root exudates. Plant physiology **57:**820-823.
57. **Phillips DA, Wery J, Joseph CM, Jones AD, Teuber LR.** 1995. Release of flavonoids and betaines from seeds of seven *Medicago* species. Crop Sci. **35:**805-808.
58. **Chambers ST, Kunin CM.** 1987. Isolation of glycine betaine and proline betaine from human urine. Assessment of their role as osmoprotective agents for bacteria and the kidney. J. Clin. Invest. **79:**731-737.
59. **Kunin CM, Hua TH, Van Arsdale White L, Villarejo M.** 1992. Growth of *Escherichia coli* in human urine: role of salt tolerance and accumulation of glycine betaine. J. Infect. Dis. **166:**1311-1315.
60. **Lever M, Sizeland PC, Bason LM, Hayman CM, Chambers ST.** 1994. Glycine betaine and proline betaine in human blood and urine. Biochim. Biophys. Acta **1200:**259-264.
61. **Phillips DA, Joseph CM, Maxwell CA.** 1992. Trigonelline and stachydrine released from alfalfa seeds activate NodD2 protein in *Rhizobium meliloti*. Plant. Physiol. **99:**1526-1531.
62. **Phillips DA, Sande ES, Vriezen JAC, de Bruijn FJ, Le Rudulier D, Joseph CM.** 1998. A new genetic locus in *Sinorhizobium meliloti* is involved in stachydrine utilization. Appl Environ Microbiol **64:**3954-3960.
63. **Boncompagni E, Osteras M, Poggi MC, le Rudulier D.** 1999. Occurrence of choline and glycine betaine uptake and metabolism in the family *Rhizobiaceae* and their roles in osmoprotection. Appl Environ Microbiol **65:**2072-2077.
64. **Barra L, Fontenelle C, Ermel G, Trautwetter A, Walker GC, Blanco C.** 2006. Interrelations between glycine betaine catabolism and methionine biosynthesis in *Sinorhizobium meliloti* strain 102F34. J Bacteriol **188:**7195-7204.
65. **Gouffi K, Bernard T, Blanco C.** 2000. Osmoprotection by pipecolic acid in *Sinorhizobium meliloti*: Specific effects of D and L isomers. Appl Environ Microbiol **66:**2358-2364.
66. **Boivin C, Camut S, Malpica CA, Truchet G, Rosenberg C.** 1990. *Rhizobium meliloti* genes encoding catabolism of trigonelline are induced under symbiotic conditions. Plant Cell **2:**1157-1170.
67. **Seymour JR, Simo R, Ahmed T, Stocker R.** 2010. Chemoattraction to dimethylsulfoniopropionate throughout the marine microbial food web. Science **329:**342-345.
68. **Cai T, Cai W, Zhang J, Zheng H, Tsou AM, Xiao L, Zhong Z, Zhu J.** 2009. Host legume-exuded antimetabolites optimize the symbiotic rhizosphere. J Mol Microbiol **73:**507-517.
69. **Weaks TE.** 1977. Differences between strains of rhizobium in sensitivity to canavanine. Plant and Soil **48:**387-395.
70. **Emmert EAB, Milner JL, Lee JC, Pulvermacher KL, Olivares HA, Clardy J, Handelsman J.** 1998. Effect of canavanine from alfalfa seeds on the population biology of *bacillus cereus*. Appl Environ Microbiol **64:**4683-4688.
71. **Li L, Sinkko H, Montonen L, Wei GH, Lindstrom K, Rasanen LA.** 2012. Biogeography of symbiotic and other endophytic bacteria isolated from medicinal *Glycyrrhiza* species in China. Fems Microbiol Ecol **79:**46-68.

72. **Keshavan ND, Chowdhary PK, Haines DC, Gonzalez JE.** 2005. L-canavanine made by *Medicago sativa* interferes with quorum sensing in *Sinorhizobium meliloti*. J Bacteriol **187:**8427-8436.
73. **Vancura V, Hanzlikova A.** 1972. Root Exudates of Plants .4. Differences in Chemical Composition of Seed and Seedlings Exudates. Plant and Soil **36:**271-+.
74. **Hartwig UA, Maxwell CA, Joseph CM, Phillips DA.** 1989. Interactions among Flavonoid nod Gene Inducers Released from Alfalfa Seeds and Roots. Plant Phys **91:**1138-1142.
75. **Akifumi Sugiyama KY.** 2012. Root exudates of legume plants and their involvement in interactions with soil microbes. Sec and Exud in Biol Sys **8:**284.
76. **Hartwig UA, Joseph CM, Phillips DA.** 1991. Flavonoids Released Naturally from Alfalfa Seeds Enhance Growth-Rate of Rhizobium-Meliloti. Plant Phys **95:**797-803.
77. **Bokhari UG, Coleman DC, Rubink A.** 1979. Chemistry of Root Exudates and Rhizosphere Soils of Prairie Plants. Can J Bot **57:**1473-1477.
78. **Prikryl Z, Vancura V.** 1980. Root Exudates of Plants .6. Wheat Root Exudation as Dependent on Growth, Concentration Gradient of Exudates and the Presence of Bacteria. Plant and Soil **57:**69-83.
79. **Zaat SAJ, Wijffelman CA, Mulders IHM, Vanbrussel AAN, Lugtenberg BJJ.** 1988. Root Exudates of Various Host Plants of Rhizobium-Leguminosarum Contain Different Sets of Inducers of Rhizobium Nodulation Genes. Plant Phys **86:**1298-1303.
80. **Bais HP, Weir TL, Perry LG, Gilroy S, Vivanco JM.** 2006. The role of root exudates in rhizosphere interactions with plants and other organisms. Annu Rev Plant Biol **57:**233-266.
81. **Lu SL, Hu HY, Sun YX, Yang J.** 2009. [Study on the growth characteristics and root exudates of three wetlands plants at different culture conditions]. Huan Jing Ke Xue **30:**1901-1905.
82. **Wu FY, Chung AKC, Tam NFY, Wong MH.** 2012. Root Exudates of Wetland Plants Influenced by Nutrient Status and Types of Plant Cultivation. Intern J Phytoremed **14:**543-553.
83. **Yang CH, Crowley DE.** 2000. Rhizosphere microbial community structure in relation to root location and plant iron nutritional status. Appl Environ Microbiol **66:**345-351.
84. **Caetanoanolles G, Bauer WD.** 1988. Feedback-Regulation of Nodule Formation in Alfalfa. Planta **175:**546-557.
85. **Caetanoanolles G, Lagares A, Bauer WD.** 1990. Rhizobium-Meliloti Exopolysaccharide Mutants Elicit Feedback-Regulation of Nodule Formation in Alfalfa. Plant Phys **92:**368-374.
86. **Iizuka M, Arima Y, Yokoyama T, Watanabe K.** 2002. Positive correlation between the number of root nodule primordia and seed sugar secretion in soybean (Glycine max L.) seedlings inoculated with a low density of Bradyrhizobium japonicum. Soil Sci Plant Nutr **48:**219-225.
87. **Weaver RW, Frederick LR.** 1974. Effect of Inoculum Rate on Competitive Nodulation of Glycine-Max-L - Merrill .2. Field Studies. Agron J **66:**233-236.
88. **Herridge DF, Roughley RJ, Brockwell J.** 1987. Low Survival of Rhizobium-Japonicum Inoculant Leads to Reduced Nodulation, Nitrogen-Fixation and Yield of Soybean in the Current Crop but Not in the Subsequent Crop. Aust J Agr Res **38:**75-82.
89. **Hiltner L.** 1904. Uber neue Erfahrungen und Probleme auf dem Gebiete der Bodenbakteriologie. Arbeiten der Deutschen Landwirtschaftgesellschaft**:**59-78.

90. **Miller LD, Yost CK, Hynes MF, Alexandre G.** 2007. The major chemotaxis gene cluster of *Rhizobium leguminosarum* bv. *viciae* is essential for competitive nodulation. J Mol Microbiol **63:**348-362.
91. **Armitage JP.** 2001. Bacterial taxis, eLS. John Wiley & Sons, Ltd.
92. **Munoz Aguilar JM, Ashby AM, Richards AJM, Loake GJ, Watson MD, Shaw CH.** 1988. Chemotaxis of *Rhizobium leguminosarum* biovar *phaseoli* towards flavonoid inducers of the symbiotic nodulation genes. J Gen Microbiol **134:**2741-2746.
93. **Barbour WM, Hattermann DR, Stacey G.** 1991. Chemotaxis of *Bradyrhizobium japonicum* to soybean exudates. Appl Environ Microbiol **57:**2635-2639.
94. **Kape R, Parniske M, Werner D.** 1991. Chemotaxis and nod gene activity of *Bradyrhizobium japonicum* in response to hydroxycinnamic acids and isoflavonoids. Appl Environ Microbiol **57:**316-319.
95. **Perret X, Staehelin C, Broughton WJ.** 2000. Molecular basis of symbiotic promiscuity. Microbiol Mol Biol Rev **64:**180-201.
96. **Hirsch AM, Lum MR, Downie JA.** 2001. What makes the rhizobia-legume symbiosis so special? Plant Phys **127:**1484-1492.
97. **Phillips DA, Joseph CM, Maxwell CA.** 1992. Trigonelline and stachydrine released from alfalfa seeds activate NodD2 protein in *Rhizobium meliloti*. Plant Phys **99:**1526-1531.
98. **Phillips DA, Tsai SM.** 1992. Flavonoids as plant signals to rhizosphere microbes. Mycorrhiza **1:**55-58.
99. **Goedhart J, Bono JJ, Gadella TW, Jr.** 2002. Rapid colorimetric quantification of lipo-chitooligosaccharides from *Mesorhizobium loti* and *Sinorhizobium meliloti*. MPMI **15:**859-865.
100. **Mulligan JT, Long SR.** 1985. Induction of *Rhizobium meliloti nodC* expression by plant exudate requires *nodD*. Proc Natl Acad Sci USA **82:**6609-6613.
101. **Mulligan JT, Long SR.** 1989. A family of activator genes regulates expression of *Rhizobium meliloti* nodulation genes. Genetics **122:**7-18.
102. **Hartwig UA, Maxwell CA, Joseph CM, Phillips DA.** 1990. Chrysoeriol and luteolin released from alfalfa seeds induce *nod* genes in *Rhizobium meliloti*. Plant Phys **92:**116-122.
103. **Schlaman HR, Spaink HP, Okker RJ, Lugtenberg BJ.** 1989. Subcellular localization of the *nodD* gene product in *Rhizobium leguminosarum*. J Bacteriol **171:**4686-4693.
104. **Fishbeck KA, Heichel GH, Vance CP.** 1987. Dry-matter, nitrogen distribution, and dinitrogen fixation in contrasting alfalfa symbioses. Crop Sci **27:**1205-1209.
105. **Zhu YP, Sheaffer CC, Russelle MP, Vance CP.** 1998. Dry matter accumulation and dinitrogen fixation of annual *Medicago* species. Agron J **90:**103-108.
106. **Jordan DC.** 1952. Studies on the legume root nodule bacteria .3. Growth factor requirements for effective, ineffective, and parasitic strains. Can J Bot **30:**693-700.
107. **Zeng ZH, Chen WX, Hu YG, Sui XH, Chen DM.** 2007. Screening of highly effective *Sinorhizobium meliloti* strains for 'Vector' alfalfa and testing of its competitive nodulation ability in the field. Pedosphere **17:**219-228.
108. **Streeter JG.** 1994. Failure of inoculant Rhizobia to overcome the dominance of indigenous strains for nodule formation. Can J Microbiol **40:**513-522.
109. **Dowling DN, Broughton WJ.** 1986. Competition for Nodulation of Legumes. Ann Rev Microbiol **40:**131-157.

110. **Singleton PW, Tavares JW.** 1986. Inoculation Response of Legumes in Relation to the Number and Effectiveness of Indigenous Rhizobium Populations. Appl Environ Microbiol **51:**1013-1018.
111. **Eardly BD, Hannaway DB, Bottomley PJ.** 1985. Characterization of Rhizobia from Ineffective Alfalfa Nodules: Ability to Nodulate Bean Plants [Phaseolus vulgaris (L.) Savi.]. Appl Environ Microbiol **50:**1422-1427.
112. **Del Papa MF, Pistorio M, Draghi WO, Lozano MJ, Giusti MA, Medina C, van Dillewijn P, Martinez-Abarca F, Moron Flores B, Ruiz-Sainz JE, Megias M, Puhler A, Niehaus K, Toro N, Lagares A.** 2007. Identification and characterization of a nodH ortholog from the alfalfa-nodulating Or191-like rhizobia. Molecular plant-microbe interactions : MPMI **20:**138-145.

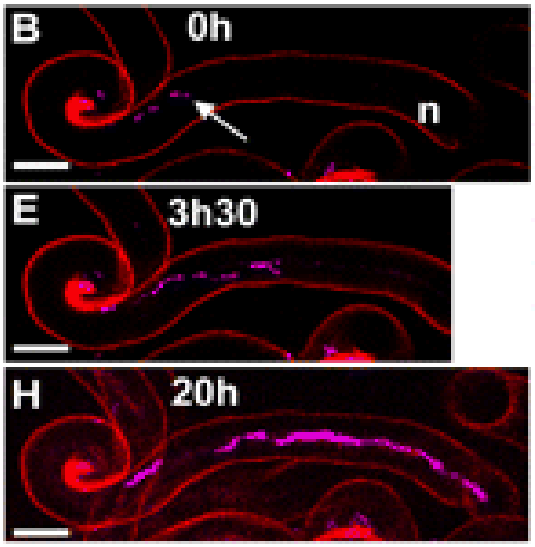

Fig 1.1. Infection thread development in *M. truncatula* root hairs. *M. truncatula* mutant *sunn* expressing the *35S-GFP-HDEL* transgene was inoculated with *S.meliloti-2011-cCFP* and successive confocal images were taken showing the fluorescence of the rhizobia (magenta) **B.,** There are only a very few bacteria in the early stage of the infection thread. **E.,** The infection thread has progressed within the root hair and the rhizobia have multiplied within. **H.,** The infection thread has grown further down the hair toward the base of the cell as the bacteria have multiplied and formed a thick stretching colony Bars = 10 µm. Figure used with permission of Fornier 2008. Plant Physiol. 148:1985-1995 (2008). Copyright 2008 American Society of Plant Biologists.

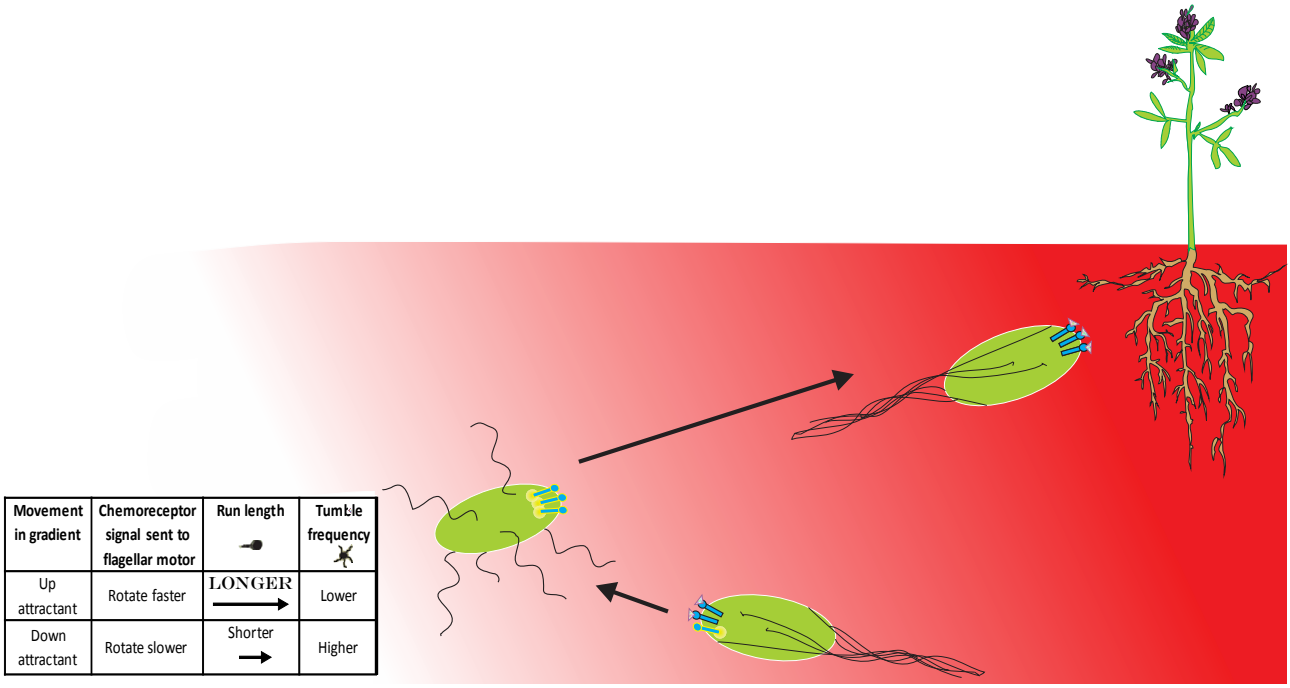

Fig 1.2. Chemotaxis to a host plant. This diagram simply depicts a microbe's journey through the soil to find the rhizosphere of its host plant alfalfa. The gradient from red to white represents a density gradient (red being densest) composed of attractant. The microbe senses the attractant and uses chemotaxis to swim up the gradient towards the host roots. The inset table describes a general behavioral scheme for chemotaxis used by *S. meliloti*. Scales are exaggerated.

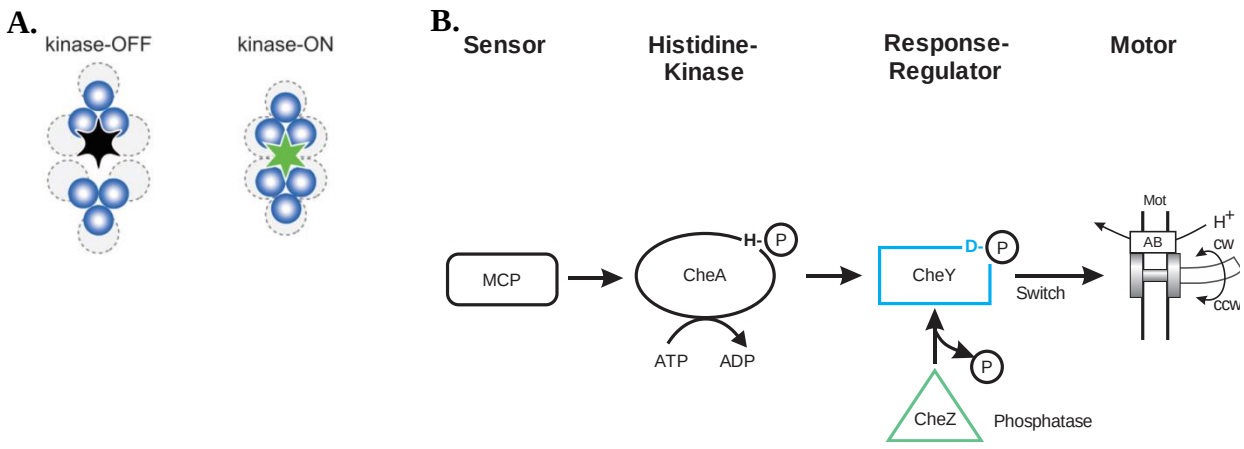

Fig 1.3. The chemotaxis signal transduction pathway of *E. coli.* A. A view of the tip of the protein interaction domain of an MCP. Signal transduction begins with the conversion of an extracellular signal into an intracellular signal mediated by an MCP. When an attractant binds the LBD of an MCP dimer, the tip of the protein interaction domains splay outward, deactivating the CheA autokinase. In the absence of an attractant or binding of a repellent, the protein interaction domains swing inward and activate the CheA autokinase. **B.,** CheA autophosphorylates and passes the signal to the response regulator CheY. CheY-P commands the flagellar motor to switch rotation from CCW to CW. The phosphatase CheZ terminates the signal by removing the phosphate from CheY. Figure **A**. used with permission of Proc Natl Acad Sci USA 2008, 105(43):16555-16560. **B** used with permission of Dr. Birgit Scharf.

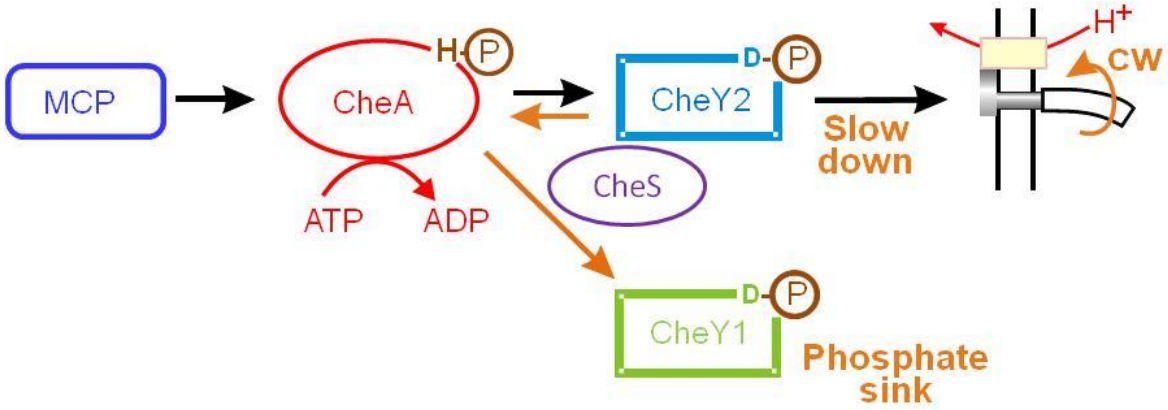

Fig 1.4. The signal transduction pathway of *S. meliloti.* In the absence of an attractant the MCP activates the CheA autokinase which is then autophosphorylated. This phosphate is relayed to CheY2 which binds to the flagellar motor signaling it to slow rotation. CheY1 acts as a phosphate sink and CheS promotes dephosphorylation of CheY1-P. Figure used with permission of Dr. Birgit Scharf.

A.

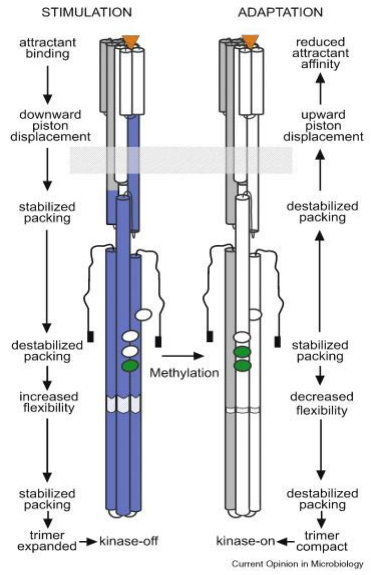

B.

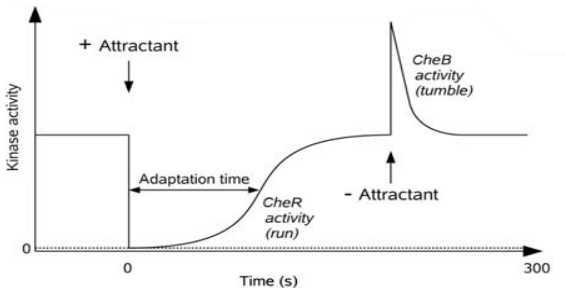

Fig 1.5. Signal adaptation in *E. coli.* A. Chemoreceptor signaling. Cartoons of a stimulated and adapted receptor dimer illustrate the conformational changes that couple stimulation by attractant binding to kinase inhibition (left-hand image and labels) and adaptation by methylation to re-establish pre-stimulation kinase activity (right-hand image and labels). Blue symbolizes the inactivated form. **B.** timecourse of a typical chemotactic response. Addition of attractant at time zero decreases CheA activity. During adaptation time, CheA activity slowly rejuvenates due to increasing CheR activity. Removal of attractant immediately increases CheA activity followed by CheB dependent adaptation through demethylation. **A.** used with permission of Curr Opin Microbiol. 2010 Apr;13(2):124-32. Epub 2010 Feb 1. **B.** Figure traced in Photoshop. Original from Vladimorov & Sourjik, Biol Chem. 2009 Nov;390(11):1097-104.

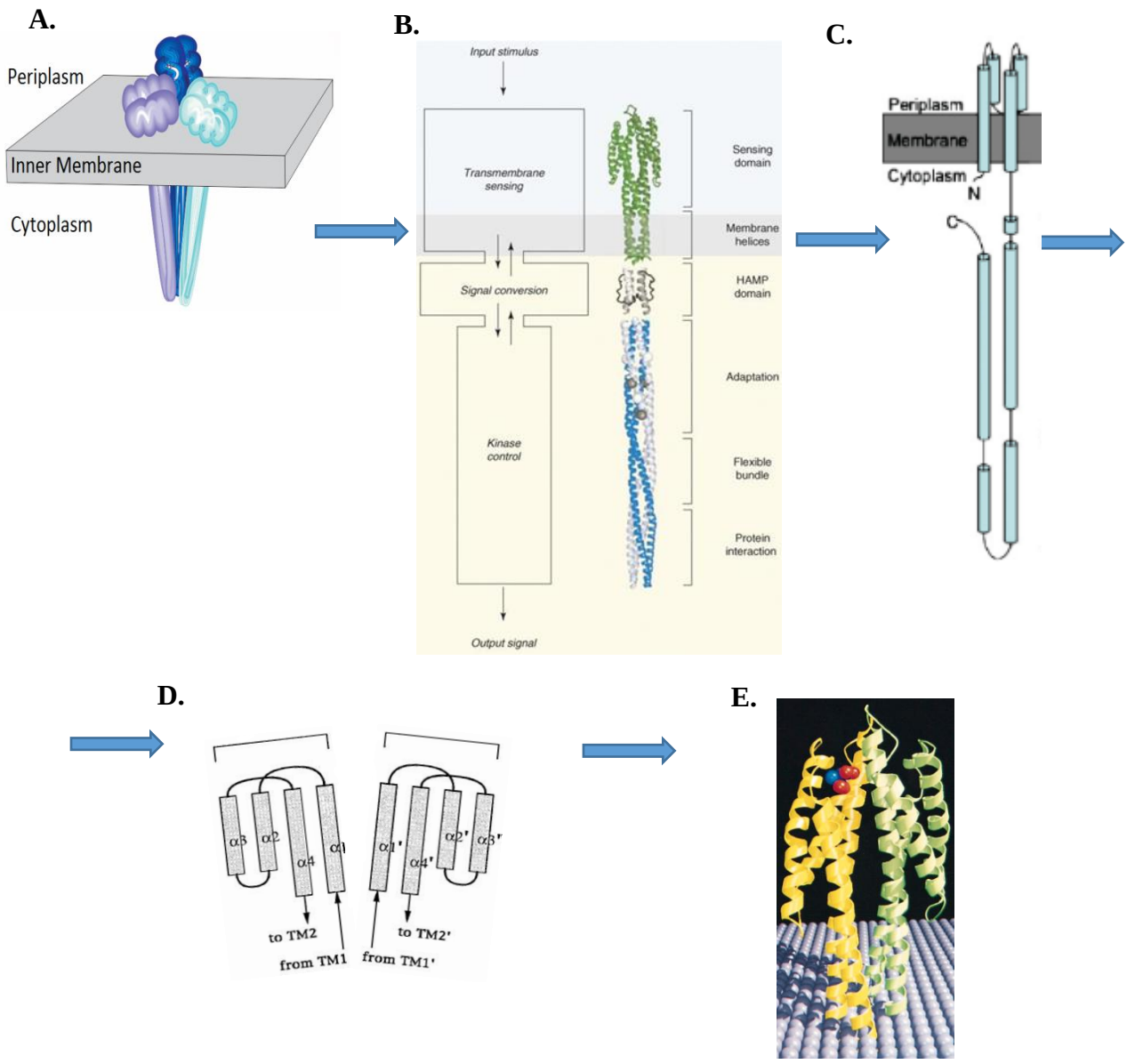

Fig 1.6. Picking apart a mechanism for bacterial chemoreception. Follow the flow chart to witness the dissection of a bacterial MCP. **A.,** Cartoon representation of typical MCP organization in the trimer dimer formation. **B.,** Zoom in to a ribbon model of the *E. coli* MCP dimer, "Tar." Domains are indicated on the left, roles or identities of module segments on the right. **C.,** Crude schematic of the Tar monomer. With this first iteration, it is obvious that the sensing domain forms a 4-helix bundle. The cytoplasmic domain contains the HAMP domain; adaptation domain where CheR and CheB act on key glutamate residues; signaling domain that binds to the CheA/CheW complex. **D.**, the second iteration is a cartoon model of the dimerized LBD from Tar that resides in the periplasm. Notice how the monomers are splayed apart. **E.,** Aspartate bound to the ribbon model of the dimerized Tar-LBD. Notice how the monomers have closed in on each other. Figure B taken from Hazelbauer et al. Trends Biochem Sci. 2008 Jan;33(1):9-19. Epub 2007 Dec 31.

Figure **C** used with permission from Bioessays. 2006 Jan;28(1):9-22. **B** used with permission of Trends Biochem Sci, 2008 January; 33(1): 9–19. doi:10.1016/j.tibs. 2007.09.01. **C** used with permission of Bioessays, 28: 9–22. doi: 10.1002/bies.20343. **D** and **E** used with permission of J. Mol Biol. 1996 Sep 20;262(2):186-201.

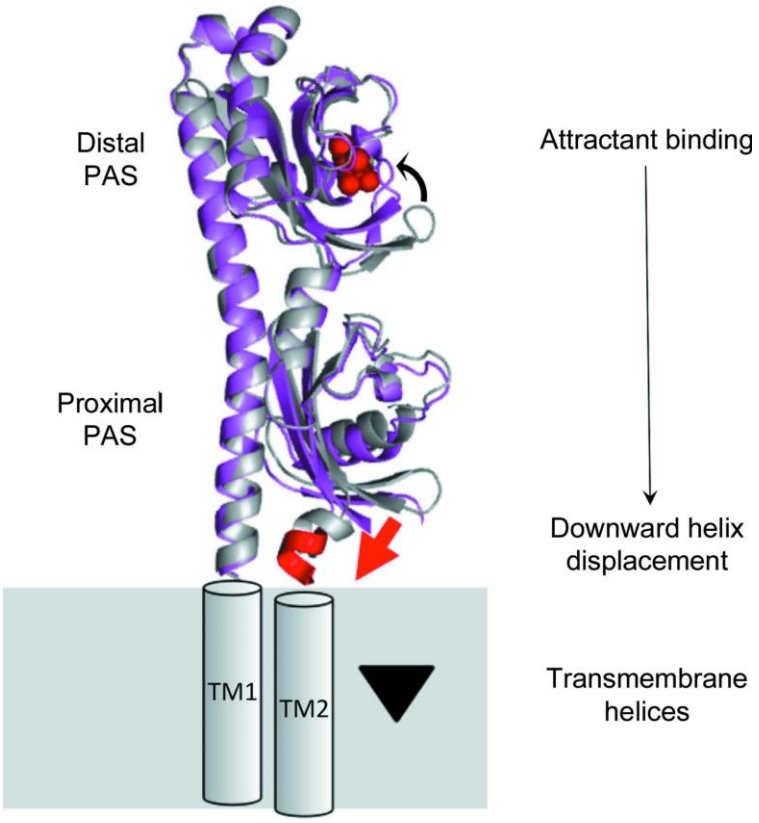

Fig 1.7. Piston model for transmembrane signaling by periplasmic tandem PAS domains. The model is based on the superimposition of the two extreme conformational states of the periplasmic region of Transducer like protein 3 (Tlp3) observed in subunit A of the free protein (shown in magenta/red), respectively. Attractant binding to the distal PAS domain locks it in the closed form, weakening its association with the proximal domain, which results in the transition of the latter into an open form, concomitant with a downward ~4 Å displacement of the C-terminal helix towards the membrane. Figure used with permission of The Journal Biological of Crystallography, doi:10.1107/S139900471501384X, Copyright 2016 International Union of Crystallography

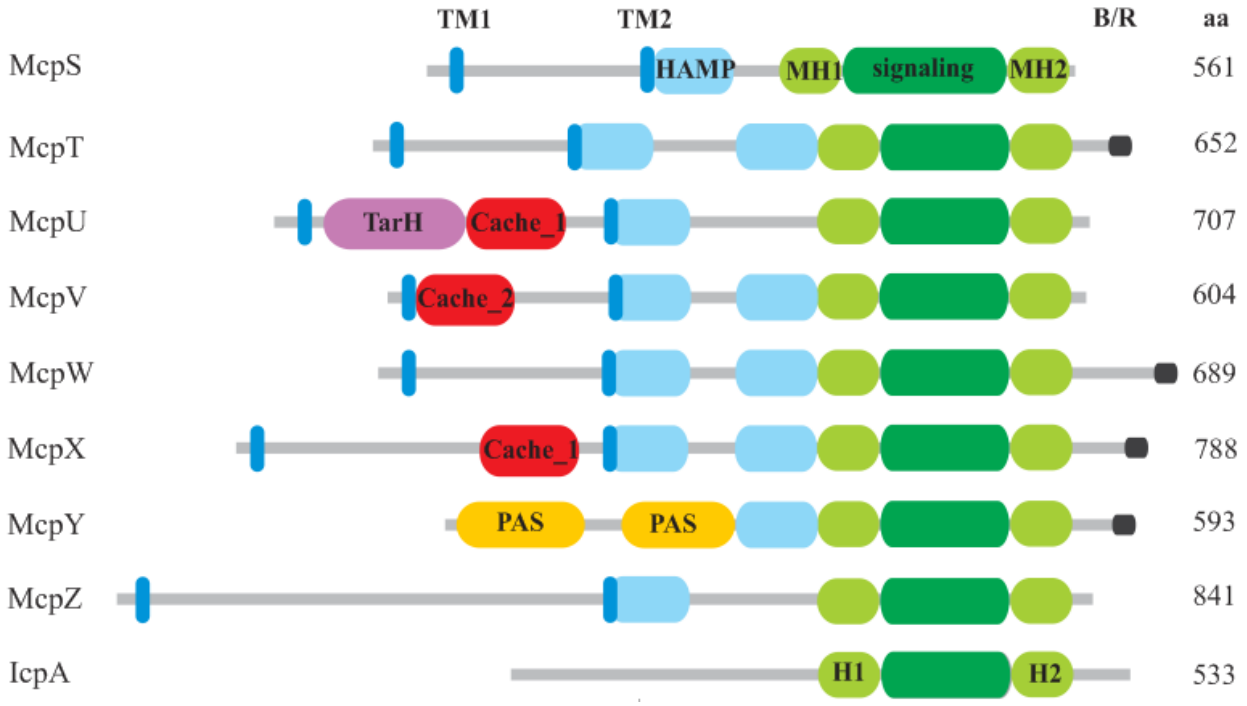

Fig 1.8. Domain organization of chemoreceptor proteins in S. meliloti. TM1 and TM2 are transmembrane regions. HAMP, is a conserved signal transduction domain. H1 and H2 helices in IcpA lack the conserved methylated helices (MH1&2). The signaling domain interacts with CheW and CheA. MH1&2 is the make up the adaptation domain. TarH is a four helix ligand binding domain motif known to mediate chemotaxis toward aspartate and related amino acids. Cache, acronym for the names of the proteins in which these signaling domains were recognized. PAS, acronym for the names of the proteins in which imperfect repeat sequences were recognized. PAS domains are typically involved in sensing redox potential, oxygen, or light.

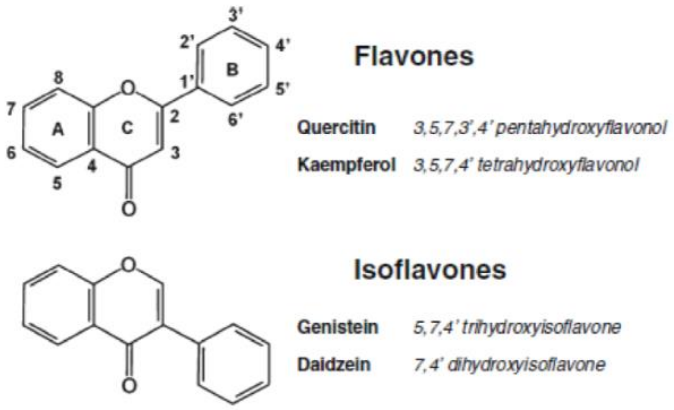

Fig 1.9. The basic structure of flavonoids. Flavones are built up from 2-Phenyl-1,4-benzopyrone while isoflavones are built up from 3-Phenyl-1,4-benzopyrone. Figure used with permission of Springer. Plant and Soil. April 2010, Volume 329, Issue 1, pp 1–25.

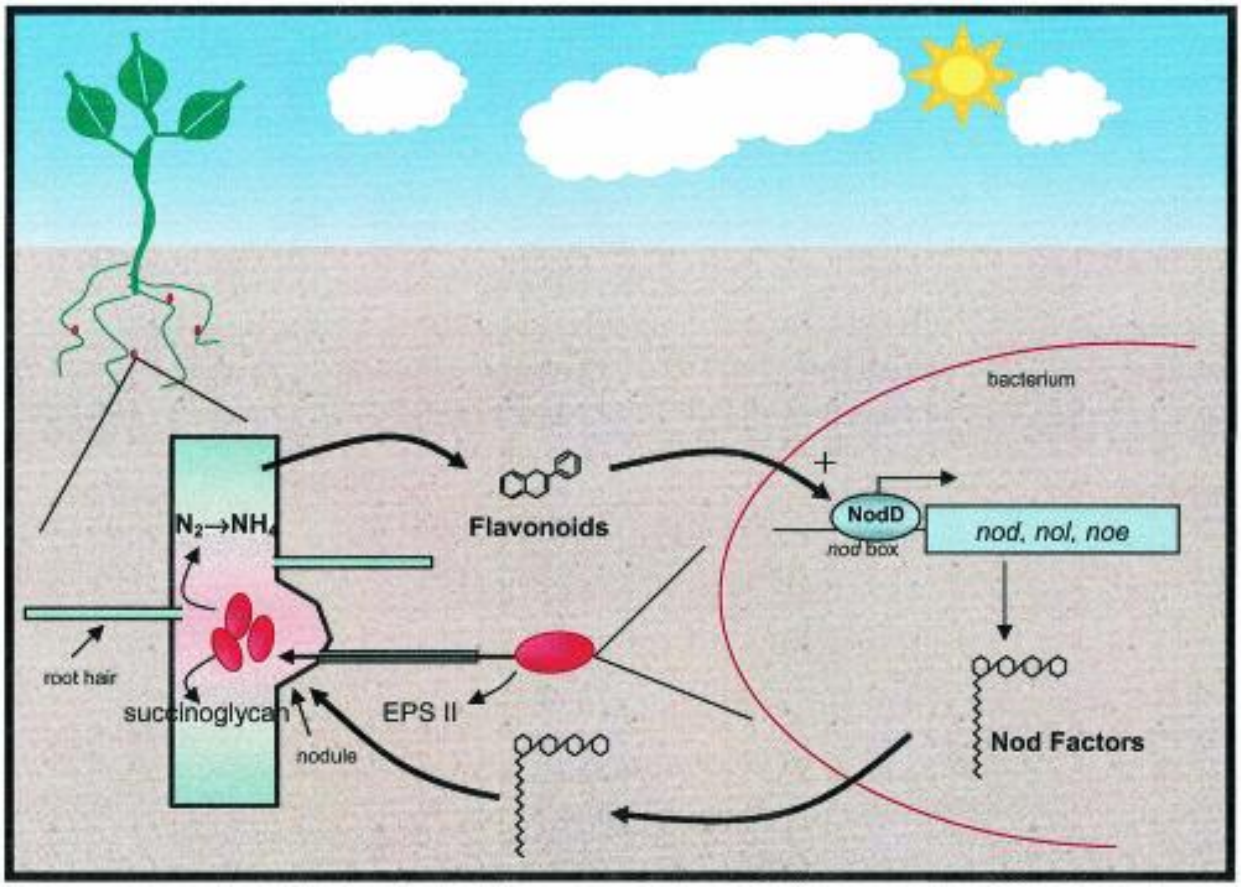

Fig 1.10. Signal exchange between rhizobia and legumes before nodulation. Figure used with permission of Microbiology and Molecular Biology Reviews. Copyright 2003, American Society for Microbiology.

Chapter 2 - The *Sinorhizobium meliloti* chemoreceptor McpU mediates chemotaxis towards host plant exudates through direct proline sensing

BENJAMIN A. WEBB[1], SHERRY HILDRETH[1], RICHARD F. HELM[2], AND BIRGIT E. SCHARF[1]*

[1]Virginia Tech, Department of Biological Sciences, Life Sciences I, Blacksburg, VA 24061;

[2]Virginia Tech, Department of Biochemistry, Life Sciences I, Blacksburg, VA 24061

Running title: McpU binds proline to mediate host exudate sensing

Key words: flagellar motor, motility, rhizosphere, symbiosis, two-component system

* For correspondence:
E-mail bscharf@vt.edu
Tel (+1) 540 231 0757
Fax (+1) 540 231 4043
Biological Sciences, Life Sciences I
Virginia Tech
Blacksburg, VA 24061, USA

Appl. Environ. Microbiol. AEM. 00115-14. 2014. Jun;80(11):3404-15. Accepted manuscript posted online 21st of March 2014, doi: 10.1128/AEM.00115-14

Attribution: BAW has generated the data shown here in Fig. 2.1 - Fig. 2.8. SH helped in determining the quantity of proline in the Results section: "The potent chemoattractant proline is exuded by germinating alfalfa seeds." BAW, RFH, and BES drafted the final manuscript.

ABSTRACT

Bacterial chemotaxis is an important attribute that aids in establishing symbiosis between rhizobia and their legume hosts. Plant roots and seeds exude a spectrum of molecules into the soil to attract their bacterial symbionts. The alfalfa symbiont *Sinorhizobium meliloti* possesses eight chemoreceptors to sense its environment and mediate chemotaxis towards its host. The methyl accepting chemotaxis protein McpU is one of the more abundant *S. meliloti* chemoreceptors and an important sensor for the potent attractant proline. We established a dominant role of McpU in sensing molecules exuded by alfalfa seeds. Mass spectrometry analysis determined that a single germinating seed exudes 3.72 nmoles of proline, producing a millimolar concentration near the seed surface which can be detected by the chemosensory system of *S. meliloti*. Complementation analysis of the *mcpU* deletion strain verified McpU as the key proline sensor. A structure-based homology search identified tandem Cache (calcium channels and chemotaxis receptors) domains in the periplasmic region of McpU. Conserved residues Asp-155 and Asp-182 of the N-terminal Cache domain were determined to be important for proline sensing by evaluating mutant strains in capillary and swim plate assays. Differential scanning fluorimetry revealed interaction of the isolated periplasmic region of McpU ($McpU_{40-284}$) with proline and the importance of Asp-182 in this interaction. Using isothermal titration calorimetry, we determined that proline binds with a K_D of 104 μM to $McpU_{40-284}$ while binding was abolished when Asp-182 was substituted by Glu. Our results show that McpU is mediating chemotaxis towards host plants by direct proline sensing.

INTRODUCTION

Rapidly changing environmental conditions make soil a challenging environment for bacteria to persist. Motile soil bacteria use chemotaxis to navigate through the soil and to find optimal surroundings for survival. One important group of soil bacteria are symbiotic rhizobia, which fix atmospheric nitrogen to forms utilizable by its host plant. In particular, crop legumes, such as peas, soybeans, and alfalfa, form symbiotic relationships with *Rhizobium leguminosarum*, *Bradyrhizobium japonicum*, and *Sinorhizobium meliloti*, respectively (1, 2). Symbiosis partners have evolved a complex and specific molecular dialogue through the exchange of chemical signals, which direct bacterial species to the roots of host plants (3, 4). The rhizosphere is a narrow zone of soil that is influenced by root secretions, while the spermosphere is defined as the zone of soil surrounding a germinating seed. Roots and seeds alike have been shown to exude different types of compounds for the ultimate purposes of successful establishment and proliferation of beneficial microbial communities (5, 6). Host plant exudates recruit symbiotic rhizobia by inducing positive chemotaxis, which allows microbes to accumulate in the rhizosphere (7). Various attractants are exuded from the roots of the *S. meliloti* host, alfalfa (*Medicago sativa*), including sugars, amino acids, carboxylic acids, and phenolic compounds (8-12), but knowledge of substances exuded by germinating seeds is greatly lacking (13-18). Information about how *S. meliloti* perceives seed-derived attractants may aid in symbiotic efficiency, and ultimately greater crop yield by enhancing the recruitment of *S. meliloti* to the spermosphere of germinating seeds.

Chemotaxis is directed movement based on the perception of chemical stimuli. *S. meliloti* and other soil bacteria from the *Rhizobiaceae* family such as *Agrobacterium tumefaciens*, *Bradyrhizobium japonicum*, and *Rhizobium leguminosarum* use their chemotactic trait to move towards roots of their host plants, while chemotaxis-compromised strains are outcompeted by

wild-type bacteria (19-23). However, little is known about the specific role of individual chemoreceptors in this process. In *R. leguminosarum,* an *mcpC* chemoreceptor mutant is severely diminished in nodulation occupancy compared to wild type (24). To date, there are no studies characterizing the specificity of a rhizobial chemoreceptor for host-derived signals.

Previous work has characterized important aspects of *S. meliloti* chemotaxis and how it differs from the *Escherichia coli* paradigm regarding the number and domain topology of chemoreceptors (9), the two-component regulatory system (25-27), and the unidirectional flagellar motor (28-31). *E. coli* has four conventional chemoreceptors, called methyl-accepting chemotaxis proteins (MCPs) and one unorthodox receptor, Aer (32). Aer and the four MCPs share a highly conserved, C-terminal signaling domain that forms a ternary complex with two cytoplasmic chemotaxis proteins, CheA, a histidine kinase, and CheW, an adaptor protein. In the absence of an attractant, CheA is autophosphorylated and subsequently transfers the phosphoryl group to the response regulator protein, CheY (33, 34). Phosphorylated CheY interacts with the cytoplasmic face of the flagellar motor and controls the swimming paths of bacteria (35-37). Orthodox MCPs have an N-terminal periplasmic ligand-binding domain, which have been extensively studied in *E. coli* along with each chemoreceptor's repertoire of detected chemotactic stimuli (38-42).

S. meliloti has nine *genes* coding for putative chemoreceptors (9, 43). We have shown that eight of these receptors participate in chemotaxis, while the *mcpS* gene is not expressed when cells are motile, and presumably regulates processes other than chemotaxis (9, 44). Seven of the *S. meliloti* chemoreceptors are classical MCPs, McpT to McpZ, and one receptor, IcpA, lacks the conserved residues that typically serve as methyl-accepting sites to control adaptation. Six of the MCPs are located in the cytoplasmic membrane via two membrane-spanning regions, whereas McpY and IcpA lack such hydrophobic regions (9). All chemoreceptors vary in their ligand-binding domains;

however, McpU, McpV, and McpX contain specialized domains such as Cache and TarH signaling domains (9), which are known to bind small molecules like amino acids (45, 46). McpY possesses two PAS domains, which typically sense redox potential, oxygen, or light (47). Deletion of individual receptor genes causes differential impairments in the chemotactic response towards various sugars, amino acids, and organic acids (9). The exact function of *S. meliloti* chemoreceptors and mode of attractant binding is not known, and the identification of ligands, and in particular, plant-borne signaling molecules, is a focus of our work.

McpU is one of the most strongly expressed chemoreceptors in *S. meliloti* and is a major sensor for the potent attractant proline (9). This study reveals that proline is sensed through direct binding to the periplasmic region of McpU. We also demonstrate that McpU mediates positive chemotaxis to host seed exudates and quantify the amount of proline exuded by germinating seeds. In conclusion, sensing of seed-derived proline by McpU plays a significant role in host plant recognition.

MATERIALS AND METHODS

Bacterial strains and plasmids

Derivatives of *E. coli* K-12 and *S. meliloti* MV II-1 (48) and the plasmids used are listed in Table 1.

Media and growth conditions

E. coli strains were grown in lysogeny broth (LB) (49) at 37°C. *S. meliloti* strains were grown in TYC (0.5% (w/v) tryptone, 0.3% (w/v) yeast extract, 0.13% $CaCl_2$ x 6 H_2O (w/v) [pH 7.0]) at 30°C (50). Motile cells for capillary assays were grown for two days in TYC, diluted 1:2 in 3 ml TYC and grown for 11 h. Cultures were then diluted 1:100 in 10 ml RB minimal medium (6.1 mM K_2HPO_4, 3.9 mM KH_2PO_4, 1 mM $MgSO_4$, 1 mM $(NH_4)_2SO_4$, 0.1 mM $CaCl_2$, 0.1 mM NaCl, 0.01 mM Na_2MoO_4, 0.001 mM $FeSO_4$, 20 μg/l biotin, 100 μg/l thiamine (11)), layered on Bromfield agar plates (27), and incubated at 30°C for 14 h to an optical density at 600 nm (OD_{600}) of 0.12 ± 0.02. All strains were motile and exhibited swimming characteristics as described by Meier *et al.* (9). The following antibiotics were used at the indicated final concentrations: for *E. coli*, ampicillin at 100 μg/ml, kanamycin at 50 μg/ml; for *S. meliloti*, neomycin at 120 μg/ml, streptomycin at 600 μg/ml.

Preparation of seed exudates

The *Medicago sativa* cultivar 'Guardsman II' (Registration number CV-203, PI 639220), used in this study was developed from the extensively studied cultivar 'Iroquois' by the Cornell University Agricultural Experiment Station, New York State College of Agriculture and Life Sciences, Cornell University, Ithaca, NY (48). Seeds (0.1 g, approximately 47 +/-1 seeds) were placed in a

50-ml conical tube and washed four times with 35 ml of autoclaved, sterile-filtered water. Next, seeds were washed once with 3 ml of 6% commercial bleach for 3 min and four times with 35 ml of autoclaved, sterile filtered water under slow agitation. Seeds were then transferred to a 125-ml Erlenmeyer flask containing 20 ml of autoclaved, sterile-filtered water. Seeds were jostled to distribute them evenly at the bottom of the flask and germinated without shaking at 30°C for 24 h. Post incubation, the germination efficiency was approximately 95% as determined by radicle emergence. To harvest the exudate, 19 ml of seed supernatant was removed from the flask, placed into a 50-ml conical tube and flash frozen in liquid nitrogen. The frozen sample was freeze-dried for 72 h and stored at -20°C. Seed exudates were tested for bacterial contamination by microscopic examination and by plating 20 µl on TYC plates and incubation at 30°C for 24 h. Contaminated samples were not included in this study.

Quantification of proline in alfalfa seed exudates by liquid chromatography mass spectrometry (LC-MS)

Seed exudate residue from three biological replicates was thawed to room temperature, resuspended in 1 ml of 0.1% formic acid in water and sonicated for 10 min. The samples were centrifuged at 3,450 x g for 10 min to remove insoluble material. Two 120 µL aliquots were removed from the supernatant of each biological replicate and transferred to separate 1.5-ml microfuge tubes and centrifuged at 14,000 x g to pellet remaining insoluble material. A 100 µL aliquot of supernatant was then processed using the "EZ:faast® for Free Physiological Amino Acid Analysis by LC-MS" kit according to the manufacturer instructions (Phenomenex, Torrance, CA). Briefly, the EZ:faast® consists of a solid phase extraction step followed by a derivatization and extraction of free amino acids. The derivatized amino acids were analyzed by LC-MS using the supplied EZ:faast AAA-MS on an Agilent 1100 series HPLC (Agilent Technologies, Santa Clara,

CA) coupled with an Applied Biosystems 3200 Q Trap LC/MS/MS System (AB SCIEX, Framingham, MA). Calibration solutions were made separately from the Phenomenex® kit with L-proline (Sigma-Aldrich, St. Louis, MO). Proline standard solutions ranging from 55 to 220 nmoles/ml were derivatized alongside the exudate samples to establish the proline calibration curve. Using Analyst software (AB Sciex, Concord, Ontario, Canada) for data analysis. the peak area of the internal standard, homoarginine, was used to normalize the concentration of proline and given as average derived from three biological replicates, each processed twice, with duplicate injections.

Swim plate assay

Swim plates containing containing RB minimal medium complemented with 10^{-4} M L-proline, 0.27% Bacto Agar and varying concentrations of isopropyl-β-D-thiogalactopyranoside (IPTG) were inoculated with 3 µl droplets of the test culture and incubated at 30°C for three to four days (9).

Traditional capillary assays

Traditional capillary assays were performed essentially as described by Adler (51), with minor modifications (9, 52). Cells were harvested by centrifugation at 3,000 x g for 5 min at room temperature and suspended in RB minimal medium to OD_{600} of 0.1. Closed U-shaped tubes (bent from 65 mm micropipettes, Drummond Scientific Co., Broomall, Pennsylvania, USA) were placed between two glass plates. For each capillary, 400 µl of bacterial suspension were used to make a bacterial pond. Capillary tubes (1-µl disposable micropipettes, Drummond Microcaps) were sealed at one end and filled with attractant dissolved in RB minimal medium. The capillaries were inserted open end first into the bacterial pond and incubated for two hours at 22.5°C. Capillaries were

removed, the sealed end was cut off and the complete content was transferred into 1 ml RB minimal medium. Dilutions were plated in duplicate on TYC plates containing streptomycin. After incubation for three days at 30°C, colonies were counted.

Agarose capillary assays

Agarose capillary assays were performed essentially as described by Grimm and Harwood (1997) (53), with minor modifications. Dried seed exudate was thawed to room temperature, dissolved in acetone:water (7:3 v/v) and centrifuged at 3,000 x g for 5 min. The soluble fraction was concentrated to dryness, dissolved in RB to a concentration of 1.5 mg/ml and diluted 1:10 in molten 1.1% low-melting temperature agarose (NuSieve GTG). To fill the capillaries, 0.5-µl capillaries (Drummond Microcaps) with one end sealed were heated with a Bunsen burner and the open end was placed into the molten mixture. The mixture was allowed to solidify and the open end of the capillary was placed into a circular chemotaxis chamber formed by a microscope slide, a rubber O-ring with an inner diameter of 8.5 mm and a height of 1 mm (Sarstedt), and a coverslip. Cells were harvested and suspended in RB to an OD_{600} of 0.20. An 81 µl aliquot of *S. meliloti* suspension was placed in the chamber before the coverslip was in place. The open end of the capillary was observed at 100x magnification under dark phase using a Nikon Optiphot-2. Pictures were taken using a Q-Imaging Micropublisher camera.

Hydrogel capillary assays

Capillaries containing a cross-linked hydrogel instead of agarose were used because of their improved properties in preventing cells from entering the capillaries. The inner glass surface of 0.5-µl capillaries (Drummond Microcaps) was cleaned with a 3:1 solution of concentrated sulfuric

acid and 30% hydrogen peroxide before capillaries were treated with 1% (v/v) solution of 3-(trichlorosilyl)propyl methacrylate (TPM) (Sigma-Aldrich, St. Louis, MO), diluted in paraffin oil at room temperature for 10 min. After a thorough rinse with 100% ethanol and removal of residual ethanol in a nitrogen gas stream, capillaries were baked at 95°C for 10 min. A 10% (w/v) solution of poly(ethylene glycol) diacrylate (PEG-DA) with an average M_n of 6,000 (Sigma-Aldrich, St. Louis, MO) in phosphate buffered saline, pH 7.4 was mixed with 10% (w/v) Irgacure®2959 (Sigma-Aldrich) in 70% ethanol at a ratio of 1:20 to form the hydrogel solution, which was subsequently pulled into the capillaries with a rubber suction bulb. After submerging the capillaries in hydrogel solution, photopolymerization was performed for 20 seconds using a 365 nm, 18 W cm−2 UV light source (Omnicure S1000, Vanier, Quebec). Hydrogel capillaries were soaked in distilled H_2O for 5 h with 5 water exchanges and equilibrated with L-proline solutions using the same method. One end of each capillary was sealed with machine grease (Apiezon, Manchester, U.K.) and chemotaxis assays were carried out as described for agarose capillary assays.

DNA methods and genetic manipulations

S. meliloti DNA was isolated and purified as described previously (27). Plasmid DNA was purified with a Wizard Plus SV Miniprep system (Promega). DNA fragments or PCR products were purified from agarose gels using a Wizard SV Gel and PCR Clean-Up System (Promega). PCR amplification of chromosomal DNA was carried out according to published protocols (54). Deletion and codon replacement constructs were created by PCR and overlap extension PCR as described by Higuchi (55). These constructs were cloned into the suicide vector pK18*mobsacB*, which was then used to transform *E. coli* S17-1. The plasmid was conjugally transferred to *S. meliloti* by filter mating according to the method of Simon *et al.* (56). Allelic replacement was

achieved by sequential selections on neomycin and 10% (w/v) sucrose as described previously (27). Confirmation of allelic replacement and elimination of the vector was obtained by gene-specific primer PCR and DNA-sequencing.

Isolation of *S. meliloti* cell membranes

S. meliloti strains BS183, BS185, RU11/001, and RU13/301 (Table 1) were grown in *Sinorhizobium* motility medium (SMM; RB minimal medium, 0.2 % mannitol, 2 % TY) (11, 57) to an OD_{600} of 0.26 ± 0.10. An amount of 250 mL of cell culture normalized to an OD_{600} of 0.26 was harvested by centrifugation at 5,000 x g for 5 min at 4°C. Cells were suspended in 20 ml of 1 mM PMSF, 20 mM Tris/HCl, pH 8.0 plus 5 μg/ml DNase I. After two passages through a French press at 20,000 psi, the resulting extract was freed of unbroken cells by centrifugation at 2,000 x g for 2 min. Broken cells were centrifuged at 200,000 x g for 60 min at 4°C, yielding the pellet as the membrane fraction. Membrane fractions were resuspended in 3.5 ml of 1 mM PMSF, 20 mM Tris/HCl, pH 8.0 and homogenized for use in immunoblots. Prior to sodium dodecyl sulfate (SDS) gel electrophoresis, 40 μl of samples were mixed with 25 μl of SDS sample buffer containing 0.5 % β-mercaptoethanol. Prior to SDS-electrophoresis, samples were heated to 100°C for 10 min.

Immunoblotting

Homogenized membrane fractions were separated in 10% acrylamide gels, transferred to Trans-Blot® nitrocellulose (Bio-Rad Laboratories, Hercules, CA) and probed using monoclonal antibodies raised against Green Fluorescent Protein (GFP) (Living Colors® GFP Monoclonal Antibody, Clontech, Mountain View, CA) at a 1:20,000 dilution. Blots were incubated with sheep anti-mouse horseradish peroxidase-linked whole immunoglobin (GE Healthcare Life Sciences,

Pittsburgh, PA) diluted 1:40,000. Detection was achieved by enhanced chemiluminescence using SuperSignal® West Pico Chemiluminescent Substrate (Thermo Scientific, Rockford, IL) using Hyperfilm™ ECL (Amersham, Pittsburgh, PA). Films were scanned by using an Epson Perfection 1640SU and Corel Photo-Paint 10 software. Analysis of the scans was performed using ImageJ and Origin 8.1 software.

Expression and purification of the periplasmic region of McpU (McpU-PR)

The recombinant ligand-binding, periplasmic region of McpU (McpU-PR, $McpU_{40-284}$) and its single amino acid substitution variants were overproduced from plasmid pBS373, pBS383, pBS384, and pBS390 in *E. coli* M15/pREP4 (Table 1). Three liters of cell culture were grown to an OD_{600} of 0.8 at 37°C in LB containing 100 μg/ml ampicillin and 50 μg/mL kanamycin and gene expression was induced by 0.6 mM isopropyl-β-D-thiogalactopyranoside (IPTG). Cultivation was continued for 4 h at 25°C until harvest. Cells were suspended in 50 ml column buffer (500 mM NaCl, 20 mM imidazole, 1 mM PMSF, 20 mM $NaPO_4$, pH 7.0) and lysed by three passages through a French pressure cell at 20,000 psi (SLM Aminco, Silver Spring, MD) and the soluble fraction was loaded on a 5-ml NTA column (GE Healthcare Life Sciences, Pittsburgh, PA) charged with Ni^{2+}. Protein was eluted from the column with elution buffer (500 mM NaCl, 500 mM imidazole, 1 mM PMSF, 20 mM $NaPO_4$, pH 7.0). Pooled fractions were concentrated by ultrafiltration on regenerated cellulose membranes (10-kDa cut-off) and further purified by Äktaprime™ Plus gel filtration HiPrep 26/60 Sephacryl S-300 HR (GE Healthcare Life Sciences, Pittsburgh, PA). The column was equilibrated and developed in 100 mM NaCl, 50 mM HEPES, pH 7.0 at 0.5 ml/min, and protein containing fractions were combined and stored at 4°C.

Thermal denaturation studies

Differential Scanning Fluorimetry experiments were performed using an ABI 7300 Real-Time PCR System (Applied Biosystems, Foster City, CA, USA). L-proline was dissolved in 20 mM imidazole, 500 mM NaCl, 20 mM $NaPO_4$, pH 6.4 and used at final concentrations of 100 μM, 1 mM, and 10 mM. McpU-PR (wild type and its variants) and SYPRO® Orange (Invitrogen, Grand Island, NY) were diluted in the same buffer to final concentrations of 10 μM and a final SYPRO® Orange concentration of 0.7x (from 5,000x stock). Thirty microliter reactions of all conditions were performed in duplicate. A temperature gradient was applied from 10–85 °C with a 30 second equilibration at each half degree °C. Fluorescence was quantified using the preset FRET parameters (excitation, 490 nm; emission, 530 nm) and normalized to the lowest and highest intensity for each data set. Melting temperatures were determined by data analysis with XLfit™ from IDBusiness Solutions (Guildford, UK).

Isothermal titration calorimetry (ITC)

McpU-PR and McpU-PR/D182E in 100 mM NaCl, 50 mM HEPES, pH 7.0 were concentrated to 812 μM using a 10-kDa regenerated cellulose membrane in a 50 ml Amicon filter unit and a 10-kDa Centricon centrifugal filter device (Millipore, Bedford, MA). Measurements were made on a VP-ITC Microcalorimeter (MicroCal, Northampton, MA) at 22°C. The protein was placed in the sample cell and titrated with 10 μl injections of 4 mM L-proline that had been dissolved in the flow-through of the protein filtration step. The flow-through fraction was titrated with the same concentration of L-proline to produce a baseline that was subtracted from the protein titration. Data analysis was carried out using the "one binding sites" model of the MicroCal version of Origin 8.1 software (OriginLab, Northampton, MA).

RESULTS

McpU mediates *S. meliloti* chemotaxis towards seed exudate of its host *Medicago sativa*

Chemotaxis of rhizobacteria in the soil towards host plant roots is important in establishing symbiosis (58, 59). Since McpU is a major receptor in *S. meliloti* chemotaxis (9, 44), we analyzed the reaction of wild type (WT, RU11/001), a strain lacking *mcpU* (Δ*mcpU*; RU11/828), and a *che* strain (Δ*mcpS,* Δ*mcpT,* Δ*mcpU,* Δ*mcpV,* Δ*mcpW,* Δ*mcpX,* Δ*mcpY,* Δ*mcpZ,* Δ*icpA* (Δ9); RU13/149) towards exudates of *Medicago sativa* (alfalfa) seeds. Exudates were prepared from surface-sterilized germinating seeds and tested with motile cell populations in qualitative agarose capillary assays. The wild-type strain revealed a strong positive response towards seed exudate as detected by the accumulation of cells at the mouth of the capillary (Fig. 2.1, top), while a strain lacking all nine chemoreceptors genes (RU13/149) showed a complete lack of cell accumulation, and is therefore defined as chemotaxis negative (*che*; Fig. 2.1, middle). In comparison, the *mcpU* deletion strain exhibited a very weak, but still visible response, observed as faint accumulation of cells at the capillary opening (Fig. 2.1, bottom). The strongly diminished response of the Δ*mcpU* strain indicates that McpU is a principal chemoreceptor for attractant components in alfalfa seed exudates.

The potent chemoattractant proline is exuded by germinating alfalfa seeds

Since capillary assays revealed that McpU is an important chemoreceptor for host seed exudates and previous studies recognized McpU as a major proline sensor (9), we analyzed the amount of proline exuded by germinating alfalfa seeds. Three biological replicates of surface-sterilized seeds were germinated, exudates harvested and processed with the Phenomenex EZ:faast® kit. Data analysis after liquid chromatography mass spectrometry (LC-MS) revealed that 1.75 ± 0.24 μmoles of proline are exuded by one gram of seeds (201 μg/g of seed), which equals an amount of 3.72

nmoles of proline per alfalfa seed. With an average seed volume of 2.17 μl, the concentration of exuded proline at the seed surface is predicted to be 1.71 mM which would then be allowed to diffuse from the seed into the spermosphere. Millimolar concentrations of proline have been reported to elicit an attractant response from *S. meliloti* (9, 11). In conclusion, proline is secreted by germinating alfalfa seeds in concentrations detectable by the chemotaxis system of *S. meliloti*.

McpU mediates chemotaxis of *S. meliloti* towards proline

In a previous study, we analyzed the chemotaxis behavior of single chemoreceptor deletion strains and identified McpU as a major receptor for the strong attractant proline (9). To further assess the importance of McpU for the attraction of *S. meliloti* to proline, we constructed the broad-host range plasmid pBS1053 which allows controlled expression of *mcpU* from an inducible *lac* promoter by the addition of varying concentrations of isopropyl β-D-1-thiogalactopyranoside (IPTG). We first performed a quantitative swim plate assay with 10^{-4} M proline (L-proline was used in all studies) as the sole carbon source. After 5 days of incubation at 30 °C, the wild type formed a swim ring with a diameter of 80 mm, while the swim ring produced by the *mcpU* deletion strain was 44% of the wild-type swim ring (Fig. 2.2A). In comparison, a *che* strain formed a ring on proline swim plates which had a diameter of 27% of the wild-type swim ring size (9). In the absence of the inducer IPTG, the complemented strain (Δ*mcpU*/*mcpU*) formed a ring larger than that of the deletion strain (64% of wild type). The observed partial complementation demonstrates that McpU is already expressed under these conditions, which can be explained by basal leakiness of the *E. coli lac* promoter/LacI^q repressor system. The swim ring size of the complemented strain increased with increasing ITPG concentration, reaching a plateau between 5 and 500 μM ITPG with a maximum of 91% of the wild-type swim ring at 500 μM IPTG (Fig. 2.2). Higher concentrations

of IPTG had a marginally inhibitory effect on swim ring size (data not shown). To serve as a second assessment, we quantified the response of *S. meliloti* strains to proline in a traditional capillary assay. This test is considered the gold standard of chemotaxis assays because of its ability to quantify cell numbers in a capillary, thus allowing for accurate classification of tested chemicals. When the response of wild-type cells to 10 mM proline was tested, 1.1 x 10^6 cells accumulated in the 1-μl capillary after 2 hour incubation at room temperature. The *che* strain exhibited a negligible response compared to wild type, while the response of the *mcpU* deletion strain was 34% of the wild-type response (Fig. 2.2B). When the complemented strain was grown in the presence of 500 μM IPTG, which caused optimal recovery of proline sensing on swim plates (Fig. 2.2A), it attained 86% of the wild-type response (Fig. 2.3B). Taken together, both assays provided consistent results showing that the response of *S. meliloti* to proline is greatly dependent on McpU. Furthermore, proline taxis can be restored by the expression of *mcpU in trans*.

A structure-based homology search identifies the ligand binding site in McpU

The periplasmic region of McpU contains a conserved Cache (calcium channels and chemotaxis receptors; (45)) signaling domain (amino acid residues 149-226; (60, 61)) and a less well-conserved TarH domain (residues 106-144; (61)). Members of the Cache family are widespread in both prokaryotic and eukaryotic organisms and are predicted to bind small molecules, including amino acids (45). A homologue search in the RCSB Protein Data Bank revealed that the periplasmic region of McpU (McpU-PR, residues 40-284) shares the greatest sequence identity (26%) with the sensor domain of McpN from *Vibrio cholerae*. The structure of the McpN sensor domain (residues 61-300, Protein Data Bank code 3C8C) appears as a homodimer (Fig. 2.3). Each polypeptide chain has an N-proximal α-helix that loops over into two consecutive Cache domains.

Zooming in on either of the N-proximal Cache domains (close up in Fig. 2.3) reveals the ligand alanine in the binding pocket formed by the domains. The carboxyl groups of two aspartate residues, Asp-172 and Asp-201, coordinate the ligand via hydrogen bonds between the oxygen atoms and the amino group of the ligand. Alignment of McpU-PR and McpN-PR revealed a 34% identity in the region of the McpN tandem Cache domains, whereas the regions outside of the tandem cache domains have only 16% identity (62), corroborating the presence of tandem Cache domains in McpU-PR. The amino acid sequence of the McpU periplasmic region was submitted for three dimensional-structure-based homology modeling in the SWISS-MODEL Workspace (63). A model was constructed with McpU-PR residues 7-245 based on the McpN template (3C8C) of *V. cholerae*. When the homology model of McpU-PR was superimposed with the structure of the McpN sensor domain, two aspartate residues, namely Asp-155 and Asp-182, were conserved in the same positions as the two ligand-coordinating residues in McpN. This finding allows the prediction that the ligand binding pocket of *V. cholerae* McpN and *S. meliloti* McpU is conserved and that McpU coordinates proline in a similar manner that McpN uses to bind the ligand alanine.

Single-point mutations in the ligand-binding pocket of McpU cause a diminished chemotaxis response to proline

Homology modeling predicted two conserved aspartate residues in McpU-PR to be involved in ligand sensing. To elucidate the role of these residues in chemotaxis towards proline, we created *S. meliloti* mutants carrying single point mutations in position 155 and 182. Initially, we made alanine substitutions and analyzed the behavior of the resulting mutants in comparison to appropriate control strains in hydrogel capillary assays. The hydrogel capillary assay is an improved variation of the agarose capillary assay used earlier (Fig. 2.1). Wild-type cells

(RU11/001) strongly accumulated around the mouth of the capillary filled with 1 mM proline (Fig. 2.4A), while the *che* (RU13/149) and the *mcpU* deletion (RU11/828) strains displayed no or a strongly reduced response to proline, respectively (Fig. 2.4B and 2.4C). Strain BS184 ($McpU^{D155A}$) exhibited a weaker response compared to wild type, yet considerably stronger than that of the *mcpU* deletion strain (RU11/828) (Fig. 2.4D). In contrast, the response of strain BS182 ($McpU^{D182A}$) to proline was almost abolished (Fig. 2.4E). Therefore, we introduced a glutamate residue in position 182, which we predicted to be a less detrimental substitution. The resulting strain, BS187 ($McpU^{D182E}$) exhibited an intermediary response (Fig. 2.4F), which was weaker than wild type, but stronger than the *mcpU* deletion strain. To quantify the importance of aspartate residues 155 and 182 for proline taxis, we performed proline swim plate assays with the mutant strains and compared their behavior to the wild type (Fig. 2.5). All mutant strains exhibited a diminished response to proline, with the order of response ranking as Δ*mcpU* < $McpU^{D182A}$ < $McpU^{D182E}$ < $McpU^{D155A}$ < wild type, correlating with the results obtained from the hydrogel capillary assays.

To verify that the altered chemotactic responses of the mutant strains are not caused by reduced levels of mutant McpU protein, we assessed the expression of McpU variant proteins in *S. meliloti* using immunoblots. Since antibodies directly targeting McpU were not available, we created mutants strains with corresponding variants of McpU-EGFP in its native chromosomal locus for $McpU^{D155A}$ and $McpU^{D182A}$ (Table 1) and compared their expression and incorporation in *S. meliloti* cell membranes with that of McpU-EGFP (44) using a commercially available monoclonal anti-GFP antibody. Full-length McpU-EGFP fusion variant proteins (101 kDa) were present in isolated membranes at similar levels compared to wild-type McpU-EGFP (Fig. 2.6). Band intensities from three independent blots quantified as 114% and 91% for $McpU^{D155A}$-EGFP and

McpU^{D182A}-EGFP, respectively, compared to McpU-EGFP. Since there is no correlation between attractant response of the mutant strains (Fig. 2.4) and the respective band intensities of variant protein (Fig. 2.6), we concluded that both aspartate residues in McpU-PR are involved in proline sensing, with Asp-182 being more important than Asp-155.

Proline interacts with the periplasmic region of McpU involving Asp-182

To test the interaction of proline with the isolated sensing domain *in vitro*, we overexpressed and purified McpU-PR and its single amino acid variants McpU-PR^{D182A} and McpU^{D182E} fused N-terminally to a His_6-tag using affinity and size exclusion chromatography. Next, we monitored the thermal unfolding of isolated proteins in the presence of the fluorescent dye SYPRO orange, which binds to the hydrophobic parts of proteins as they unfold. This technique, named differential scanning fluorimetry (DSF), enables the identification of ligands that bind and stabilize purified proteins (64). Characteristically, the transition midpoint, T_m, shifts to higher temperatures upon binding of a low-molecular weight ligand. We determined the T_m of McpU-PR as 37°C, which shifted upon addition of 10 mM proline to 52°C (Fig. 2.7). The drastic T_m increase of McpU-PR in the presence of proline indicates that it stabilizes the protein through direct interaction. Furthermore, we observed a promotion of McpU-PR stability at lower concentrations of proline (1.0 and 0.1 mM, data not shown). When we tested the protein variants, we found that McpU-PR^{D182A} has a T_m of 29°C, which is 8°C lower than that of McpU-PR, indicative of reduced protein stability. In the presence of proline, no change in T_m was observed, demonstrating lack of interaction. For McpU-PR^{D182E}, the T_m in the absence of proline was 34°C, which only marginally increased by 2°C to 36°C. While the general stability of McpU-PR^{D182E} appears to be comparable to the wild-type protein, the small increase of T_m in the presence of proline infers a relatively weak

interaction. Altogether, proline directly interacts with the sensing domain of McpU, while mutations in the binding pocket that affect ligand coordination reduce the affinity between receptor and proline.

Proline binds directly to McpU-PR

Next, we used isothermal titration calorimetry (ITC) to quantitatively assess binding of proline to the sensing domain of McpU and its binding site variant (McpU-PR^{D182E}). As shown in Fig. 2.8A, titration of McpU-PR with proline resulted in large exothermic heat signals that dissipate into heats of dilution. The affinity derived from the binding curve yielded a K_D of 104 μM, a value well within the range of reported bacterial chemoreceptor-ligand interactions (65-67). Titration of the McpU-PR^{D182E} variant caused very small exothermic heat signals and earlier saturation of heat release (Fig. 2.8B). Due to the extremely weak interaction, a K_D was not derived. The ITC results confirm direct binding of proline to McpU and the importance of Asp-182 for ligand binding.

DISCUSSION

The symbiotic soil bacterium *S. meliloti* uses chemotaxis to optimize movements towards nutrients and host plant-secreted attractants (9-13). This early step in host interaction allows bacteria to effectively locate infection sites along emerging roots and therefore more effectively compete for nodulation (19, 58). Alfalfa roots release a spectrum of phytochemicals in the soil, including carbohydrates, amino acids, organic acids, fatty acids, sterols, growth factors, vitamins, and flavonoids, to initiate and modulate the dialogue with its microbial symbiont (14, 68, 69). Similarly, germinating seeds exude many organic compounds and we have shown that alfalfa seed exudates elicit a prevailing chemotactic response from *S. meliloti* (Fig. 2.1). An early recruitment of the microbial symbiont to the growing root, e.g. during seed germination, appears to be a plausible strategy to maximize interaction. While flavonoids have been suggested as host-specific attractants, they elicit only a weak chemotactic response (8, 59), and likely have a short diffusion range in aqueous soil due to their hydrophobic nature. Therefore, amino acids, organic acids, and sugars are more attractive candidates to function as recruiting agents, because they are hydrophilic and many of these substances have been shown to serve as chemoattractants for *S. meliloti* (9, 11, 12).

In this study, we rationally related proline exudation by germinating alfalfa seeds with *S. meliloti* chemotaxis towards proline. We found that proline is exuded from germinating alfalfa seeds in millimolar concentrations. It is known that plants exude most proteinogenic amino acids into the soil where they can serve as biological sources of carbon and nitrogen for soil bacteria (70). In addition, certain amino acids, including proline and glutamate, function as osmoprotectants and are accumulated by a variety of bacteria during osmotic stress. This ability is particularly valuable in environments that are prone to significant variation in solute concentration such as the

rhizosphere (70, 71). Therefore, it is beneficial for microbes to seek higher concentrations of proline in the soil and proline taxis has been reported for several soil bacteria, including *Agrobacterium* sp. H13-3, *Bacillus subtilis*, *Pseudomonas fluorescens*, and *S. meliloti* (11, 65, 72). Our current work and other studies presented that *S. meliloti* can sense and migrate towards proline in the micro to millimolar range (Figs. 2.2 & 2.4; (9, 11)). Furthermore, preliminary analyses revealed a greater attraction of *S. meliloti* to host compared to non-host legume seed exudates (data not shown). It would be interesting to see whether the capacity of host plants to exude amino acids such as proline has co-evolved with the capability of bacterial symbionts to chemotactically react to these substances, thereby increasing symbiotic effectiveness. Studies are on the way to comparatively examine the secretomes of host and non-host legumes.

Based on previous results, we focused our studies on McpU, one of eight chemoreceptors mediating *S. meliloti* chemotaxis. McpU is one of the more abundant chemoreceptors in *S. meliloti* (44), and capillary and swim plate assays of single deletion mutants identified McpU as major receptor for proline (9). We first investigated the reaction of an in-frame *mcpU* deletion strain towards exudates harvested from germinating alfalfa seeds and established that its chemotaxis response is strongly diminished (Fig. 2.1). Since proline is exuded in millimolar concentrations by germinating alfalfa seeds and proline elicits a strong chemotactic response of *S. meliloti* wild-type but not the *mcpU* deletion strain (Figs. 2.2 & 2.4), we concluded that McpU is mediating chemotaxis towards host plants through proline sensing. However, proline is likely not the sole chemoattractant. The function of individual *S. meliloti* chemoreceptors for root colonization or nodulation has not been investigated. It will be interesting to see whether the *mcpU* deletion strain is impaired in its ability to induce nodule formation. It is worth mentioning that proline chemotaxis is not completely abolished in the Δ*mcpU* strain, which suggests an overlap in specificity by other

chemoreceptors. It has been reported that at least three chemoreceptors in *Pseudomonas putida* have overlapping specificity for organic acids (14). In fact, *S. meliloti* McpX and McpY have been identified previously through capillary assays to contribute to proline taxis (9). McpX and McpU both possess Cache domains, which are known to bind small ligands such as amino acids (45), while McpY is a cytosolic protein with dual Per-Arnt-Sim (PAS;(73)) domains (9). Since detailed information about the proline sensing characteristics of McpX and McpY is lacking, we can only speculate about their involvement in the recognition of plant-derived proline. Proline binding and/or cooperative signaling of receptor homodimers forming mixed trimers-of-dimers are among the possible explanations for the behavior of *mcpX* and *mcpY* receptor mutants. Behavioral studies of *S. meliloti* are hampered by the circumstance that chemoreceptor function appears to depend on the presence of a receptor ensemble (9). A strain bearing only a chromosomal copy of *mcpU* but lacking all other receptor genes (RU13/285) behaves like a *che* strain on swim plates and in the agarose capillary assay. In addition, overexpression of *mcpU* from pBS1053 in a strain lacking all chemoreceptors (RU13/149) failed to restore proline taxis (data not shown). One plausible hypothesis for this behavior is a reduced capability of an individual chemoreceptor to form a signaling cluster (44). This rules out the possibility of analyzing the sensing range of single chemoreceptor species *in vivo* without the influence of other chemoreceptors.

Bacterial chemoreceptors can bind attractants directly to their periplasmic domains or indirectly through periplasmic substrate-binding proteins (74). Our *in-vitro* binding studies revealed that McpU binds proline directly to its periplasmic region (Figs. 2.7&2.8). Using ITC we determined the K_D to be 104 μM, which is within the range of K_D values obtained for proline binding to the periplasmic regions of McpC of *B. subtilis* and McpX of *V. cholerae* with 14 μM and 75 μM, respectively (65, 66). It is worth mentioning that McpU exhibited exothermic binding, similar to

McpX, while McpC displayed endothermic binding. The structures of their periplasmic domains were modeled after *V. cholera* McpN and proposed to have tandem Cache domains. Interestingly, McpC and McpX were shown to bind multiple amino acid ligands (65, 66). It remains to be seen whether similar binding characteristics hold true for McpU and to what extent these putative ligands are exuded by the alfalfa host.

Since no structural data are available for McpU, we used the crystal structure of *V. cholerae* McpN complexed with alanine to model the ligand binding pocket and identify residues that coordinate proline (Fig. 2.3). Two conserved residues, Asp-155 and Asp-182 (Asp-172 and Asp-201 in McpN) in the N-terminal Cache domain were predicted to bind the ligand proline and were chosen for further phenotypic analyses. The moderate decrease in proline taxis caused by a mutation of Asp-155 to Ala indicates the involvement of this residue in proline binding. However, the effect is not as detrimental as an Asp to Ala mutation in position 182, which abolished proline taxis mediated by McpU and *in-vitro* binding of proline to McpU-PR^{D182A} (Figs. 2.4, 2.5, 2.7). We hypothesize that a change in the side chain of residue 155 can be relatively promiscuous, while the nature of the residue in position 182 is critical for proper proline binding. This conclusion is supported by the less impaired phenotype of a strain carrying an Asp to Glu mutation in position 182, which conserves the carboxyl group of the side chain (Figs. 2.4&2.5). The carboxyl moiety of the glutamate residue likely allows coordination of the ligand via hydrogen bonds to the amino group of the ligand, yet the increased length of the side chain possibly reduces the size of the binding pocket thereby weakening ligand affinity. Reduced affinity of proline to McpU-PR^{D182E} was confirmed by *in-vitro* DSF and ITC binding analyses (Figs. 2.7&2.8). Additional information delivered by DSF was the moderate decrease in stability of the proteins with a variation in position 182. We found DSF to be a useful technique for monitoring interactions with proline. Although

this technique does not provide K_D values, it can be beneficial as a first screen of mutant proteins or potential ligand interactions.

Chemoreceptor proteins vary in their genomic abundance, sequence, and domain topologies throughout the bacterial kingdom (67, 75). The number of MCPs in bacteria that establish pathogenic or symbiotic interactions with plant roots is typically high, e.g., 20 in *Agrobacterium tumefaciens* (76) and 36 in *Bradyrhizobium japonicum* (77). In this view, *S. meliloti* is an ideal model organism to study chemoreception of phytochemicals, because it only has eight receptors directing chemotaxis (9, 43). Four of these receptors have un-annotated ligand binding domains, while the remaining four contain either Cache or PAS domains (9). We showed that the Cache domain in McpU directly binds proline. McpU is the first chemoreceptor in *S. meliloti* or other rhizobial bacteria for which a host plant-derived ligand was identified. Furthermore, we presented the importance of proline sensing for the recognition of the *S. meliloti* host alfalfa. Lastly, we drew the conclusion that McpU has a major contribution in host recognition. It will be interesting to decipher the role of the remaining seven chemoreceptor proteins in host recognition, as we continue the search for, possibly unique, host plant-specific attractants.

ACKNOWLEDGMENTS

This study was supported by NSF grant MCB-1253234 and start-up funds from Virginia Tech to Birgit Scharf. We are indebted to Florian Schubot for sharing instrument ABI 7300 real-time PCR system, technical advice on differential scanning fluorimetry, and support with protein modeling. The Virginia Tech Mass Spectrometry Incubator is maintained with funding from the Fralin Life Science Institute of Virginia Tech as well as NIFA (Hatch Grant 228344). We are indebted to the Cornell University College of Agriculture and Life Sciences New York State Agricultural

Experiment Station for donation of alfalfa seeds, Mahama Aziz Traore and Bahareh Behkam for help with the preparation of hydrogel capillaries, Veronika Meier for her help in the construction of RU13/285, Emily Koiner for the construction of pBS1053, and Katherine Broadway for critical reading of the manuscript.

REFERENCES

1. **van Rhijn P, Vanderleyden J.** 1995. The *Rhizobium*-plant symbiosis. Microbiol. Rev. **59:**124-142.
2. **Gage DJ.** 2004. Infection and invasion of roots by symbiotic, nitrogen-fixing rhizobia during nodulation of temperate legumes. Microbiol. Mol. Biol. Rev. **68:**280-300.
3. **Bais HP, Weir TL, Perry LG, Gilroy S, Vivanco JM.** 2006. The role of root exudates in rhizosphere interations with plants and other organisms. Annu. Rev. Plant Biol. **57:**233-266.
4. **Uren NC.** 2000. Types, amounts and possible functions of compounds released into the rhizosphere by soil-grown plants, p. 19-40. *In* Pinton R, Varanini Z, Nannipiero P (ed.), The Rhizosphere: Biochemistry and Organic Substances at the Soil-Plant Interface, New York.
5. **Nelson EB.** 2004. Microbial dynamics and interactions in the spermosphere. Annu. Rev. Phytopathol. **42:**271-309.
6. **Berendsen RL, Pieterse CM, Bakker PA.** 2012. The rhizosphere microbiome and plant health. Trends Plant Sci. **17:**478-486.
7. **Hiltner L.** 1904. Über neue Erfahrungen und Probleme auf dem Gebiete der Bodenbakteriologie. Arbeiten der Deutschen Landwirtschaftsgesellschaft **98:**59-78.
8. **Dharmatilake AJ, Bauer WD.** 1992. Chemotaxis of *Rhizobium meliloti* towards Nodulation Gene-Inducing Compounds from Alfalfa Roots. Appl. Environ. Microbiol. **58:**1153-1158.
9. **Meier VM, Muschler P, Scharf BE.** 2007. Functional analysis of nine putative chemoreceptor proteins in *Sinorhizobium meliloti*. J. Bacteriol. **189:**1816-1826.
10. **Burg D, Guillaume J, Tailliez R.** 1982. Chemotaxis by *Rhizobium meliloti*. Microbiology **133:**162-163.
11. **Götz R, Limmer N, Ober K, Schmitt R.** 1982. Motility and chemotaxis in two strains of *Rhizobium* with complex flagella. J. Gen. Microbiol. **128:**789-798.
12. **Malek W.** 1989. Chemotaxis in *Rhizobium meliloti* strain L5.30. Microbiology **152:**611-612.
13. **Hartwig UA, Joseph CM, Phillips DA.** 1991. Flavonoids Released Naturally from Alfalfa Seeds Enhance Growth Rate of *Rhizobium meliloti*. Plant Physiol. **95:**797-803.
14. **Hartwig UA, Maxwell CA, Joseph CM, Phillips DA.** 1990. Chrysoeriol and Luteolin Released from Alfalfa Seeds Induce *nod* Genes in *Rhizobium meliloti*. Plant Physiol. **92:**116-122.
15. **Hartwig UA, Phillips DA.** 1991. Release and Modification of *nod*-Gene-Inducing Flavonoids from Alfalfa Seeds. Plant Physiol. **95:**804-807.
16. **Phillips DA, Wery J, Joseph CM, Jones AD, Teuber LR.** 1995. Release of flavonoids and betaines from seeds of seven *Medicago* species. Crop Sci. **35:**805-808.
17. **Phillips DA, Joseph CM, Maxwell CA.** 1992. Trigonelline and Stachydrine Released from Alfalfa Seeds Activate NodD2 Protein in *Rhizobium meliloti*. Plant. Physiol. **99:**1526-1531.
18. **Hartwig UA, Maxwell CA, Joseph CM, Phillips DA.** 1989. Interactions among Flavonoid *nod* Gene Inducers Released from Alfalfa Seeds and Roots. Plant Physiol. **91:**1138-1142.
19. **Gulash M, Ames P, Larosiliere RC, Bergman K.** 1984. Rhizobia are attracted to localized sites on legume roots. Appl. Environ. Microbiol. **48:**149-152.

20. **Hawes MC, Smith LY.** 1989. Requirement for chemotaxis in pathogenicity of *Agrobacterium tumefaciens* on roots of soil-grown pea plants. J. Bacteriol. **171:**5668-5671.
21. **Barbour WM, Hattermann DR, Stacey G.** 1991. Chemotaxis of *Bradyrhizobium japonicum* to soybean exudates. Appl. Environ. Microbiol. **57:**2635-2639.
22. **Miller LD, Yost CK, Hynes MF, Alexandre G.** 2007. The major chemotaxis gene cluster of *Rhizobium leguminosarum* bv. *viciae* is essential for competitive nodulation. Mol. Microbiol. **63:**348-362.
23. **Althabegoiti MJ, Lopez-Garcia SL, Piccinetti C, Mongiardini EJ, Perez-Gimenez J, Quelas JI, Perticari A, Lodeiro AR.** 2008. Strain selection for improvement of *Bradyrhizobium japonicum* competitiveness for nodulation of soybean. FEMS Microbiol. Lett. **282:**115-123.
24. **Yost CK, Rochepeau P, Hynes MF.** 1998. Rhizobium leguminosarum contains a group of genes that appear to code for methyl-accepting chemotaxis proteins. Microbiology **144 (Pt 7):**1945-1956.
25. **Dogra G, Purschke FG, Wagner V, Haslbeck M, Kriehuber T, Hughes JG, Van Tassell ML, Gilbert C, Niemeyer M, Ray WK, Helm RF, Scharf BE.** 2012. *Sinorhizobium meliloti* CheA complexed with CheS exhibits enhanced binding to CheY1, resulting in accelerated CheY1 dephosphorylation. J. Bacteriol. **194:**1075-1087.
26. **Riepl H, Maurer T, Kalbitzer HR, Meier VM, Haslbeck M, Schmitt R, Scharf B.** 2008. Interaction of CheY2 and CheY2-P with the cognate CheA kinase in the chemosensory-signalling chain of *Sinorhizobium meliloti*. Mol. Microbiol. **69:**1373-1384.
27. **Sourjik V, Schmitt R.** 1996. Different roles of CheY1 and CheY2 in the chemotaxis of *Rhizobium meliloti*. Mol. Microbiol. **22:**427-436.
28. **Scharf B.** 2002. Real-time imaging of fluorescent flagellar filaments of *Rhizobium lupini* H13-3: flagellar rotation and pH-induced polymorphic transitions. J. Bacteriol. **184:**5979-5986.
29. **Eggenhofer E, Haslbeck M, Scharf B.** 2004. MotE serves as a new chaperone specific for the periplasmic motility protein, MotC, in *Sinorhizobium meliloti*. Mol. Microbiol. **52:**701-712.
30. **Eggenhofer E, Rachel R, Haslbeck M, Scharf B.** 2006. MotD of *Sinorhizobium meliloti* and related alpha-proteobacteria is the flagellar-hook-length regulator and therefore reassigned as FliK. J. Bacteriol. **188:**2144-2153.
31. **Attmannspacher U, Scharf B, Schmitt R.** 2005. Control of speed modulation (chemokinesis) in the unidirectional rotary motor of *Sinorhizobium meliloti*. Mol. Microbiol. **56:**708-718.
32. **Baker MD, Wolanin PM, Stock JB.** 2006. Signal transduction in bacterial chemotaxis. Bioessays **28:**9-22.
33. **Lukat GS, Lee BH, Mottonen JM, Stock AM, Stock JB.** 1991. Roles of the highly conserved aspartate and lysine residues in the response regulator of bacterial chemotaxis. J. Biol. Chem. **266:**8348-8354.
34. **Borkovich KA, Kaplan N, Hess JF, Simon MI.** 1989. Transmembrane signal transduction in bacterial chemotaxis involves ligand-dependent activation of phosphate group transfer. Proc. Natl. Acad. Sci. U S A **86:**1208-1212.
35. **Welch M, Oosawa K, Aizawa S, Eisenbach M.** 1993. Phosphorylation-dependent binding of a signal molecule to the flagellar switch of bacteria. Proc. Natl. Acad. Sci. USA. **90:**8787-8791.
36. **Scharf BE, Fahrner KA, Turner L, Berg HC.** 1998. Control of direction of flagellar rotation in bacterial chemotaxis. Proc. Natl. Acad. Sci. USA. **95:**201-206.

37. **Alon U, Camarena L, Surette MG, Aguera y Arcas B, Liu Y, Leibler S, Stock JB.** 1998. Response regulator output in bacterial chemotaxis. EMBO J. **17:**4238-4248.
38. **Grebe TW, Stock J.** 1998. Bacterial chemotaxis: the five sensors of a bacterium. Curr. Biol. **8:**R154-157.
39. **Hazelbauer GL.** 1988. The bacterial chemosensory system. Can. J. Microbiol. **34:**466-474.
40. **Bibikov SI, Biran R, Rudd KE, Parkinson JS.** 1997. A signal transducer for aerotaxis in *Escherichia coli*. J. Bacteriol. **179:**4075-4079.
41. **Hazelbauer GL, Falke JJ, Parkinson JS.** 2008. Bacterial chemoreceptors: high-performance signaling in networked arrays. Trends Biochem. Sci. **33:**9-19.
42. **Hazelbauer GL, Lai WC.** 2010. Bacterial chemoreceptors: providing enhanced features to two-component signaling. Curr. Opin. Microbiol. **13:**124-132.
43. **Galibert F, Finan TM, Long SR, Pühler A, Abola P, Ampe F, Barloy-Hubler F, Barnett MJ, Becker A, Boistard P, Bothe G, Boutry M, Bowser L, Buhrmester J, Cadieu E, Capela D, Chain P, Cowie A, Davis RW, Dreano S, Federspiel NA, Fisher RF, Gloux S, Godrie T, Goffeau A, Golding B, Gouzy J, Gurjal M, Hernandez-Lucas I, Hong A, Huizar L, Hyman RW, Jones T, Kahn D, Kahn ML, Kalman S, Keating DH, Kiss E, Komp C, Lelaure V, Masuy D, Palm C, Peck MC, Pohl TM, Portetelle D, Purnelle B, Ramsperger U, Surzycki R, Thebault P, Vandenbol M, Vorholter FJ, Weidner S, Wells DH, Wong K, Yeh KC, Batut J.** 2001. The composite genome of the legume symbiont *Sinorhizobium meliloti*. Science **293:**668-672.
44. **Meier VM, Scharf BE.** 2009. Cellular localization of predicted transmembrane and soluble chemoreceptors in *Sinorhizobium meliloti*. J. Bacteriol. **191:**5724-5733.
45. **Anantharaman V, Aravind L.** 2000. Cache - a signaling domain common to animal Ca(2^+)-channel subunits and a class of prokaryotic chemotaxis receptors. Trends Biochem. Sci. **25:**535-537.
46. **Ulrich LE, Zhulin IB.** 2005. Four-helix bundle: a ubiquitous sensory module in prokaryotic signal transduction. Bioinformatics **21 Suppl 3:**iii45-iii48.
47. **Taylor BL, Zhulin IB.** 1999. PAS domains: internal sensors of oxygen, redox potential, and light. Microbiol. Mol. Biol. Rev. **63:**479-506.
48. **Kamberger W.** 1979. An Ouchterlony double diffusion study on the interaction between legume lectins and rhizobial cell surface antigens. Arch. Microbiol. **121:**83-90.
49. **Bertani G.** 1951. Studies on lysogenesis. I. The mode of phage liberation by lysogenic *Escherichia coli*. J. Bacteriol. **62:**293-300.
50. **Platzer J, Sterr W, Hausmann M, Schmitt R.** 1997. Three genes of a motility operon and their role in flagellar rotary speed variation in *Rhizobium meliloti*. J. Bacteriol. **179:**6391-6399.
51. **Adler J.** 1973. A method for measuring chemotaxis and use of the method to determine optimum conditions for chemotaxis by *Escherichia coli*. J. Gen. Microbiol. **74:**77-91.
52. **Götz R, Schmitt R.** 1987. *Rhizobium meliloti* swims by unidirectional, intermittent rotation of right-handed flagellar helices. J. Bacteriol. **169:**3146-3150.
53. **Grimm AC, Harwood CS.** 1997. Chemotaxis of *Pseudomonas* spp. to the polyaromatic hydrocarbon naphthalene. Appl. Environ. Microbiol. **63:**4111-4115.
54. **Sourjik V, Sterr W, Platzer J, Bos I, Haslbeck M, Schmitt R.** 1998. Mapping of 41 chemotaxis, flagellar and motility genes to a single region of the *Sinorhizobium meliloti* chromosome. Gene **223:**283-290.
55. **Higuchi R.** 1989. Using PCR to engineer DNA, p. 61-70. *In* Erlich HA (ed.), PCR technology. Principles and applications for DNA amplification. Stockton Press, New York.

56. **Simon R, O'Connell M, Labes M, Pühler A.** 1986. Plasmid vectors for the genetic analysis and manipulation of rhizobia and other gram-negative bacteria. Methods Enzymol. **118:**640-659.
57. **Rotter C, Mühlbacher S, Salamon D, Schmitt R, Scharf B.** 2006. Rem, a new transcriptional activator of motility and chemotaxis in *Sinorhizobium meliloti*. J. Bacteriol. **188:**6932-6942.
58. **Ames P, Bergman K.** 1981. Competitive advantage provided by bacterial motility in the formation of nodules by *Rhizobium meliloti*. J. Bacteriol. **148:**728-908.
59. **Caetano-Anolles G, Wall LG, De Micheli AT, Macchi EM, Bauer WD, Favelukes G.** 1988. Role of Motility and Chemotaxis in Efficiency of Nodulation by *Rhizobium meliloti*. Plant Physiol. **86:**1228-1235.
60. **Ulrich LE, Zhulin IB.** 2009. The MiST2 database: a comprehensive genomics resource on microbial signal transduction. Nucleic Acids Res.
61. **Bateman A, Coin L, Durbin R, Finn RD, Hollich V, Griffiths-Jones S, Khanna A, Marshall M, Moxon S, Sonnhammer EL, Studholme DJ, Yeats C, Eddy SR.** 2004. The Pfam protein families database. Nucleic Acids Res. **32:**D138-141.
62. **Altschul SF, Madden TL, Schaffer AA, Zhang J, Zhang Z, Miller W, Lipman DJ.** 1997. Gapped BLAST and PSI-BLAST: a new generation of protein database search programs. Nucleic acids research **25:**3389-3402.
63. **Arnold K, Bordoli L, Kopp J, Schwede T.** 2006. The SWISS-MODEL workspace: a web-based environment for protein structure homology modelling. Bioinformatics **22:**195-201.
64. **Niesen FH, Berglund H, Vedadi M.** 2007. The use of differential scanning fluorimetry to detect ligand interactions that promote protein stability. Nat Protoc **2:**2212-2221.
65. **Glekas GD, Mulhern BJ, Kroc A, Duelfer KA, Lei V, Rao CV, Ordal GW.** 2012. The *Bacillus subtilis* chemoreceptor McpC senses multiple ligands using two discrete mechanisms. J. Biol. Chem. **287:**39412-39418.
66. **Nishiyama S, Suzuki D, Itoh Y, Suzuki K, Tajima H, Hyakutake A, Homma M, Butler-Wu SM, Camilli A, Kawagishi I.** 2012. Mlp24 (McpX) of *Vibrio cholerae* implicated in pathogenicity functions as a chemoreceptor for multiple amino acids. Infection and immunity **80:**3170-3178.
67. **Lacal J, Alfonso C, Liu X, Parales RE, Morel B, Conejero-Lara F, Rivas G, Duque E, Ramos JL, Krell T.** 2010. Identification of a chemoreceptor for tricarboxylic acid cycle intermediates: differential chemotactic response towards receptor ligands. J. Biol. Chem. **285:**23126-23136.
68. **Dakora FD, Joseph CM, Phillips DA.** 1993. Alfalfa (*Medicago sativa* L.) Root Exudates Contain Isoflavonoids in the Presence of *Rhizobium meliloti*. Plant Physiol. **101:**819-824.
69. **Lipton DS, Blanchar RW, Blevins DG.** 1987. Citrate, Malate, and Succinate Concentration in Exudates from P-Sufficient and P-Stressed *Medicago sativa* L. Seedlings. Plant Physiol. **85:**315-317.
70. **Moe LA.** 2013. Amino acids in the rhizosphere: from plants to microbes. Am. J. Bot. **100:**1692-1705.
71. **Csonka LN, Hanson AD.** 1991. Prokaryotic osmoregulation: genetics and physiology. Annu. Rev. Microbiol. **45:**569-606.
72. **Oku S, Komatsu A, Tajima T, Nakashimada Y, Kato J.** 2012. Identification of chemotaxis sensory proteins for amino acids in *Pseudomonas fluorescens* Pf0-1 and their involvement in chemotaxis to tomato root exudate and root colonization. Microbes Environ. **27:**462-469.
73. **Ponting CP, Aravind L.** 1997. PAS: a multifunctional domain family comes to light. Curr.

Biol. **7:**R674-677.
74. **Neumann S, Hansen CH, Wingreen NS, Sourjik V.** 2010. Differences in signalling by directly and indirectly binding ligands in bacterial chemotaxis. EMBO J **29:**3484-3495.
75. **Alexander RP, Zhulin IB.** 2007. Evolutionary genomics reveals conserved structural determinants of signaling and adaptation in microbial chemoreceptors. Proc. Natl. Acad. Sci. USA **104:**2885-2890.
76. **Wood DW, Setubal JC, Kaul R, Monks DE, Kitajima JP, Okura VK, Zhou Y, Chen L, Wood GE, Almeida NF, Jr., Woo L, Chen Y, Paulsen IT, Eisen JA, Karp PD, Bovee D, Sr., Chapman P, Clendenning J, Deatherage G, Gillet W, Grant C, Kutyavin T, Levy R, Li MJ, McClelland E, Palmieri A, Raymond C, Rouse G, Saenphimmachak C, Wu Z, Romero P, Gordon D, Zhang S, Yoo H, Tao Y, Biddle P, Jung M, Krespan W, Perry M, Gordon-Kamm B, Liao L, Kim S, Hendrick C, Zhao ZY, Dolan M, Chumley F, Tingey SV, Tomb JF, Gordon MP, Olson MV, Nester EW.** 2001. The genome of the natural genetic engineer *Agrobacterium tumefaciens* C58. Science **294:**2317-2323.
77. **Kaneko T, Nakamura Y, Sato S, Minamisawa K, Uchiumi T, Sasamoto S, Watanabe A, Idesawa K, Iriguchi M, Kawashima K, Kohara M, Matsumoto M, Shimpo S, Tsuruoka H, Wada T, Yamada M, Tabata S.** 2002. Complete genomic sequence of nitrogen-fixing symbiotic bacterium *Bradyrhizobium japonicum* USDA110. DNA Res. **9:**189-197.
78. **Hanahan D, Meselson M.** 1983. Plasmid screening at high colony density. Methods Enzymol. **100:**333-342.
79. **Pleier E, Schmitt R.** 1991. Expression of two *Rhizobium meliloti* flagellin genes and their contribution to the complex filament structure. J. Bacteriol. **173:**2077-2085.
80. **Chang AC, Cohen SN.** 1978. Construction and characterization of amplifiable multicopy DNA cloning vehicles derived from the P15A cryptic miniplasmid. J. Bacteriol. **134:**1141-1156.
81. **Kovach ME, Elzer PH, Hill DS, Robertson GT, Farris MA, Roop RM, 2nd, Peterson KM.** 1995. Four new derivatives of the broad-host-range cloning vector pBBR1MCS, carrying different antibiotic-resistance cassettes. Gene **166:**175-176.
82. **Schäfer A, Tauch A, Jager W, Kalinowski J, Thierbach G, Pühler A.** 1994. Small mobilizable multi-purpose cloning vectors derived from the *Escherichia coli* plasmids pK18 and pK19: selection of defined deletions in the chromosome of *Corynebacterium glutamicum*. Gene **145:**69-73.
83. **Bachmann BJ.** 1990. Linkage map of *Escherichia coli* K-12, edition 8 [published erratum appears in Microbiol Rev 1991 Mar;55(1):191]. Microbiol. Rev. **54:**130-197.
84. **Novick RP, Clowes RC, Cohen SN, Curtiss R, 3rd, Datta N, Falkow S.** 1976. Uniform nomenclature for bacterial plasmids: a proposal. Bacteriol. Rev. **40:**168-189.

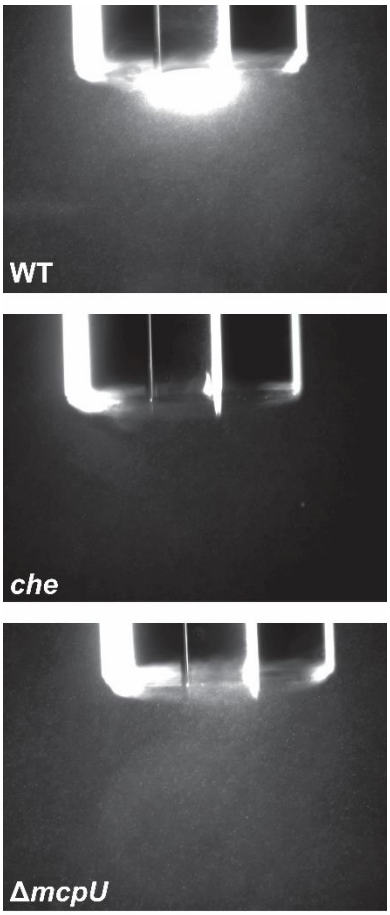

Fig 2.1 Chemotactic responses of *S. meliloti* wild type (WT, RU11/001), *mcpU* deletion (Δ*mcpU*, RU11/828) and *che* strain (RU13/149, Δ*mcpS*, Δ*mcpT*, Δ*mcpU*, Δ*mcpV*, Δ*mcpW*, Δ*mcpX*, Δ*mcpY*, Δ*mcpZ*, Δ*icpA* (Δ9)) towards alfalfa seed exudate. Strains from early log phase in RB were tested with agarose capillaries containing 0.15 mg/ml of alfalfa seed exudate in RB solidified with 1% agarose. Photographs were taken at 100x magnification under dark field microscopy after 10 min for wild type and 20 min for the *mcpU* and *che* strain, respectively.

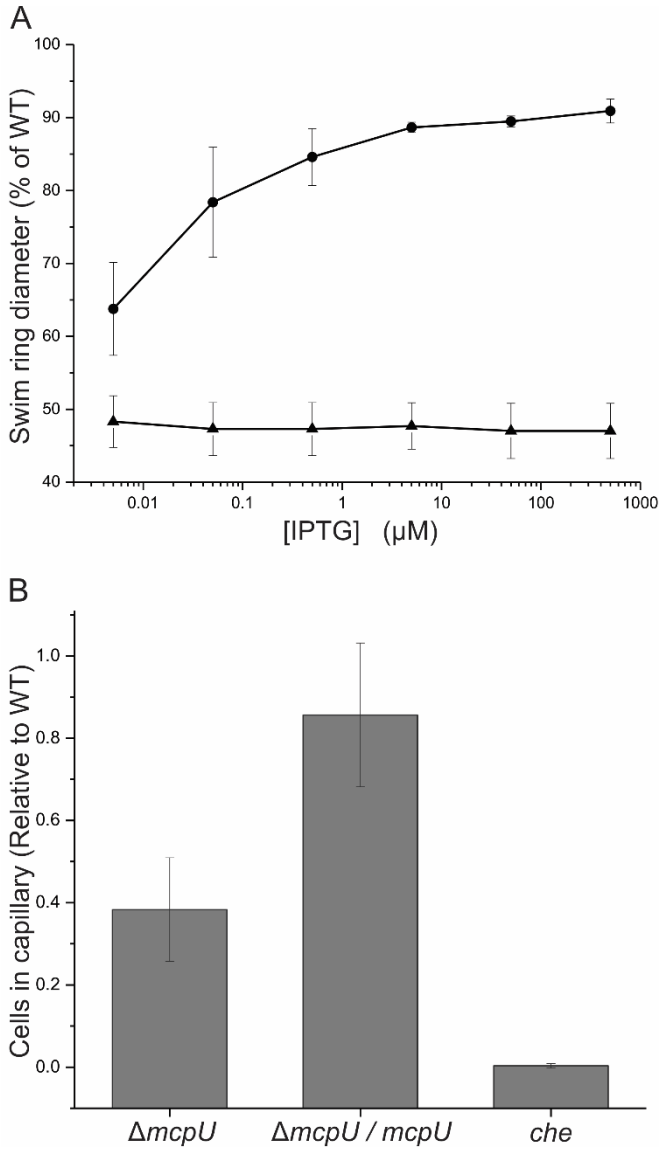

Fig 2.2 Complementation of the chemotactic response of the *S. meliloti* mcpU deletion strain to proline. **A.** Quantitative proline swim plate assay with increasing amounts of IPTG. Strains RU11/828 (▲-▲) and RU11/828 with pBS1053 (●-●) were pipetted onto RB plates containing 10^{-4} M proline with varying concentrations of IPTG to induce expression of *mcpU* under control of the *lac* promoter from plasmid pBS1053. Percentages of the wild-type swim diameter on 0.27% agar are the means of three replicates, each in duplicate. Error bars represent the standard deviation from the mean. **B.** Quantitative capillary assay of the *mcpU* deletion strain (Δ*mcpU*, RU11/828), the complemented strain (Δ*mcpU*/*mcpU*, RU11/828 with pBS1053) induced with 500 μM IPTG, and the chemotaxis negative strain (*che*, RU13/149) with 10 mM proline. Results for each strain are the means of three experiments, each in triplicate. The means of each strain were normalized to the number of wild-type cells per capillary. Error bars represent the standard deviation from the mean.

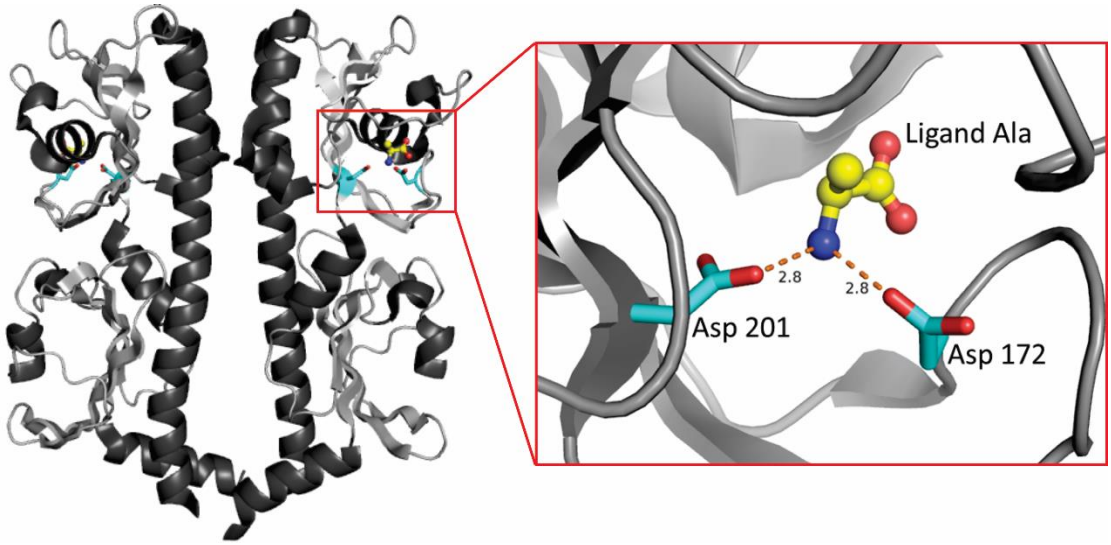

Fig 2.3 Identification of McpU residues involved in proline sensing using the structure of the *Vibrio cholerae* McpN as a model. The structure of the periplasmic amino-terminal domain of the McpN dimer (Protein data bank code 3C8C) is oriented to display the tandem Cache domains of *V. cholera* McpN. The view on the right provides a close up of the alanine ligand in the binding pocket of the N-terminal Cache domain on the monomer on the right. Two aspartate residues (Asp172 and Asp201) likely coordinate the ligand. The corresponding residues in *S. meliloti* McpU, Asp155 and Asp182, were chosen for further studies.

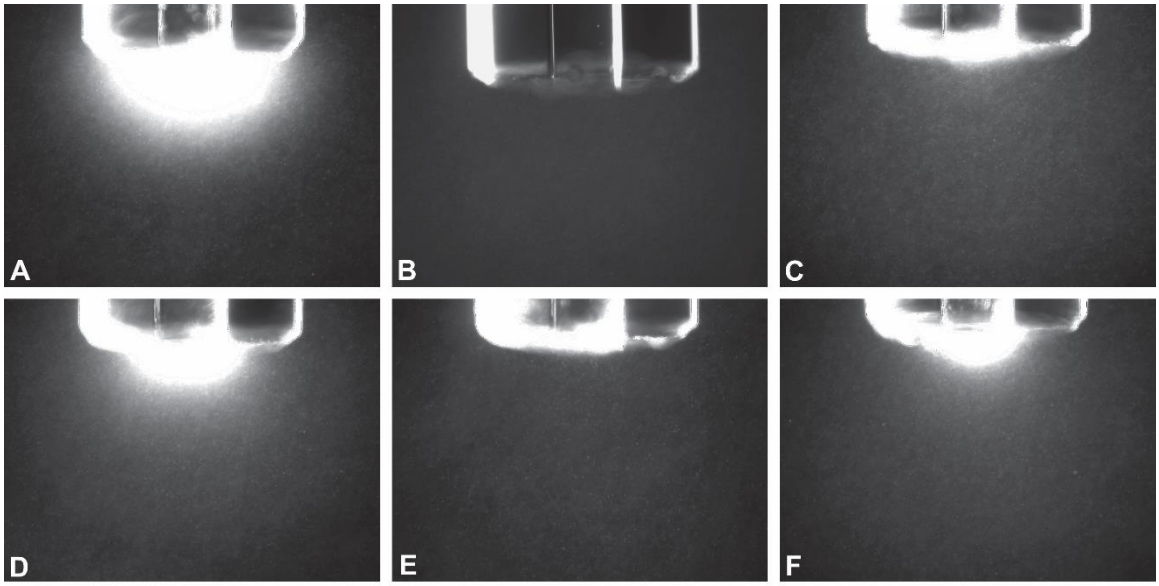

Fig 2.4 Chemotactic responses of *S. meliloti* mcpU mutant strains towards proline in hydrogel capillaries. A. wild type (RU11/001), **B.** *che* (RU13/149), **C.** Δ*mcpU* (RU11/828), **D.** McpU^{D155A} (BS184), **E.** McpU^{D182A} (BS182), **F.** McpU^{D182E} (BS187). Strains from early log phase in RB were tested with hydrogel capillaries containing 1 mM proline. Photographs were taken at 100x magnification under dark field microscopy after 20 min.

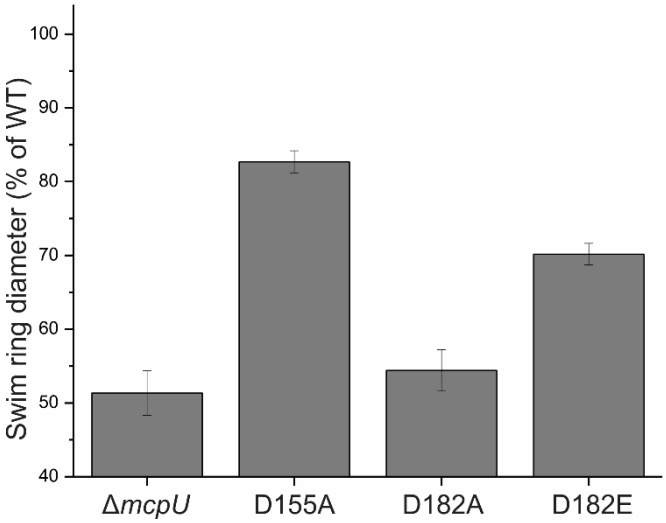

Fig 2.5 Chemotactic responses of S. meliloti mcpU mutant strains towards proline in a quantitative swim plate assay compared to the wild-type strain. The *mcpU* deletion strain (Δ*mcpU*, RU11/828), McpU^{D155A} (D155A, BS184), McpU^{D182A} (D182A, BS182), McpU^{D182E} (D182E, BS187) were pipetted onto RB plates containing 10^{-4} M proline. Percentages of the wild-type swim diameter on 0.27% agar are the means of three replicates, each in duplicate. Error bars represent the standard deviation from the mean.

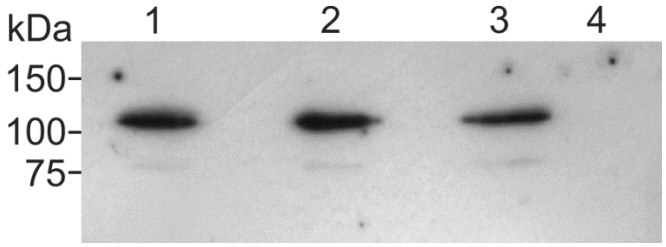

Fig 2.6 Immunoblot analysis of McpU and McpU-variant EGFP fusions in *S. meliloti* membrane fractions. *S. meliloti* cells were fractionated, and equal volumes of membrane fractions were electrophoretically separated, blotted on nitrocellulose and detected with anti-GFP monoclonal antibody. Lane 1, BS183 ($McpU^{D182A}$-EGFP), lane 2, RU13/301 (McpU-EGFP), lane 3, BS185 ($McpU^{D155A}$-EGFP), lane 4, RU11/001 (wt).

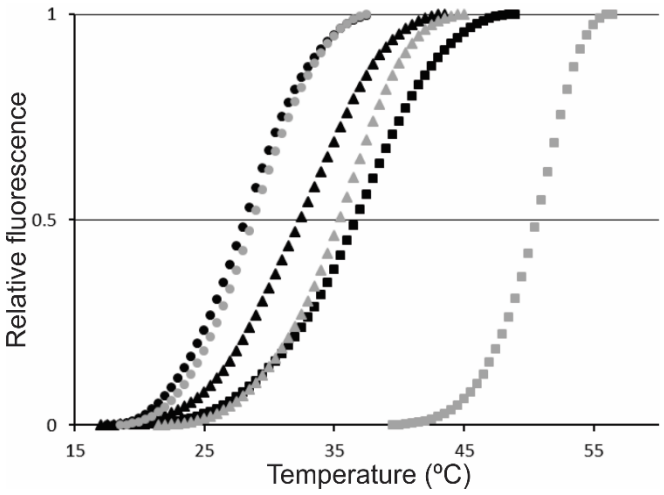

Fig 2.7 Differential scanning fluorimetry profiles for binding of proline to McpU-PR and McpU-PR variants. Protein stability was monitored as a function of fluorescence intensity. Proteins were tested at a concentration of 10 μM with or without 10 mM proline. McpU-PR (■), McpU-PR with proline (■), McpU-PR^{D182A} (●), McpU-PR^{D182A} with proline (●) McpU-PR^{D182E} (▲), and McpU-PR^{D182E} with proline (▲).

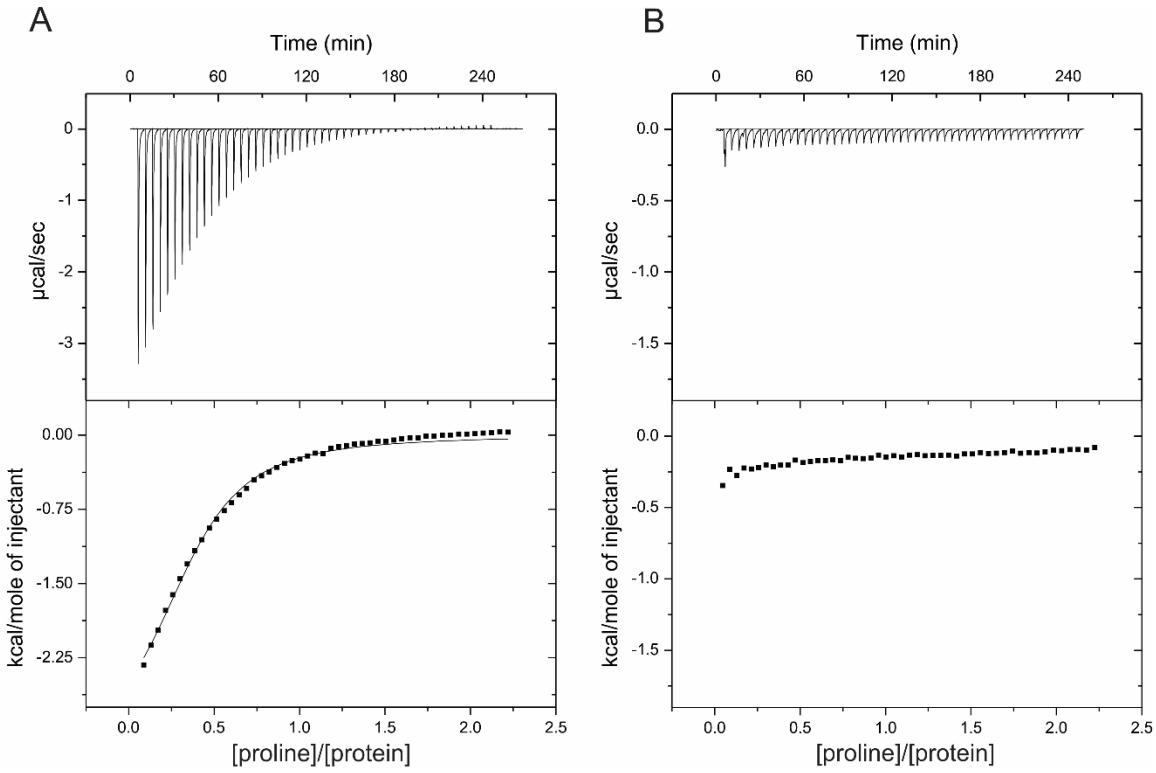

Fig 2.8 Isothermal titration calorimetry of McpU-PR and McpU-PRD182E with proline. Titration of **A.** McpU-PR and **B.** McpU-PR^{D182E} was carried out at a protein concentration of 812 µM with 10 µl injections of 9.8 mM proline. Reference data were produced by titrating buffer with proline and subtracting the resulting heat of ligand dilution from the experimental curves shown. Upper panels show the raw titration data and lower panels show the normalized and dilution corrected peak areas of the raw titration data. Data were fitted with the One-set-of-sites model of the MicroCal version of Origin7.

Table 2.1. Bacterial strains and plasmids

Strain/Plasmid	Relevant characteristics [a]	Source or Reference
Strain		
E. coli		
DH5α	*recA1 endA1*	(78)
M15/pREP4	Km^r; *lac ara gal mtl F recA uvr*	Qiagen
S17-1	*recA endA thi hsdR* RP4-2 Tc::Mu::Tn7 Tp^r Sm^r	(56)
S. meliloti		
BS182	Sm^r; *mcpU* with codon 182 changed from GAT to GCC (D182A)	This work
BS183	Sm^r; *mcpU*-EGFP gene with codon 182 changed from GAT to GCC (D182A)	This work
BS184	Sm^r; *mcpU* with codon 155 changed from GAC to GCC (D155A)	This work
BS185	Sm^r; *mcpU*-EGFP gene with codon 155 changed from GAC to GCC (D155A)	This work
BS187	Sm^r; *mcpU* with codon 182 changed from GAT to GAG (D182E)	This work
RU11/001	Sm^r; spontaneous streptomycin-resistant wild-type strain	(79)
RU11/828	Sm^r; Δ*mcpU*	(9)
RU13/149	Sm^r; Δ*mcpS,* Δ*mcpT,* Δ*mcpU,* Δ*mcpV,* Δ*mcpW,* Δ*mcpX,* Δ*mcpY,* Δ*mcpZ,* Δ*icpA* (Δ9)	(26)
RU13/285	Sm^r; Δ*mcpS,* Δ*mcpT,* Δ*mcpV,* Δ*mcpW,* Δ*mcpX,* Δ*mcpY,* Δ*mcpZ,* Δ*icpA* (Δ8); *mcpU* crossed-back into RU13/149	This work
RU13/301	Sm^r; *mcpU*-EGFP gene	(44)
Plasmid		
pACYC184	Cp^r, Tc^r; source of *lacI^q*	(80)
pBBR1-MCS2	Km^r	(81)
pBS189	Ap^r , *lacI^q* fragment from pBS189 cloned into the *Sac*I site of pBBR1-MCS2	This work
pBS373	Ap^r; 735 bp *Sph*I/*Hin*dIII PCR fragment containing *mcpU* 118-852 bps (aa 40-284) cloned into pQE30	This work
pBS383	Ap^r; 735 bp *Sph*I/*Hin*dIII PCR fragment containing *mcpU* 118-852 bps (aa 40-284) with *mcpU* codon 155 changed from GAC to GCC (D155A) cloned into pQE30	This work
pBS384	Ap^r; 735 bp *Sph*I/*Hin*dIII PCR fragment containing *mcpU* 118-852 bps (aa 40-284) with *mcpU* codon 182 changed from GAT to GCC (D182A) cloned into pQE30	This work
pBS390	Ap^r; 735 bp *Sph*I/*Hin*dIII PCR fragment containing *mcpU* 118-852 bps (aa 40-284) with *mcpU* codon 182 changed from GAT to GAG (D182E) cloned into pQE30	This work
pBS1053	2124 bp *Hin*dIII/*Xba*I PCR fragment containing *mcpU* cloned into pBS189	This work
pK18*mobsacB*	Km^r, *lacZ mob sacB*	(82)
pQE30	Ap^r; expression vector	Qiagen

[a] Nomenclature according to Bachmann (83) and Novick et al. (84).

Chapter 3 - Contribution of individual chemoreceptors to *Sinorhizobium meliloti* chemotaxis towards amino acids of host and non-host seed exudates

BENJAMIN A. WEBB[1], RICHARD F. HELM[2], AND BIRGIT E. SCHARF[1]*

[1]Virginia Tech, Department of Biological Sciences, Life Sciences I, Blacksburg, VA 24061;

[2]Virginia Tech, Department of Biochemistry, Life Sciences I, Blacksburg, VA 24061

Running title: Chemotaxis towards host and non-host seed exudates

Key words: flagellar motor, motility, rhizosphere, symbiosis, two-component system

* For correspondence:
E-mail bscharf@vt.edu
Tel (+1) 540 231 0757
Fax (+1) 540 231 4043
Biological Sciences, Life Sciences I
Virginia Tech
Blacksburg, VA 24061, USA

Mol Plant Microbe Interact. MPMI. 2016 Mar;29(3):231-9. doi: 10.1094/MPMI-12-15-0264-R. Accepted manuscript posted online 22nd of February 2016, doi: 10.1128/AEM.00115-14

Attribution: BAW has generated the data shown here in Fig. 3.1 - Fig. 3.7. BAW, RFH, and BES drafted the final manuscript.

ABSTRACT

Plant seeds and roots exude a spectrum of molecules into the soil that attract bacteria to the spermosphere and rhizosphere, respectively. The alfalfa symbiont *Sinorhizobium meliloti* utilizes eight chemoreceptors (McpT-Z, IcpA) to mediate chemotaxis. Using a modified hydrogel capillary chemotaxis assay that allows data quantification and larger throughput screening, we defined the role of *S. meliloti* chemoreceptors in sensing its host, *Medicago sativa*, and a closely related non-host, *Medicago arabica*. *S. meliloti* wild type and most single deletion strains displayed comparable chemotaxis responses to host or non-host seed exudate. However, while the *mcpZ* mutant responded like wild type to *M. sativa* exudate, its reaction to *M. arabica* exudate was reduced by 80%. Even though the amino acid amounts released by both plant species were similar, synthetic amino acid mixtures that matched exudate profiles contributed differentially to the *S. meliloti* wild-type response to *M. sativa* (23%) and *M. arabica* (37%) exudates, with McpU identified as the most important chemoreceptor for amino acids. Our results show that *S. meliloti* is equally attracted to host and non-host legumes; however, amino acids play a greater role in attraction to *M. arabica* than to *M. sativa*, with McpZ being specifically important in sensing *M. arabica*.

INTRODUCTION

The legume-rhizobia symbiosis is characterized by the infection of a legume root by rhizobia resulting in the formation of an organ called the nodule. Inside the nodule, rhizobia transform into bacteroids, which fix atmospheric nitrogen into a utilizable nitrogen source resulting in greater legume biomass. In return, the legume provides nutrients to the rhizobia. A key step in the initiation of nodulation is the rhizobial recognition of compatible host-legume secreted flavonoids followed by the legume recognition of compatible microsymbiont-borne Nod factors (Cooper, 2007; Hirsch et al., 2001; Jones et al., 2007; van Rhijn and Vanderleyden, 1995). The symbiotic partners have developed very specific means of molecular dialogue resulting in interactions that can be highly exclusive (Garau et al., 2005; Sprent, 2007). For example, the soil dwelling bacterium *Sinorhizobium meliloti* is hosted by the agriculturally important legume, *Medicago sativa* (alfalfa) (Jones et al., 2007) as well as *Melilotus alba* (white sweet clover) (Yan et al., 2000) and *Medicago truncatula* (barrel medic) (Terpolilli et al., 2008). However, the closely related *Medicago arabica* (spotted medic) cannot serve as a host for *S. meliloti* (Garau et al., 2005).

There are several steps prior to nodulation that contribute to propagation of the symbiosis including rhizobial chemotaxis, attachment mediated by Type IVb pili, exopolysaccharide synthesis and biofilm formation, and flavonoid-Nod factor recognition (Downie, 2010; Fujishige et al., 2006; González et al., 1996; Gulash et al., 1984; Kamberger, 1979; Rinaudi and González, 2009; Sorroche et al., 2010; Wang et al., 2012; Zatakia et al., 2014). Chemotaxis is one of the earliest steps in symbiosis, which enables rhizobia to respond to compounds released by host seed and roots and actively swim towards and accumulate in the spermosphere and rhizosphere (Ames and Bergman, 1981; Bergman et al., 1988; Caetano-Anolles et al., 1988b; Dharmatilake and Bauer, 1992; Malek, 1989; Soby and Bergman, 1983; Uren, 2000). This initial step has proven to be

important for successful symbiotic interactions in several rhizobia-legume partnerships including *S. meliloti* – alfalfa, *Rhizobium trifolii* – clover, and *Rhizobium leguminosarum* – pea (Ames and Bergman, 1981; Caetano-Anolles et al., 1988b; Mellor et al., 1987; Miller et al., 2007). Even more, a strain of *Bradyrhizobium japonicum* with enhanced chemotaxis had a greater nodulation efficiency than the wild type (Althabegoiti et al., 2008b).

A germinating seed exudes a multitude of compounds into the soil creating a spermosphere that is unique to that species and even to that seed (Miller and Oldroyd, 2012; Nelson, 2004). The molecular composition of seed exudate includes amino acids, sugars, lipids, phenolics, proteins, and other metabolites (Barbour et al., 1991; Nelson, 2004; Webb et al., 2014). Chemotaxis to their host seed exudates has been shown for *S. meliloti*, *B. japonicum*, and *R. leguminosarum* (Barbour et al., 1991; Gaworzewska and Carlile, 1982; Webb et al., 2014), but knowledge of the compounds responsible is mostly lacking. A more comprehensive study of the attractants exuded by alfalfa seeds and the corresponding *S. meliloti* chemoreceptors is required for the development of strains with enhanced chemotaxis towards the host.

Previous work has characterized particular aspects of the *S. meliloti* chemotaxis system regarding the number and domain topology of chemoreceptors (Meier et al., 2007), chemoreceptor-ligand specificity (Meier et al., 2007; Webb et al., 2014), the two-component regulatory components (Amin et al., 2014; Dogra et al., 2012; Riepl et al., 2004; Sourjik and Schmitt, 1998), and the unidirectional, speed-variable flagellar motor (Attmannspacher et al., 2005; Eggenhofer et al., 2004; Platzer et al., 1997; Sourjik and Schmitt, 1996). *S. meliloti* has eight genes coding for putative chemoreceptors called methyl-accepting chemotaxis proteins (McpS-Z) and one internal chemotaxis protein (IcpA) lacking typical methyl-accepting sites (Galibert et al., 2001; Meier et al., 2007). McpS, encoded from a second chemotaxis operon on the pSymA plasmid, is not

expressed when cells are motile, and a contribution to chemotaxis can be excluded (Meier et al., 2007; Meier and Scharf, 2009). The eight chemoreceptors contributing to chemotaxis share a highly conserved, C-terminal signaling domain, which forms a ternary complex with two cytoplasmic chemotaxis proteins, CheA, an autohistidine kinase, and CheW, an adaptor protein. In the absence of an attractant, CheA is autophosphorylated and subsequently transfers the phosphoryl group to the response regulator protein, CheY2, which interacts with the cytoplasmic face of the flagellar motor and controls the swimming paths of bacteria (Scharf, 2002; Sourjik and Schmitt, 1996). Seven of the *S. meliloti* MCPs possess two transmembrane regions and a periplasmic region harboring the ligand-binding domain located between the transmembrane helices. In contrast, McpY and IcpA lack such hydrophobic regions and thus exhibit a cytosolic localization (Meier et al., 2007). All the chemoreceptors vary in their ligand-binding domains, however, McpU, McpV, and McpX share specialized domains such as Cache_1 and Cache_2 signaling domains (Meier et al., 2007), which are known to bind small molecules, such as amino acids (Anantharaman and Aravind, 2000; Ulrich and Zhulin, 2005). McpY possesses a PAS domain, which typically senses redox potential, oxygen, or light (Taylor and Zhulin, 1999). Deletion of individual receptor genes causes differential impairments in the chemotactic response towards a variety of small biomolecules tested, including various sugars, five amino acids, and four organic acids (Meier et al., 2007), but a more complete study is needed to establish their significance in host sensing.

While *S. meliloti* chemotaxis mutants are less competitive in inducing nodule formation with alfalfa (Ames and Bergman, 1981; Caetano-Anolles et al., 1988b), little is known about the specific role of individual chemoreceptors in chemotactic host recognition. To date, only McpU has been characterized in playing a significant role in host plant recognition by mediating

chemotaxis to host-derived proline (Webb et al., 2014). To identify *S. meliloti* chemoreceptors important for host sensing, quantitative chemotaxis assays of wild type and single receptor deletion strains were performed with *M. sativa* seed exudate. In comparison, the seed exudate of the closely related non-host, *M. arabica*, was tested to identify differential responses of mutant strains, and concomitantly, differences in exudate attractant composition. Since amino acids are relatively strong attractants for *S. meliloti* (Götz et al., 1982; Meier et al., 2007), we also analyzed the amino acid profiles of host and non-host exudates, their contribution to chemotaxis, and the involvement of individual chemoreceptors in amino acid sensing.

RESULTS

A modified agarose capillary assay with automated data acquisition and quantification

The classic Adler capillary assay allows for the direct quantitative measurement of the response of a population of cells to an attractant or repellent gradient (Adler, 1973). However, when several variables are to be tested, such as multiple strains and/or attractants, this method can become tedious and time consuming. In addition, reproducible removal of the capillary contents can be difficult (Sampedro et al., 2014). The modified agarose or hydrogel capillary assays ease the assessment of chemotaxis, but the results are purely qualitative (Parales and Harwood, 2002; Webb et al., 2014). To avoid disadvantages of the classic capillary assay but still generate quantitative data, we combined the simplicity of the modified hydrogel capillary assay with a quantifiable measure of the chemotactic response at the mouths of the capillaries.

Fig. 3.1A illustrates the setup of the chemotaxis chambers on a microscope slide. The dimensions of the setup allow for testing of up to ten different variables such as strains and attractants, or repetitions. Once the slide is set on the microscope stage, it is important to utilize a motorized focusing drive with software that allows for memorization of the x-, y-, and z-coordinates for each capillary. Fig. 3.1B illustrates the pipeline for image acquisition and analysis for one chemotaxis chamber (for more details, refer to the Materials and Methods section). The combination of the hydrogel capillary assay, motorized focusing drive, and image analysis software enabled quantitative time-course assessments of the chemotactic response, providing detailed comparative information on multiple experimental variables.

Chemotaxis of *S. meliloti* wild type toward seed exudate of *M. sativa* and *M. arabica*

To assess the potencies of germinating seed exudates from *M. sativa* (host) and *M. arabica* (non-

host), the *S. meliloti* wild-type strain RU11/001 was tested with the hydrogel capillary assay for its ability to sense either exudate. In this assay, capillaries contained a hydrogel that was equilibrated with seed exudate. This format allowed efflux of liquid material, but prevented cells from swimming into the capillary, thus cells that were attracted to the exudate accumulated at the mouth of the capillary. A control experiment was performed to rule out a chemotactic response of *S. meliloti* to Rhizobial Basal medium (RB) used to dissolve the exudate. Comparatively, wild type and the *che* strain, which lacks all chemoreceptor genes, exhibited no response to RB, whereas wild type displayed a strong response to *M. sativa* exudate, which is abolished for the *che* strain (Fig. 3.2A). For quantitative analyses, photographs were taken at the mouth of the capillary every four minutes under a pseudo dark field, the pixel intensity in front of the capillaries was quantified using the Time Series Analyzer V3 plug-in of the ImageJ software (Balaji, 2014), and the intensities were normalized to the greatest intensity observed from the wild type. In this assay, pixel intensity positively correlates with the amount of cells present and thus with strength of the chemotactic response. To determine the optimal exudate concentration for optical observation and pixel intensity quantification, a dose response assay was performed (data not shown). During the first 12 min, the wild type appeared to show a slightly greater response to the *M. arabica* exudate. However, after 12 min the response to either exudate did not differ from each other (Fig. 3.2B). The responses plateaued between 20 and 34 min before declining. It should be noted that the plateau in the response is purely physiological, because pixel intensities did not reach a level of saturation in the images. Upon microscopic examination, it was observed that the declination in response after 34 min was due to the dissemination of cells away from the capillary. This is most likely due to depletion of the attractants from the capillary into the bacterial pond. Taken together, these results support the claim that the chemotactic potencies of *M. arabica* and *M. sativa* seed

exudate are relatively equal.

Chemotaxis of single *S. meliloti* chemoreceptor deletion strains to *M. sativa* and *M. arabica* seed exudates

To elucidate the importance of each chemoreceptor in *M. sativa* and *M. arabica* exudate sensing, eight single deletion strains were assessed for their maximum chemotactic response using the hydrogel capillary assay. The wild type exhibited a maximum response to exudate of *M. sativa* and *M. arabica* between 20 and 34 min (Fig. 3.2B); therefore, the pixel intensities of the mutant images pertaining to this time period were averaged and normalized to the greatest average intensity observed for the wild type for the same time period (Fig. 3.3). McpT, U, V, Y, and IcpA appeared to contribute similarly to the chemotaxis response toward either legume exudate. A strain lacking *mcpU* showed the most diminished response toward *M. sativa* and *M. arabica* legume exudates with reductions to 35% and 20% of the wild-type response, respectively. Strains lacking *mcpW* and *mcpX* displayed significant reductions in response to the exudate of *M. sativa* and *M. arabica*, respectively. Interestingly, the strain lacking *mcpZ* displayed a pronounced differential response toward the two legume exudates. While this strain responded like wild type to the *M. sativa* exudate, its reaction to the *M. arabica* exudate was reduced by 80%. The results indicate that the attractant compositions of the two legume exudates are different, and that *S. meliloti* senses an altered, but presumably overlapping attractant spectrum in *M. sativa* and *M. arabica* exudates.

Chemotaxis of *S. meliloti* toward *M. sativa* and *M. arabica* seed exudates and synthetic amino acid mixtures

S. meliloti is able to utilize each proteinogenic amino acid (AA) for growth and displays positive chemotaxis of varied strengths to all of them (Burg et al., 1982; Götz et al., 1982; Jordan, 1952;

Malek, 1989). Therefore, we first analyzed the AA composition of *M. sativa* and *M. arabica* seed exudates to investigate their contribution to host sensing. Exudates from surface sterilized and germinated seeds of *M. sativa* and *M. arabica* were quantified with LC-MS in conjunction with authentic AA standards. The amounts of each AA exuded by one seed was determined and the concentration of these AAs at the seed surface was calculated using the average *M. sativa* and *M. arabica* seed volumes of 2.17 μl and 1.84 μl, respectively. Fig. 3.4 gives a comparison of the concentration of each AA on the seed surface of *M. sativa* or *M. arabica*. Since both legume species are closely related, there appears to be no striking differences between the amounts of each AA exuded. It should be noted that the concentration of each AA is within range of eliciting a chemotactic response, thus making the individual amounts exuded relevant for attraction of *S. meliloti* to the spermosphere, and therefore for symbiosis with *M. sativa*. Since chemotaxis has been observed for the non-proteinogenic AA, ornithine, citrulline, and cystine (data not shown), their analysis was included in this study.

To assess the chemotactic contribution of the AA fraction in the exudate (proteinogenic AAs plus cystine, ornithine, and citrulline), synthetic AA mixtures were created mimicking the exact quantities detected in the seed exudates of *M. sativa* and *M. arabica*, and the wild-type responses to the exudates were compared to the responses to their respective synthetic AA mixture. Here, responses to *M. sativa* exudate and the *M. sativa* synthetic AA mixture were normalized to the highest response observed to the exudate. The same normalization procedure was done for the *M. arabica* exudate and synthetic AA mixture. In both cases, the wild-type response toward the exudate is greater than it is toward the respective synthetic AA mixture (Fig. 3.5A and 3.5B). By adding up the normalized response values for each data set, we determined that the wild-type response to the *M. sativa* and *M. arabica* synthetic AA mixtures is 23% and 37% of its response

to the corresponding exudates, respectively. In conclusion, AA have a greater contribution to non-host than to host exudate chemotaxis, indicating that host sensing is mediated by additional attractants other than measured AAs.

Chemotaxis of single *S. meliloti* chemoreceptor deletion strains to synthetic amino acid mixture mimicking *M. sativa* exudate composition

To determine the chemotactic contribution of individual chemoreceptors toward the synthetic AA mixture of the *S. meliloti* host, *M. sativa*, the single receptor deletion strains were assessed for their maximum chemotactic response using the hydrogel capillary assay and responses were quantified in Fig. 3.6. All deletion strains but Δ*mcpY* exhibited a decreased response, although this reduction was not statistically significant for Δ*mcpT*, Δ*mcpV*, Δ*mcpW*, and Δ*mcpZ*. The single deletion strains Δ*mcpX* and Δ*icpA* displayed significantly reduced responses of approximately 35% and 40%, respectively, whereas a strain lacking *mcpY* exhibited a significantly increased response. Most interestingly, a strain lacking *mcpU* showed the largest reduction compared to wild type, namely a 90% decrease. This result may indicate that McpU is not only a receptor for proline, as previously shown (Webb et al., 2014), but proposes a function as a general AA sensor. The intermediate response levels of strains lacking *mcpT*, *mcpV*, *mcpW*, *mcpX*, and *icpA* suggests that these chemoreceptors also play a role in AA sensing.

Chemotaxis to synthetic amino acid mixtures with and without proline

To determine if McpU is important for chemotaxis to AAs other than proline, the chemotactic responses of the wild type and the Δ*mcpU* strain to the synthetic AA mixture were compared to their responses to a synthetic AA mixture lacking proline. When exposed to the synthetic mixture with proline, as expected, the Δ*mcpU* strain exhibited a reduced response compared to the wild

type (Fig. 3.7A and 3.7C); however, there appeared to be no difference in the responses to the synthetic mixtures without proline (Fig.3.7B and 3.7D). This result implies that McpU senses amino acids other than proline and is likely a general amino acid sensor.

DISCUSSION

S. meliloti uses chemotaxis to direct its movements toward host seed and root exuded attractants (Dharmatilake and Bauer, 1992; Malek, 1989). This early host-microbe interaction is important for increasing nodulation efficiency, because it allows the bacterial cells to effectively locate infection sites and compete for nodulation (Ames and Bergman, 1981; Gulash et al., 1984). Germinating alfalfa seeds release compounds that attract *S. meliloti*, which can be viewed as an early recruitment phase of the microsymbiont to the spermosphere. The initial recruitment and establishment of a positional advantage on the roots may be attained by attractants with a longer diffusion range such as hydrophilic amino acids, organic acids, sugars, and sugar alcohols (Ma et al., 2005), whereas hydrophobic substances such as phenolic compounds might only have short range effects (King and Srinivas, 2011). In fact, organic metabolites have been reported to be effective chemoattractants for *S. meliloti* (Burg et al., 1982; Götz et al., 1982; Meier et al., 2007; Robinson and Bauer, 1993), while flavonoids, although proposed as host-specific attractants, elicit a rather small chemotactic response (Caetano-Anolles et al., 1988a; Dharmatilake and Bauer, 1992). Since chemical compounds are commonly exuded by many plant species during germination, comparing the attractant profile of *S. meliloti* host and non-host legumes can lead to a better understanding of the initial stages of symbiont recruitment.

We observed no obvious difference in the strength or time course of attraction of *S. meliloti* wild type to seed exudate of the host, *M. sativa*, and the closely related non-host, *M. arabica*, in the

hydrogel capillary assay (Fig. 3.2B). This may be simply due to the high phylogenetic proximity of the two medics; however, the specific molecular composition of host and non-host exudates is unknown. Therefore, we cannot conclude that (i) the attractant spectrum is the same for both exudates, and (ii) *S. meliloti* will accumulate equally well in host and non-host spermosphere and rhizosphere. To address the first point, a detailed analysis of the secretome and attractome of host versus non-host exudate is required. The second idea can be challenged by analyzing preferential accumulation of *S. meliloti* in a microfluidic device with competing host and non-host exudates (Sahari et al., 2014).

When we analyzed the chemotaxis response of single receptor deletion strains to both exudates, certain parallels and differences emerged. McpU and IcpA appeared to be most important for general exudate sensing, followed by McpV, W, X, and Y (Fig. 3.3). While the role of McpU in proline (Webb et al., 2014) and general amino acid sensing (Fig. 3.6) has been uncovered, little is known about the ligand spectrum of the remaining receptors (Meier et al., 2007). In particular, a function of the cytosolic IcpA in sensing the metabolic state of the cell has been discussed (Meier et al., 2007). Most interestingly, McpZ plays no role in host sensing, but is equally important as McpU for non-host sensing (Fig. 3.3). Thus, the attractants sensed by McpZ are absent in the host exudate, which is a clear indication that the attractant profiles of both exudates differ. In conclusion, *S. meliloti* senses a divergent, but most likely overlapping attractant spectrum in *M. sativa* and *M. arabica* exudates.

Amino acids are documented as potent attractants (Burg et al., 1982; Götz et al., 1982), and our previous work revealed McpU as proline sensor (Webb et al., 2014). The present study identified McpU as the most important receptor for host sensing (Fig. 3.3). Therefore, we quantified each proteinogenic amino acid (AA), citrulline, cystine, and ornithine in the host and non-host seed

exudates, determining their millimolar concentrations per seed to classify their abundances in the spermosphere. Götz *et al.* specified the chemotactic thresholds for each proteinogenic AA ranging from 10^{-6} M (proline) to 10^{-4} M (aspartate) (Götz et al., 1982). Thus, single seeds from both medics exude chemotactically relevant amounts of most proteinogenic AAs. The AA profiles appear very similar between the two medics, although with slightly higher amounts exuded by *M. arabica* (Fig. 3.4). The only significant difference between the two profiles is the concentration of alanine, which is approximately 40% higher in *M. arabica* exudate. While this difference is small, it could still be influential on the scale of chemotactic strength.

Using the hydrogel capillary assay, we observed the wild-type response to the *M. sativa* and *M. arabica* synthetic AA mixtures to be 23% and 37% of the respective exudates (Fig. 3.5), suggesting that non-amino acid attractants contribute significantly more to the chemotactic response than amino acids. Potential attractants based upon the metabolomes of *Medicago* seeds include non-reducing oligosaccharides, phenolics as well as betaines (Horbowicz et al., 1995; Phillips et al., 1995). Due to the presence of these compounds in the exudate, it is conceivable that they modulate chemotaxis to AAs. Thus, reported contributions of the AAs based upon synthetic mixtures may not directly correlate to AA-based chemotaxis in exudate samples. Studies are currently under way to identify the remaining attractants and characterize differences in the attractant profile between host and non-host secretomes. The majority of the single deletion strains exhibited a reduced response to the synthetic *M. sativa* AA mixture, inferring that most receptors, directly or indirectly, play a role in AA sensing. Clearly, this study revealed that the proline receptor McpU also senses other AAs (Figs. 3.6 and 3.7). McpU binds proline in its amino-proximal Cache domain (Webb et al., 2014), and it remains to be shown whether the same holds true for other AAs.

Identifying environmentally relevant chemotaxis signals in soil bacteria, in particular plant

symbionts, and matching them to respective chemoreceptors is a difficult task, due to the complex composition of the rhizosphere. Additionally, bacterial chemoreceptors are known to sense chemically diverse ligands through two different mechanisms; via direct binding to the periplasmic region or indirectly involving specialized periplasmic binding proteins. As an example, the *E. coli* chemoreceptor Tar mediates positive chemotaxis to aspartate through direct binding and senses maltose through binding of maltose-bound maltose binding protein (Kossmann et al., 1988). McpU appears to be the most important chemoreceptor for host sensing, and it remains to be seen whether it is mediating chemotaxis to attractants other than AAs. Furthermore, the attractant profiles of the remaining seven *S. meliloti* chemoreceptors need to be identified to understand their role in host sensing. With this knowledge, a promising avenue for enhancement of *S. meliloti* chemotaxis toward its host would be opened. This goal could be attained by (i) increased expression of receptors dedicated to host sensing; (ii) genetic tuning of receptors to induce a greater positive chemotactic response towards host-specific exuded attractants; and (iii) increased exudation of host-borne attractants. Fine-tuning the chemotaxis process could assist in microsymbiont positioning early during rhizosphere formation, resulting in a greater recruitment of *S. meliloti* to the plant host and thus greater crop yields.

MATERIALS AND METHODS

Bacterial strains and plasmids

Derivatives of *S. meliloti* MV II-1 (Kamberger, 1979) used are listed in Table 1.

Media and growth conditions

(Bertani, 1951) *S. meliloti* strains were grown in TYC (0.5% (w/v) tryptone, 0.3% (w/v) yeast extract, 0.13% $CaCl_2$ x 6 H_2O (w/v) [pH 7.0], streptomycin (600 μg/ml.)) at 30°C (Platzer et al., 1997). Motile cells for hydrogel capillary assays were grown for two days in TYC, diluted 1:1000 in 3 ml TYC and grown overnight. Cultures were then diluted 1:100 in 10 ml Rhizobial Basal minimal medium (RB) (6.1 mM K_2HPO_4, 3.9 mM KH_2PO_4, 1 mM $MgSO_4$, 1 mM $(NH_4)_2SO_4$, 0.1 mM $CaCl_2$, 0.1 mM NaCl, 0.01 mM Na_2MoO_4, 0.001 mM $FeSO_4$, 20 μg/l biotin, 100 μg/l thiamine (Götz et al., 1982)), layered on Bromfield agar plates with no antibiotics (Sourjik and Schmitt, 1996), and incubated at 30°C for approximately 15 h to an optical density at 600 nm (OD_{600}) of 0.17 ± 0.02.

Preparation of seed exudates

The *Medicago sativa* cultivar 'Guardsman II' (Registration number CV-203, PI 639220), used in this study was developed from the extensively studied cultivar 'Iroquois' by the Cornell University Agricultural Experiment Station, New York State College of Agriculture and Life Sciences, Cornell University, Ithaca, NY (Althabegoiti et al., 2008a). Seeds were harvested in 2012 and stored at 4 °C prior to experiments. *Medicago arabica* (L.) Huds. (accession SA7746) from a wild population in Siena, Italy in 2008, was cultivated *ex situ* in Lodi, Italy in 2010, and seeds were harvested and stored at 4 °C prior to experiments. Seeds (0.1 g, approximately 47 ± 1 *M. sativa*

seeds and 49 ± 1 *M. arabica* seeds) were placed in a 50-ml conical tube and washed four times with 35 ml of autoclaved, sterile-filtered water. Next, seeds were washed once with 8 ml of commercial hydrogen peroxide (3% in water) for 12 min and then four times with 35 ml of autoclaved, sterile filtered water under slow agitation. Seeds were then transferred to a 125-ml Erlenmeyer flask containing 20 ml of autoclaved, sterile-filtered water. Seeds were jostled to distribute them evenly at the bottom of the flask and germinated without shaking at 30 °C for 24 h. To harvest the exudate, the contents were mixed by swirling, a 19-ml aliquot of seed supernatant was removed from the flask, placed into a 50-ml conical tube and flash frozen in liquid nitrogen. The frozen sample was freeze-dried for approximately 48 h and stored at -20 °C. Prior to flash freezing, seed exudates were tested for bacterial contamination by microscopic examination and by plating on TYC plates and observation of colony forming units after incubation at 30 °C for 48 h. Contaminated samples were not included in this study. Seed exudate powders were resuspended to a volume less than the original volume in the flask, thus concentrating the contents to 50x. Aliquots were stored at -30°C and prior to a chemotaxis assay, they were thawed and then diluted in RB to working concentrations. Post incubation, the germination efficiency was approximately 90-95% for both Medics as determined by radicle emergence. Seed exudate powders were resuspended to a 50x smaller volume than the original volume in the flask, thus concentrating the contents. Aliquots were stored at -30°C, thawed prior to a chemotaxis assay, and then diluted in RB to working concentrations.

Quantification of amino acids (AA) in M. arabica and M. sativa seed exudates by liquid chromatography mass spectrometry (LC-MS)

For each Medic, seed exudate residue from six biological replicates was thawed to room

temperature, suspended in 250 µl of RB and sonicated for 10 min. The samples were centrifuged at 4,000 x g for 10 min to pellet insoluble material. The six biological replicates were combined in pairs yielding three biological replicates consisting of 500 µl per combined sample. The samples were briefly vortexed and split into 120 µl aliquots to be used for either amino acids (AA) quantification or chemotaxis experiments. Aliquots were stored at -20 °C prior to use. Aliquots were thawed on ice, briefly vortexed, sonicated for 5 min, centrifuged at 14,000 x g for 5 min to pellet any remaining insoluble material, and transferred to microfuge tubes that had been previously rinsed with 100% ethanol. Exudate samples were diluted 1:1, 1:3, 1:5, and 1:7 in RB, titrated to pH 3.5 with HCl, and 100 µL of material per sample was processed using the "EZ:faast® for Free Physiological Amino Acid Analysis by LC-MS" as previously described (Webb et al., 2014). Amino acid standard solutions ranging from 55 to 220 nmoles/ml made from the Phenomenex® kit (Sigma-Aldrich, St. Louis, MO) were derivatized alongside the exudate samples to establish a calibration curve for each amino acid. Using Analyst software (AB Sciex, Concord, Ontario, Canada) for data analysis, the peak area of the internal standard homoarginine was used to normalize the concentration of the amino acids Ala, Arg, Asn, Asp, Cit, Gln, Glu, Gly, His, Lys, Met, Orn, Pro, Ser, Thr, Trp, and the peak area of the internal standard homophenylalanine was used to normalize Ile, Leu, Phe, cystine (C-C), and Tyr. The Phenomenex kit does not allow for quantification of cysteine. Results are given as the average concentration derived from three biological replicates, with two to four technical replicates, and duplicate injections per technical replicate.

Creation of synthetic amino acid mixtures

Synthetic mixtures were made with amino acids from the Fluka Analytical kit, "21 L-Amino acids

+ glycine" (lot number 09416) which were dissolved in RB to 50x the concentrations observed in seed exudates, aliquoted, and stored at -30 °C until ready for experiments.

Preparation of hydrogel capillaries

Capillaries containing a cross-linked hydrogel were essentially prepared according to Webb *et al*., 2014 with minor modifications (Webb et al., 2014). Briefly, capillaries (0.5 µl Drummond Microcaps) were sealed at one end in a Bunsen burner flame and the inner glass surface was hydroxylated by placing the mouth of the capillaries into a 1% (v/v) solution of 3-(trichlorosilyl) propyl methacrylate (TPM) (Sigma-Aldrich, St. Louis, MO) diluted in paraffin oil at room temperature for 10 min. After excess TPM was removed via desiccation, the capillaries were submerged in 100% ethanol and put under desiccation for approximately 30 seconds. Ethanol was removed via desiccation and capillaries were wiped with a micro-fiber cloth to remove any residual material. Capillaries were then quickly passed once through a Bunsen burner flame. A 10% (w/v) solution of poly(ethylene glycol) diacrylate (PEG-DA) with an average M_n of 6,000 (Sigma-Aldrich, St. Louis, MO) in phosphate buffered saline, pH 7.4 was mixed with 10% (w/v) Irgacure®2959 (Sigma-Aldrich) in 70% ethanol at a ratio of 1:20 to form the precursor solution, which was subsequently pulled into the capillaries by placing them under vacuum for approximately 30 seconds. The mouths of the capillaries were submersed in the precursor solution, and photopolymerization was performed for 20 seconds using a 365 nm, 18 W cm^{-2} UV light source (Omnicure S1000, Vanier, Quebec). Hydrogel capillaries were observed under 100x magnification to check for hydrogel integrity. If any hydrogel extended from the mouth of the capillary, the mouth was gently scraped with a wet Kimwipe and re-checked for hydrogel integrity. Only capillaries with a flush surface at the mouth were used for experiments. Hydrogel capillaries

were washed with distilled water and then soaked in distilled water with 1 μg/ml ampicillin, 1 μg/ml kanamycin, 1 ug/ml neomycin, and 1 μg/ml gentamicin for at least 4 h at room temperature, followed by three subsequent washes with the same solution. Hydrogel capillaries could be stored in distilled water with antibiotics at 4 °C for at least two months.

Hydrogel capillary assay

Prior to experiments, hydrogel capillaries were washed and equilibrated for four hours twice with RB. Amino acid mixtures and seed exudates suspended in RB were thawed to room temperature, briefly vortexed, centrifuged at 13 x g for three minutes and diluted to working concentrations in RB. For experiments including only seed exudates, the solutions were tested at 5x concentration. For experiments including seed exudates and amino acid mixtures, the solutions were tested at 7.6x concentration. For experiments with only the amino acid mixtures, the solutions were tested at 7.6x concentration. For equilibration of the capillaries with attractant, capillaries were placed into 50 μl of attractant solution per capillary and left overnight at 4 °C. Cells were harvested by centrifugation at 4,000 x g for 5 min at room temperature, suspended with RB to an OD_{600} of 0.12 and 81 μl of each strain suspension was added to a circular chemotaxis chamber formed by a microscope slide (100 mm x 50 mm), a cut rubber O-ring with an inner diameter of 8.5 mm and a thickness of 1 mm (Sarstedt), and a coverslip. The open end of a hydrogel capillary was inserted into the chemotaxis chamber before the coverslip was placed on top. After the assembly of ten such chambers (Fig. 3.1A), the microscope slide was placed on the computer-assisted stage of a Zeiss Axio Observer Research microscope. By programming the Zen software module, the X, Y, and Z positions of all ten chambers were observed at 25x magnification under pseudo dark field and images were taken with a 1.3 millisecond exposure every two minutes.

Quantification of chemotaxis responses

Images from the hydrogel capillary assay were imported to GIMP 2.0 Image Manipulation Program (The GIMP Team) and adjusted by rotation to align the capillaries in such a way that the capillaries rest precisely on top of one another when images were stacked. Rotated images were then imported to ImageJ (Rasband) as an image sequence and the Time Series Analyzer V3 plugin (Balaji, 2014) was utilized to obtain the total intensity from a rectangular region of interest (ROI) spanning 551 pixels wide and 294 pixels high. The total intensity of an ROI is reported as "area," but will be referred to as "intensity" in this study. The placement of the ROI was centered in front of the mouth of the capillary to encapsulate the chemotactic response in the images. Images were maintained as .TIFF files with no compression. For a single repetition, the mean intensity obtained for the chemotaxis-negative strain (*che*) at each time point was subtracted from the mean intensities obtained for all other strains. These intensity values were then normalized to the greatest average intensity value observed from the wild-type (wt) strain. In all experiments, intensity values were normalized to the highest wt response observed. Due to small variations in experimental start time, each area value for a strain is plotted against the average time point. An average time point was derived from the three closest time points for an intensity value from three independent experiments.

ACKNOWLEDGMENTS

This study was supported by NSF grant MCB-1253234, the Thomas F. and Kate Miller Jeffress Memorial Trust J-1039, and start-up funds from Virginia Tech to Birgit Scharf. The Virginia Tech Mass Spectrometry Incubator is maintained with funding from the Fralin Life Science Institute of Virginia Tech as well as NIFA (Hatch Grant 228344). We are indebted to Bahareh Behkam for sharing the Zeiss Axio Observer Research microscope and the Omnicure S1000 UV light source, to Luciano Pecetti for donation of spotted medic seeds, and Timofey Arapov, Keith Compton, and Rafael Castaneda Saldana for critical reading of the manuscript.

REFERENCES

1. **van Rhijn P, Vanderleyden J.** 1995. The *Rhizobium*-plant symbiosis. Microbiol. Rev. **59:**124-142.
2. **Hirsch AM, Lum MR, Downie JA.** 2001. What makes the rhizobia-legume symbiosis so special? Plant Physiol. **127:**1484-1492.
3. **Cooper JE.** 2007. Early interactions between legumes and rhizobia: disclosing complexity in a molecular dialogue. J. Appl. Microbiol. **103:**1355-1365.
4. **Jones KM, Kobayashi H, Davies BW, Taga ME, Walker GC.** 2007. How rhizobial symbionts invade plants: the *Sinorhizobium-Medicago* model. Nat. Rev. Microbiol. **5:**619-633.
5. **Garau G, Reeve WG, Brau L, Deiana P, Yates RJ, James D, Tiwari R, O'Hara GW, Howieson JG.** 2005. The symbiotic requirements of different *Medicago* spp. suggest the evolution of *Sinorhizobium meliloti* and *S. medicae* with hosts differentially adapted to soil pH. Plant Soil **276:**263-277.
6. **Sprent JI.** 2007. Evolving ideas of legume evolution and diversity: a taxonomic perspective on the occurrence of nodulation. New Phytol. **174:**11-25.
7. **Yan AM, Wang ET, Kan FL, Tan ZY, Sui XH, Reinhold-Hurek B, Chen WX.** 2000. *Sinorhizobium meliloti* associated with *Medicago sativa* and *Melilotus* spp. in arid saline soils in Xinjiang, China. International journal of systematic and evolutionary microbiology **50 Pt 5:**1887-1891.
8. **Terpolilli JJ, O'Hara GW, Tiwari RP, Dilworth MJ, Howieson JG.** 2008. The model legume *Medicago truncatula* A17 is poorly matched for N_2 fixation with the sequenced microsymbiont *Sinorhizobium meliloti* 1021. New Phytol. **179:**62-66.
9. **Gulash M, Ames P, Larosiliere RC, Bergman K.** 1984. Rhizobia are attracted to localized sites on legume roots. Appl. Environ. Microbiol. **48:**149-152.
10. **Kamberger W.** 1979. An Ouchterlony double diffusion study on the interaction between legume lectins and rhizobial cell surface antigens. Arch. Microbiol. **121:**83-90.
11. **Wang D, Yang S, Tang F, Zhu H.** 2012. Symbiosis specificity in the legume: rhizobial mutualism. Cellular microbiology **14:**334-342.
12. **Zatakia HM, Nelson CE, Syed UJ, Scharf BE.** 2014. ExpR coordinates the expression of symbiotically important, bundle-forming Flp pili with quorum sensing in *Sinorhizobium meliloti*. Appl. Environ. Microbiol. **80:**2429-2439.
13. **Downie JA.** 2010. The roles of extracellular proteins, polysaccharides and signals in the interactions of rhizobia with legume roots. FEMS Microbiol. Rev. **34:**150-170.
14. **Sorroche FG, Rinaudi LV, Zorreguieta A, Giordano W.** 2010. EPS II-dependent autoaggregation of S*inorhizobium meliloti* planktonic cells. Current microbiology **61:**465-470.
15. **González JE, York GM, Walker GC.** 1996. *Rhizobium meliloti* exopolysaccharides: synthesis and symbiotic function. Gene **179:**141-146.
16. **Rinaudi LV, González JE.** 2009. The low-molecular-weight fraction of exopolysaccharide II from *Sinorhizobium meliloti* is a crucial determinant of biofilm formation. J. Bacteriol. **191:**7216-7224.
17. **Fujishige NA, Kapadia NN, De Hoff PL, Hirsch AM.** 2006. Investigations of *Rhizobium* biofilm formation. FEMS Microbiol. Ecol. **56:**195-206.

18. **Ames P, Bergman K.** 1981. Competitive advantage provided by bacterial motility in the formation of nodules by *Rhizobium meliloti*. J. Bacteriol. **148:**728-908.
19. **Bergman K, Gulash-Hoffee M, Hovestadt RE, Larosiliere RC, Ronco PG, 2nd, Su L.** 1988. Physiology of behavioral mutants of *Rhizobium meliloti*: evidence for a dual chemotaxis pathway. J. Bacteriol. **170:**3249-3254.
20. **Caetano-Anolles G, Wall LG, De Micheli AT, Macchi EM, Bauer WD, Favelukes G.** 1988. Role of motility and chemotaxis in efficiency of nodulation by *Rhizobium meliloti*. Plant Physiol. **86:**1228-1235.
21. **Dharmatilake AJ, Bauer WD.** 1992. Chemotaxis of *Rhizobium meliloti* towards nodulation gene-inducing compounds from alfalfa roots. Appl. Environ. Microbiol. **58:**1153-1158.
22. **Malek W.** 1989. Chemotaxis in *Rhizobium meliloti* strain L5.30. Microbiology **152:**611-612.
23. **Uren NC.** 2000. Types, amounts and possible functions of compounds released into the rhizosphere by soil-grown plants, p. 19-40. *In* Pinton R, Varanini Z, Nannipiero P (ed.), The Rhizosphere: Biochemistry and Organic Substances at the Soil-Plant Interface. CRC Press, New York.
24. **Soby S, Bergman K.** 1983. Motility and chemotaxis of *Rhizobium meliloti* in soil. Appl. Environ. Microbiol. **46:**995-998.
25. **Miller LD, Yost CK, Hynes MF, Alexandre G.** 2007. The major chemotaxis gene cluster of *Rhizobium leguminosarum* bv. *viciae* is essential for competitive nodulation. Mol. Microbiol. **63:**348-362.
26. **Mellor HY, Glenn AR, Arwas R, Dilworth MJ.** 1987. Symbiotic and competitive properties of motility mutants of *Rhizobium trifolii* Ta1. Arch. Microbiol. **148:**34-39.
27. **Althabegoiti MJ, Lopez-Garcia SL, Piccinetti C, Mongiardini EJ, Perez-Gimenez J, Quelas JI, Perticari A, Lodeiro AR.** 2008. Strain selection for improvement of *Bradyrhizobium japonicum* competitiveness for nodulation of soybean. FEMS Microbiol. Lett. **282:**115-123.
28. **Nelson EB.** 2004. Microbial dynamics and interactions in the spermosphere. Annu. Rev. Phytopathol. **42:**271-309.
29. **Miller JB, Oldroyd GED.** 2012. The role of diffusible signals in the establishment of rhizobial and mycorrhizal symbioses, p. 1-30. *In* Perotto S, Baluŝka F (ed.), Signaling and Communication in Plants vol. 11, Springer-Verlag Berlin Heidelberg.
30. **Barbour WM, Hattermann DR, Stacey G.** 1991. Chemotaxis of *Bradyrhizobium japonicum* to soybean exudates. Appl. Environ. Microbiol. **57:**2635-2639.
31. **Webb BA, Hildreth S, Helm RF, Scharf BE.** 2014. *Sinorhizobium meliloti* chemoreceptor McpU mediates chemotaxis toward host plant exudates through direct proline sensing. Appl. Environ. Microbiol. **80:**3404-3415.
32. **Gaworzewska ET, Carlile MJ.** 1982. Positive Chemotaxis of *Rhizobium leguminosarum* and other bacteria towards root Exudates from legumes and other plants. J. of Gen. Microbiol. **128:**1179-1188.
33. **Meier VM, Muschler P, Scharf BE.** 2007. Functional analysis of nine putative chemoreceptor proteins in *Sinorhizobium meliloti*. J. Bacteriol. **189:**1816-1826.
34. **Sourjik V, Schmitt R.** 1998. Phosphotransfer between CheA, CheY1, and CheY2 in the chemotaxis signal transduction chain of Rhizobium meliloti. Biochemistry-Us **37:**2327-2335.
35. **Riepl H, Scharf B, Schmitt R, Kalbitzer HR, Maurer T.** 2004. Solution structures of the inactive and BeF_3-activated response regulator CheY2. J. Mol. Biol. **338:**287-297.

36. **Dogra G, Purschke FG, Wagner V, Haslbeck M, Kriehuber T, Hughes JG, Van Tassell ML, Gilbert C, Niemeyer M, Ray WK, Helm RF, Scharf BE.** 2012. *Sinorhizobium meliloti* CheA complexed with CheS exhibits enhanced binding to CheY1, resulting in accelerated CheY1 dephosphorylation. J. Bacteriol. **194:**1075-1087.
37. **Amin M, Kothamachu VB, Feliu E, Scharf BE, Porter SL, Soyer OS.** 2014. Phosphate sink containing two-component signaling systems as tunable threshold devices. PLoS computational biology **10:**e1003890.
38. **Sourjik V, Schmitt R.** 1996. Different roles of CheY1 and CheY2 in the chemotaxis of *Rhizobium meliloti*. Mol. Microbiol. **22:**427-436.
39. **Platzer J, Sterr W, Hausmann M, Schmitt R.** 1997. Three genes of a motility operon and their role in flagellar rotary speed variation in *Rhizobium meliloti*. J. Bacteriol. **179:**6391-6399.
40. **Eggenhofer E, Haslbeck M, Scharf B.** 2004. MotE serves as a new chaperone specific for the periplasmic motility protein, MotC, in *Sinorhizobium meliloti*. Mol. Microbiol. **52:**701-712.
41. **Attmannspacher U, Scharf B, Schmitt R.** 2005. Control of speed modulation (chemokinesis) in the unidirectional rotary motor of *Sinorhizobium meliloti*. Mol. Microbiol. **56:**708-718.
42. **Galibert F, Finan TM, Long SR, Pühler A, Abola P, Ampe F, Barloy-Hubler F, Barnett MJ, Becker A, Boistard P, Bothe G, Boutry M, Bowser L, Buhrmester J, Cadieu E, Capela D, Chain P, Cowie A, Davis RW, Dreano S, Federspiel NA, Fisher RF, Gloux S, Godrie T, Goffeau A, Golding B, Gouzy J, Gurjal M, Hernandez-Lucas I, Hong A, Huizar L, Hyman RW, Jones T, Kahn D, Kahn ML, Kalman S, Keating DH, Kiss E, Komp C, Lelaure V, Masuy D, Palm C, Peck MC, Pohl TM, Portetelle D, Purnelle B, Ramsperger U, Surzycki R, Thebault P, Vandenbol M, Vorholter FJ, Weidner S, Wells DH, Wong K, Yeh KC, Batut J.** 2001. The composite genome of the legume symbiont *Sinorhizobium meliloti*. Science **293:**668-672.
43. **Meier VM, Scharf BE.** 2009. Cellular localization of predicted transmembrane and soluble chemoreceptors in *Sinorhizobium meliloti*. J. Bacteriol. **191:**5724-5733.
44. **Scharf B.** 2002. Real-time imaging of fluorescent flagellar filaments of *Rhizobium lupini* H13-3: flagellar rotation and pH-induced polymorphic transitions. J. Bacteriol. **184:**5979-5986.
45. **Anantharaman V, Aravind L.** 2000. Cache - a signaling domain common to animal $Ca(2^{+})$-channel subunits and a class of prokaryotic chemotaxis receptors. Trends Biochem. Sci. **25:**535-537.
46. **Ulrich LE, Zhulin IB.** 2005. Four-helix bundle: a ubiquitous sensory module in prokaryotic signal transduction. Bioinformatics **21 Suppl 3:**iii45-iii48.
47. **Taylor BL, Zhulin IB.** 1999. PAS domains: internal sensors of oxygen, redox potential, and light. Microbiol. Mol. Biol. Rev. **63:**479-506.
48. **Götz R, Limmer N, Ober K, Schmitt R.** 1982. Motility and chemotaxis in two strains of *Rhizobium* with complex flagella. J. Gen. Microbiol. **128:**789-798.
49. **Adler J.** 1973. A method for measuring chemotaxis and use of the method to determine optimum conditions for chemotaxis by *Escherichia coli*. J. Gen. Microbiol. **74:**77-91.
50. **Sampedro I, Parales RE, Krell T, Hill JE.** 2014. *Pseudomonas* chemotaxis. FEMS Microbiol. Rev.

51. **Parales RE, Harwood CS.** 2002. Bacterial chemotaxis to pollutants and plant-derived aromatic molecules. Curr. Opin. Microbiol. **5:**266-273.
52. **Balaji J.** 2014. Time Series Analyzer Version 3.0. Dept. of Neurobiology, UCLA.
53. **Jordan DC.** 1952. Studies on the legume root nodule bacteria. 3. Growth factor requirements for effective, ineffective, and parasitic strains. Can. J. Bot. **30:**693-700.
54. **Burg D, Guillaume J, Tailliez R.** 1982. Chemotaxis by *Rhizobium meliloti*. Microbiology **133:**162-163.
55. **Ma Y, Zhu C, Ma P, Yu KT.** 2005. Studies on the diffusion coefficients of amino acids in aqueous solutions. J. Chem. Eng. Data **50(4):**1192–1196.
56. **King JW, Srinivas K.** 2011. Measurement of binary diffusion coefficients of compounds at infinite dilution in water as a function of temperature using teledyne isco syringe pumps. Syringe Pump Application Note, Teledyne ISCO, AN26.
57. **Robinson JB, Bauer WD.** 1993. Relationships between C_4 dicarboxylic acid transport and chemotaxis in *Rhizobium meliloti*. J. Bacteriol. **175:**2284-2291.
58. **Caetano-Anolles G, Crist-Estes DK, Bauer WD.** 1988. Chemotaxis of *Rhizobium meliloti* to the plant flavone luteolin requires functional nodulation genes. J. Bacteriol. **170:**3164-3169.
59. **Sahari A, Traore MA, Scharf BE, Behkam B.** 2014. Directed transport of bacteria-based drug delivery vehicles: bacterial chemotaxis dominates particle shape. Biomed. Microdevices **16:**717-725.
60. **Phillips DA, Wery J, Joseph CM, Jones AD, Teuber LR.** 1995. Release of flavonoids and betaines from seeds of seven *Medicago* species. Crop Sci. **35:**805-808.
61. **Horbowicz M, Obendorf RL, McKersiec BD, Viands DR.** 1995. Soluble saccharides and cyclitols in alfalfa (*Medicago sativa* L.) somatic embryos, leaflets, and mature seeds. Plant Science **109:**101-198.
62. **Kossmann M, Wolff C, Manson MD.** 1988. Maltose chemoreceptor of *Escherichia coli:* interaction of maltose-binding protein and the Tar signal transducer. J. Bacteriol. **170:**4516-4521.
63. **Bertani G.** 1951. Studies on lysogenesis. I. The mode of phage liberation by lysogenic *Escherichia coli*. J. Bacteriol. **62:**293-300.
64. **Althabegoiti MJ, Lopez-Garcia SL, Piccinetti C, Mongiardini EJ, Perez-Gimenez J, Quelas JI, Perticari A, Lodeiro AR.** 2008. Strain selection for improvement of *Bradyrhizobium japonicum* competitiveness for nodulation of soybean. FEMS Microbiol. Lett. **282:**115-123.
65. **Rasband WS.** ImageJ, U. S. National Institutes of Health, Bethesda, Maryland, USA. http://imagej.nih.gov/ij/**:**1997-2014.
66. **Pleier E, Schmitt R.** 1991. Expression of two *Rhizobium meliloti* flagellin genes and their contribution to the complex filament structure. J. Bacteriol. **173:**2077-2085.
67. **Bachmann BJ.** 1990. Linkage map of *Escherichia coli* K-12, edition 8 [published erratum appears in Microbiol Rev 1991 Mar;55(1):191]. Microbiol. Rev. **54:**130-197.

Table 3.1. Bacterial strains

Strain/Plasmid	Relevant characteristics [a]	Source or Reference
Strain		
S. meliloti		
RU11/001	Sm^r; spontaneous streptomycin-resistant wild-type strain	(Pleier and Schmitt, 1991)
RU11/803	Sm^r; Δ*mcpW*	(Meier et al., 2007)
RU11/804	Sm^r; Δ*mcpY*	(Meier et al., 2007)
RU11/805	Sm^r; Δ*mcpX*	(Meier et al., 2007)
RU11/815	Sm^r; Δ*icpA*	(Meier et al., 2007)
RU11/818	Sm^r; Δ*mcpZ*	(Meier et al., 2007)
RU11/828	Sm^r; Δ*mcpU*	(Meier et al., 2007)
RU11/830	Sm^r; Δ*mcpV*	(Meier et al., 2007)
RU11/838	Sm^r; Δ*mcpT*	(Meier et al., 2007)
RU13/149	Sm^r; Δ*mcpS,* Δ*mcpT,* Δ*mcpU,* Δ*mcpV,* Δ*mcpW,* Δ*mcpX,* Δ*mcpY,* Δ*mcpZ,* Δ*icpA* (*che*)	(Meier et al., 2007)

[a] Nomenclature according to Bachmann (Bachmann, 1990).

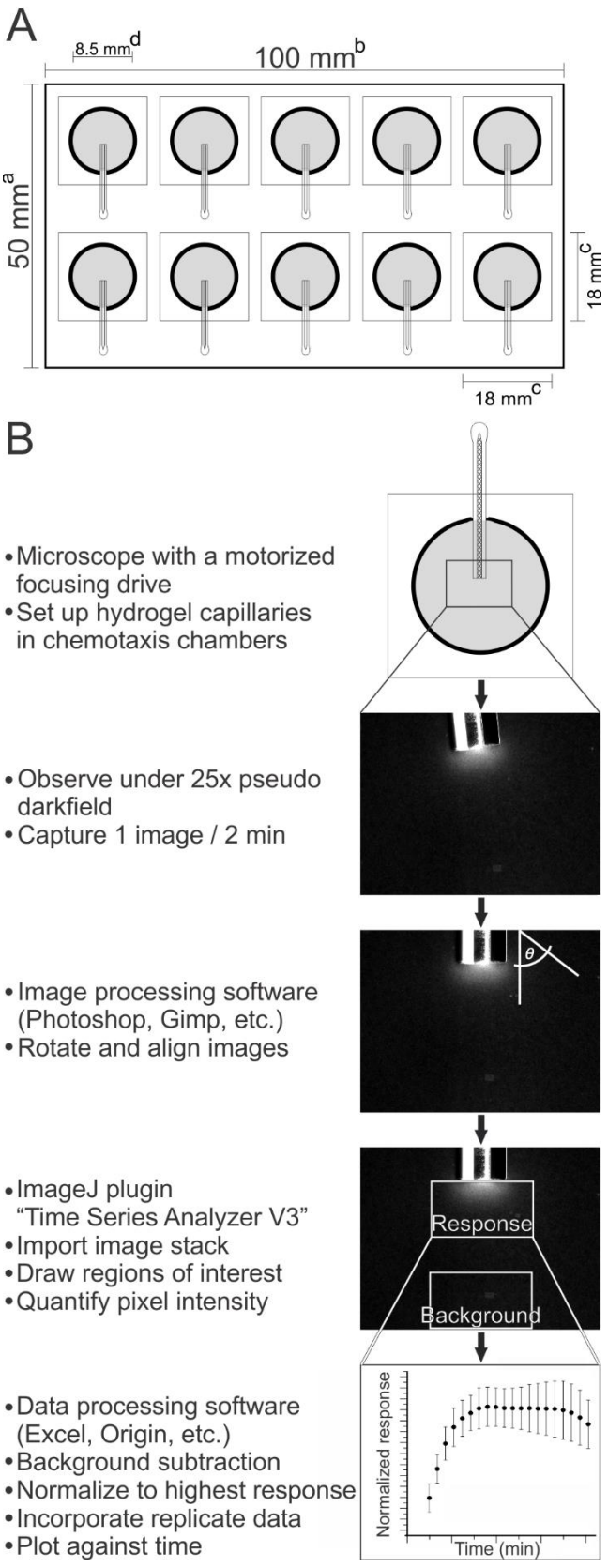
A
8.5 mm[d]
100 mm[b]
50 mm[a]
18 mm[c]
18 mm[c]
B
•Microscope with a motorized focusing drive
•Set up hydrogel capillaries in chemotaxis chambers
•Observe under 25x pseudo darkfield
•Capture 1 image / 2 min
•Image processing software (Photoshop, Gimp, etc.)
•Rotate and align images
θ
•ImageJ plugin "Time Series Analyzer V3"
•Import image stack
•Draw regions of interest
•Quantify pixel intensity
Response
Background
•Data processing software (Excel, Origin, etc.)
•Background subtraction
•Normalize to highest response
•Incorporate replicate data
•Plot against time
Normalized response
Time (min)

Fig. 3.1 Hydrogel capillary assay set up and flow chart of image acquisition and analysis. **A.** Ten chemotaxis chambers are constructed on a microscope slide (100 mm x 50 mm x 1 mm). Each chamber consists of an O-ring 8.5 mm in diameter obtained from the cap of a Sarstedt 1.5 ml screw-cap tube that is sealed to the slide with an application of machine grease. A bacterial suspension (81 µl) is placed within the O-ring and a 0.5 µl hydrogel capillary is slid into the chamber via a pre-cut section of the O-ring. A glass coverslip is placed on top of the O-ring that is sealed by an application of machine grease. The chemotaxis response is considered to start when the coverslip is set in place. **B.** Upon microscopic observation of a chemotaxis chamber, the guidelines in the flow chart are followed to acquire images of the chemotaxis response and to quantify the response in each image.

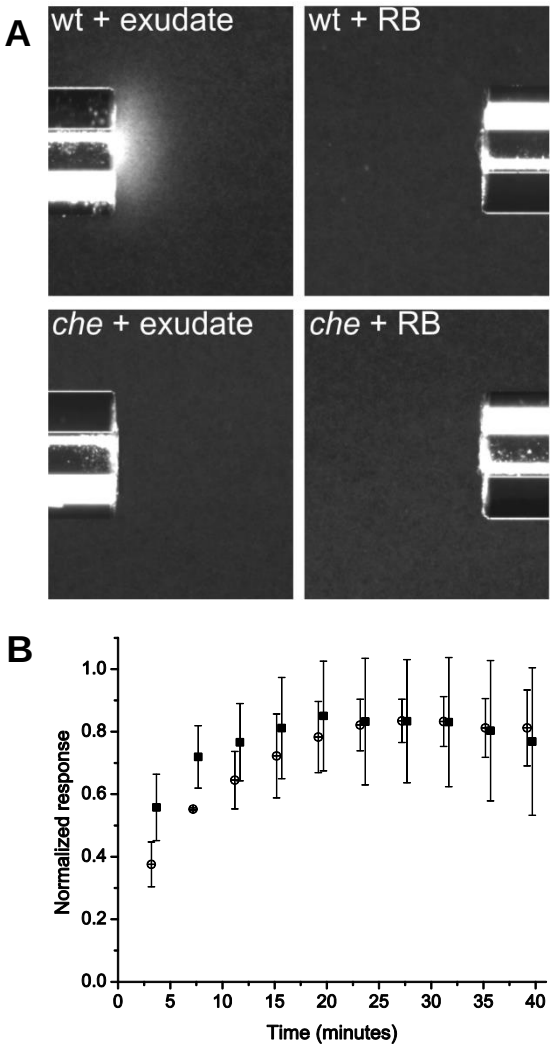

Fig. 3.2 *S. meliloti* wild-type response to M. sativa and M. arabica exudates. **A.** Responses of *S. meliloti* wild type and the *che* strain to *M. sativa* seed exudate (exudate) and Rhizobial Basal medium (RB) were observed at 25 x magnification under pseudo dark field and images were taken at 20 min. Exudate was diluted with RB and tested at 5x concentration of the original exudate sample. To allow for ease of visualization, the image brightness, contrast, and intensity were adjusted equally for each image. **B.** Responses to *M. sativa* (○) and *M. arabica* (●) exudates were observed at 25x magnification under pseudo dark field and images were taken with a 1.3

millisecond exposure every four minutes. Normalized response values are the mean and standard deviation of the pixel intensities from three independent experiments. Each response value for a strain is plotted against an average time point. Exudates were tested at 5x concentration of the original exudate samples.

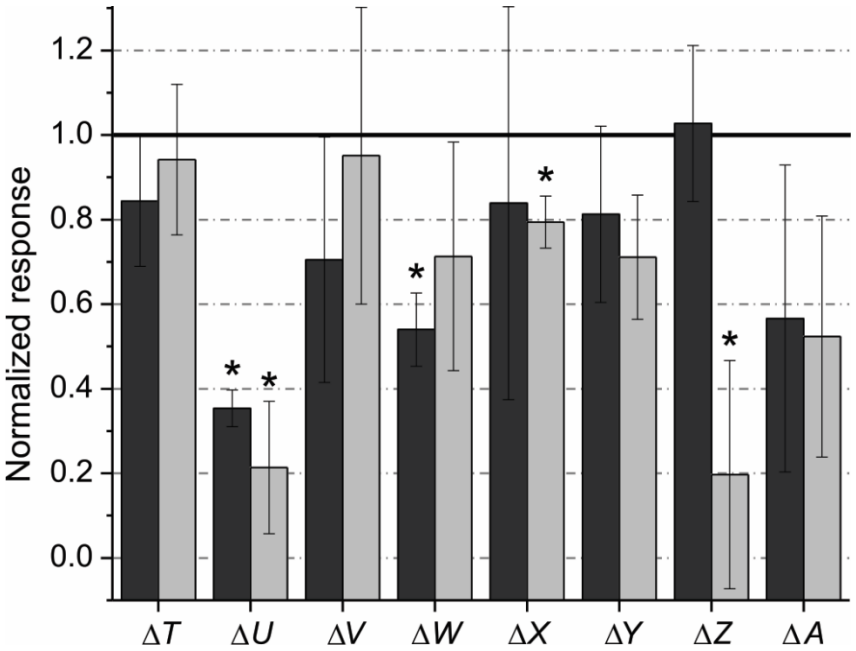

Fig. 3.3 Responses of *S. meliloti* wild type and single *mcp* deletion strains to exudates of *M. sativa* and *M. arabica*. Responses to *M. sativa* (dark gray bars) and *M. arabica* (light gray bars) exudates were observed at 25x magnification under pseudo dark field. The wild type exhibited a maximum response to exudates of *M. sativa* and *M. arabica* between 20 and 34 min (see Fig. 3.2B). Therefore, images taken during this time period were averaged. Responses were normalized to the wild type response (horizontal line at 1.0) and are the mean and standard deviation from three independent experiments. Exudates were tested at 5x concentration of the original exudate samples. Data were analyzed for statistical significance using the one sample t-test, $P \leq 0.05$ or two sample t-test. Responses marked with * are significantly smaller than the wild type, and the responses of Δ*mcpZ* marked with ** are significantly different from each other ($P \leq 0.01$).

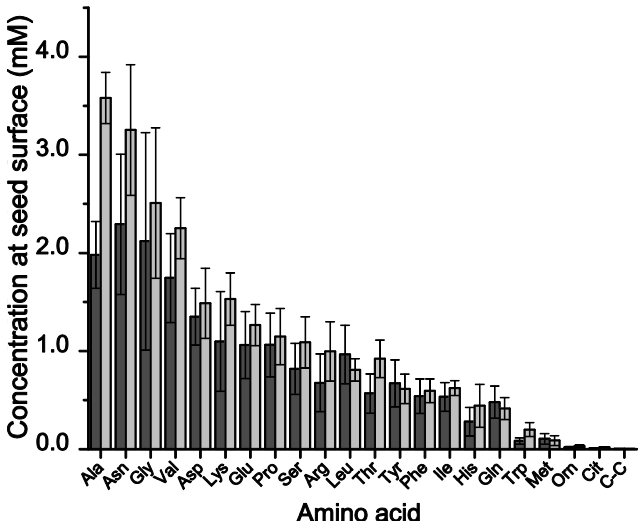

Fig. 3.4 Amino acids exuded by germinating seeds. Bars indicate the concentrations of amino acids at the surface of a germinating seed as determined by liquid chromatography-mass spectrometry for *M. sativa* (dark gray bar) and *M. arabica* (light gray bar). The seed volumes are 2.17 μl and 1.84 μl for *M. sativa* and *M. arabica*, respectively. Data are organized from highest to lowest concentrations and are the mean and standard deviation from three biological replicates and two to four technical replicates.

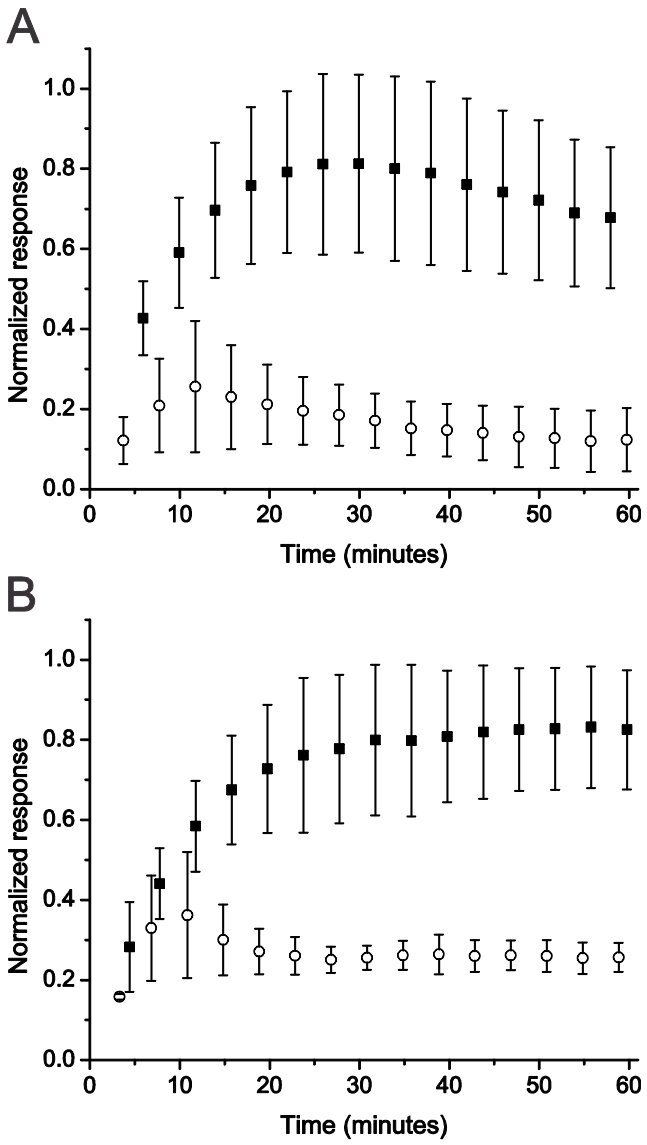

Fig. 3.5 Wild-type responses to exudates and synthetic AA mixtures. **A.** *M. sativa* exudate (■) and synthetic *M. sativa* AA mixture (○). **B.** *M. arabica* exudate (■) and *M. arabica* synthetic AA mixture (○). To observe responses that are visibly bright enough for quantification, seed exudate and AA mixtures were tested at a 7.6x concentration of the original exudate samples. Normalized response values are the mean and standard deviation from three independent experiments. Each response value for a strain is plotted against an average time point.

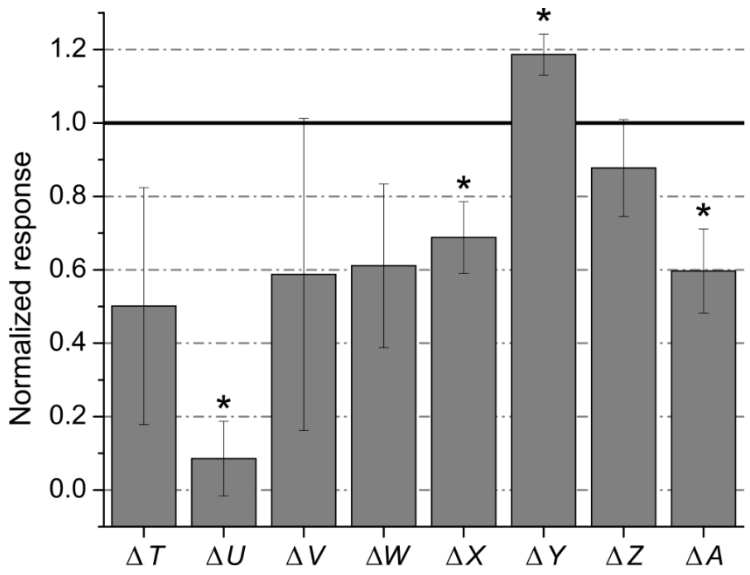

Fig. 3.6 Responses of single *mcp* deletion strains to M. sativa synthetic AA mixture. Responses were observed at 25x magnification under pseudo dark field. Images taken between 20 and 34 min were averaged and responses are normalized to the wild-type response (horizontal line at 1.0). Data are the mean and standard deviation from three independent experiments. Each response value for a strain is plotted against an average time point. Exudates were tested at 7.6x concentration of the original exudate samples. Data were analyzed for statistical significance using the one sample t-test, $P \leq 0.05$. Responses marked with * are significantly smaller (Δ*mcpU*, Δ*mcpX*, Δ*icpA*) or larger (Δ*mcpY*) than the wild type.

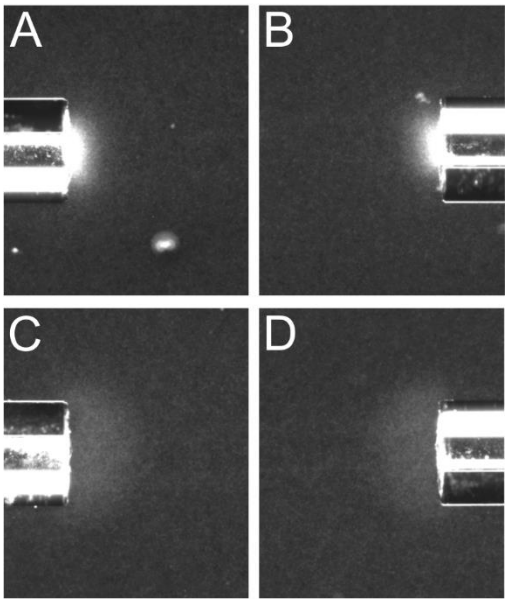

Fig. 3.7 Responses of wild type and the *ΔmcpU* strain to M. sativa synthetic amino acid mixtures with and without proline. **A.** Wild-type response to AA mixture with proline. **B.** Wild-type response to AA mixture without proline. **C.** Δ*mcpU* response to AA mixture with proline. **D.** Δ*mcpU* response to AA mixture without proline. AA mixtures were tested at a 7.6x concentration of the original exudate samples. Responses were observed at 25x magnification under pseudo dark field and images were taken at 10 min. To allow for ease of visualization, the image brightness, contrast, and intensity were adjusted equally for each image.

Chapter 4 - *Sinorhizobium meliloti* chemotaxis to multiple amino acids is mediated by chemoreceptor McpU

BENJAMIN A. WEBB, DORIS TAYLOR, AND BIRGIT E. SCHARF*

Virginia Tech, Department of Biological Sciences, Life Sciences I, Blacksburg, VA 24061

Key words: flagellar motor, plant host exudate, motility, rhizosphere, symbiosis

* For correspondence:
E-mail bscharf@vt.edu
Tel (+1) 540 231 0757
Fax (+1) 540 231 4043
Biological Sciences, Life Sciences I
Virginia Tech
Blacksburg, VA 24061, USA

Present address: Doris Taylor, Department of Biochemistry and Molecular Biology, Baylor University, Houston, TX 77030

Mol Plant Microbe Interact. MPMI. 2016 May;9. Manuscript # MPMI-04-16-0075-R Manuscript is in revision.

Attribution: BAW has generated the data shown here in Fig. 4.1 - Fig. 4.7. DT helped to generate data for Fig. 4.3. BAW, and BES drafted the final manuscript.

ABSTRACT

The legume symbiont *Sinorhizobium meliloti* is chemo-attracted to compounds exuded by germinating seeds of its host alfalfa. This response is mediated greatly by one of the *S. meliloti* chemoreceptors, namely McpU. McpU also has a prominent contribution in sensing a synthetic amino acid mixture mimicking the amounts and composition observed in seed exudate. Here, we used the hydrogel capillary assay to quantify chemotactic responses of *S. meliloti* to individual amino acids (AAs) exuded by germinating alfalfa seeds and to define the role of McpU in this behavior. *S. meliloti* exhibited positive chemotaxis responses of different intensities to all proteinogenic AAs except for aspartate, and also to citrulline, cystine, gamma-aminobutyric acid, and ornithine. Opposing, a strain lacking *mcpU* displayed strongly diminished responses towards these compounds. Differential scanning fluorimetry demonstrated an interaction of the purified periplasmic region of McpU (McpU-PR) with the AAs, except glutamate and aspartate. We additionally tested organic acids and sugars, but with mostly negative results. Using isothermal titration calorimetry, we confirmed the interaction of McpU-PR with select AAs representing strong and weak attractants. Our results show that *S. meliloti* McpU is a broad-range AA receptor mediating differential responses to individual attractants, but does not bind negatively charged AAs.

INTRODUCTION

Soil dwelling bacteria from the *Rhizobiaceae* family form a species-specific symbiosis with their legume hosts that is characterized by the formation of a plant organ known as a nodule (1-3). In developing nodules, bacteria undergo metamorphosis into bacteroids, which fix atmospheric nitrogen into ammonium. This form of nitrogen is utilized by the plant to aid in prolific growth (1, 4). Bacterial chemotaxis precedes symbiosis and enables rhizobia to actively swim towards and accumulate in the host spermosphere and rhizosphere by responding to host-released compounds (5-12). In particular, rhizobial motility and chemotaxis have been proven to enhance successful symbiotic interactions of *Bradyhizobium japonicum*, *Rhizobium leguminosarum*, *Rhizobium trifolii*, and *Sinorhizobium meliloti*, with soybean, pea, clover, and alfalfa, respectively (5, 7, 13-15).

A germinating seed exudes a multitude of compounds into the soil creating a unique and species-specific spermosphere (16). The complex molecular composition of seed exudates comprises amino acids (AAs), sugars, lipids, phenolics, proteins, and other metabolites (16-18). Positive chemotactic responses to host seed exudates were described for *B. japonicum*, *R. leguminosarum*, and *S. meliloti* (17-19). However, the heterogeneous nature of exudates hamper the identification of individual molecules responsible for the chemotactic responses.

Preceding work characterized the response of *S. meliloti* to exudate of germinating alfalfa seeds and identified that host seed-derived AAs contribute to 23% of this response (20). *S. meliloti* uses eight chemoreceptors, namely seven methyl-accepting chemotaxis proteins (McpT to McpZ) and one internal chemotaxis protein (IcpA), for chemotaxis (21). Each chemoreceptor is composed of a variable sensing domain and a highly conserved signaling domain. A variety of molecules have been identified to serve as chemoattractants, including AAs, organic acids, and sugars, but the

functions of the corresponding chemoreceptors are mostly unknown (21).

We previously presented that McpU senses proline via tandem Cache domains located in its periplasmic region (18, 22). Moreover, McpU is the most important chemoreceptor for host exudate and AAs recognition (20). Homology modeling of the periplasmic region of McpU with the crystal structure of *Vibrio cholerae* McpN as the template identified the ligand-binding site and specifically two conserved aspartate residues (asp-155 and asp-182) of the N-terminal Cache domain to be involved in ligand sensing. The prediction was supported by chemotaxis behavioral assays of single point mutants and *in vitro* binding analysis of purified mutant variant proteins (18). The recognized motif, also known as a double PhoQ-DcuS-CitA (PDC) domain, recognizes AAs directly as well as indirectly through ABC transport-binding lipoproteins (18, 22-26).

In this study, we characterized the strength and temporal reaction profile of all proteinogenic AAs as well as to citrulline, cystine, gamma-aminobutyric acid, and ornithine in *S. meliloti* chemotaxis, as they are present in alfalfa seed exudates. Since the proline sensor McpU is the most important chemoreceptor for host exudate and AAs recognition, we elucidated its role in AA sensing using quantitative *in vivo* chemotaxis assays and *in vitro* binding assays with the purified periplasmic region of McpU.

RESULTS

Chemotaxis of *S. meliloti* wild type and the *mcpU* deletion strain toward amino acids

Since host seed-derived AAs are contributing to 23% of the chemotactic response to whole seed exudates (20), we determined the chemotactic strength of individual proteinogenic AAs, citrulline (cit), cystine (c-c), gamma-aminobutyric acid (gaba), and ornithine (orn) in *S. meliloti* chemotaxis. We also tested the response of the *mcpU* deletion strain, because experimental and bioinformatics evidence suggested that McpU serves as general amino acid sensor (18, 20). Chemotactic responses of both strains were observed in a modified hydrogel capillary assay, which enables quantitative time-course assessments (20). Each capillary contained a hydrogel that was equilibrated with 1 mM compound dissolved in Rhizobial Basal medium (RB). Cells exhibiting positive chemotaxis accumulated at the mouth of the capillary, whereas no accumulation was observed for the control capillary with RB or for a chemotaxis negative strain (*che*) ((20); data not shown). Photographs were taken near the mouth of the capillary every four minutes under a pseudo dark field, and the pixel intensity in front of the capillary, correlating with the number of cells, was quantified as described ((20).

The wild-type strain responded to all AAs except asp, but with different intensities and time courses. The strongest wild-type response occurred after exposure to arg for 16 min and all responses depicted in Fig. 4.1 were normalized to this value. Response curves in Fig. 4.1 are categorized in four classes from strongest (Fig. 4.1A) to weakest (Fig. 4.1D). Peak responses to ala, arg, his, leu, phe, and thr in Fig. 4.1A ranged from 0.51 to 1.00 with differently shaped response curves. While responses to ala, arg, leu, and thr peaked at around 14-16 min, responses to his and phe gradually increased to a plateau response at around 25 min. Responses to ile, lys, met, pro, ser, and trp grouped in Fig. 4.1B are medium to strong ranging from 0.38 to 0.50.

Responses to lys, pro, and ser peaked relatively early between 8 and 12 min, whereas those to ile and met came to a plateau at around 25 min. Interestingly, the response to trp increased steadily during the 40-min observation period. The third group comprises weak to medium responses to asn, cit, gly, orn, tyr, and val. Responses to asn, cit, gly, and val reached a plateau between 12 and 16 min, while the response to orn plateaued at about 22 min. Similar to the trp response, the response to tyr increased steadily during the 40-min observation period. The last group contains weak responses to c-c, cys, gaba, gln, and glu, and no response to asp. The responses to gln and glu peaked at 12 and 20 min, respectively. The c-c response stayed at a constant level, while responses to cys and gaba steadily increased or decreased, respectively. Upon closer microscopic examination, it was noticed that declining responses towards the end of the observation period are due to the dissemination of cells away from the capillary. This response can be explained by attractant depletion due to diffusion from the capillaries into the bacterial ponds, bacterial metabolism of the attractant, or production of repellent.

The response of the *mcpU* deletion strain to all AAs was decreased substantially as compared to the wild-type response. In particular, responses to arg, cit, cys, c-c, gaba, glu, lys, orn, phe, and ser fell within the region of no response (pink box in Fig. 4.1A-D). Responses to the remaining AAs increased steadily during the observation period, but remained much lower than that of wild type. Peak responses of wild type and the *mcpU* deletion strain are compared in Fig. 4.2. Taken together, these results establish that all AAs but asp are chemoattractants for *S. meliloti* with distinct responses to individual compounds. Furthermore, we demonstrated that AA chemotaxis is mediated through McpU.

Thermal denaturation of McpU-PR with AAs

To monitor direct interactions of AAs with McpU, we performed differential scanning fluorimetry (DSF) with the isolated periplasmic region of McpU (McpU-PR) and a single amino acid variant, McpU-PR^{D182E}, which is strongly reduced in function. Homology modeling predicted the involvement of asp-182 in ligand coordination, which was experimentally supported for the binding of proline to McpU *in vivo* and *in vitro* (18), thus this variant protein serves as a negative control for binding. Thermal unfolding of both proteins, wild-type and mutant McpU-PR, in the presence of the fluorescence dye SYPRO Orange and individual AAs was monitored. A resulting sigmoidal melting curve yields an inflection point, which denotes the melting temperature (T_m) of half the protein population. In the presence of stabilizing ligands, the T_m shifts to higher temperatures (27). McpU-PR and McpU-PR^{D182E} in the absence of ligand yielded an average T_m of 36 °C and 34 °C, respectively, which were subtracted from the T_m determined in the presence of a compound. Background fluctuations in fluorescence in reactions with McpU-PR and McpU-PR^{D182E} in the absence of a compound were determined to be ± 1.5 °C each. T_m shifts were plotted against corresponding AAs in Fig. 4.3. All AAs except asp and glu shifted the T_m of McpU-PR significantly above the background level between 2.5 and 15.5 °C. In contrast, McpU-PR^{D182E} only experienced T_m shifts slightly above background in the presence of cit, cys, pro, and trp. We also tested for the interactions of two non-metabolizable analogs of arginine and proline, namely canavanine and azetidine-2-carboxylate, which produced substantial T_m shifts of 11.5 and 13.0 °C, respectively. Additional compounds tested for binding to McpU-PR included six organic acids, three inorganic salts, and ten sugars and sugar derivatives with corresponding T_m shifts listed in Table 1. With the exception of citric acid, none of the tested compounds produced a significant T_m shift. Taken together, these results demonstrate that McpU-PR directly interacts with non-acidic AAs and citric acid.

Isothermal titration calorimetry of McpU-PR with AAs

To assess the correlation between strength of chemotactic response *in vivo* and binding affinity to AAs *in vitro*, we performed isothermal titration calorimetry (ITC) of McpU-PR with the two strongest (arg and phe) and weakest (glu and asp) AA attractants, respectively. Since we observed that McpU-PR unfolding starts at around 20 °C during thermal denaturation studies, temperature conditions for ITC measurements were set to 10 °C. First, we performed a titration with pro, to compare results with previously published data collected at 22 °C, which resulted in a K_d of 104 μM (18). Titration of McpU-PR with pro at 10 °C resulted in exothermic heat signals yielding a K_d of 29 μM (Fig. 4.4A). Titration with the strong attractant phe resulted in endothermic heat signals and a K_d of 458 μM (Fig. 4.4B), while titration with arg caused large erratic exothermic heat signals that could not be resolved into a binding isotherm (data not shown). Titrations with the weakest attractant glu, and the non-attractant asp, both resulted in large exothermic heats of dilution (Fig. 4.4C+D) indicating that these two AAs do not bind to McpU-PR. In conclusion, ITC data confirmed results gained from the DSF experiments, in particular, the binding of phe and pro to McpU-PR and a lack of interaction with asp and glu.

DISCUSSION

Chemotaxis towards host seed and root-exuded attractants is an important step in early host-microbe interaction (12). Since 23% of the chemotactic response of *S. meliloti* RU11/001 to exudates from germinating alfalfa seeds is due to amino acid chemotaxis, we evaluated the chemotactic potency of 24 AAs using a recently developed hydrogel capillary assay that enables quantitative time-course assessments (20). While the *S. meliloti* wild-type response to a synthetic AA mixture peaked at 12 min, peak maxima for the reaction to individual AAs varied greatly from 4 to 36 min, with responses to trp and tyr still increasing at the end of the observation time at 40 min (Fig. 4.1). This complex reaction pattern likely stems from the diverse chemical nature of the amino acid side chains and molecule size, although no obvious correlation between hydrophobicity and charge was observed. Similarly, relative strength of attraction was not related to the AA class, with arg and phe as the two strongest attractants being positively charged and hydrophobic, respectively. A similar lack of correlation was reported for AA taxis in *E. coli* and *B. subtilis* (24, 28). Furthermore, no relationship was seen between the strength of attraction and the amount exuded by germinating alfalfa seeds (20). *S. meliloti* RU11/001 is attracted to most AAs, which is consistent with previous findings of the parental strain, MVII-1, using traditional Adler capillary assays (29). Recognition and chemotaxis towards a broad range of AAs enables *S. meliloti* to benefit from these carbon compounds as energy sources and host-plant signaling molecules.

Previous observations linked the proline sensor McpU to AA taxis (20). Here, we observed that a strain lacking *mcpU* displayed a drastically reduced response to all AAs in the hydrogel capillary assay. Specifically, the Δ*mcpU* strain showed no reaction towards arg, cit, c-c, cys, gaba, glu, lys, orn, phe, and ser, indicating that these AAs are solely sensed by McpU (Figs. 4.1 & 4.2). The response of the Δ*mcpU* strain at the time of the wild-type peak response to most AAs was lower

than its maximal response and is included in Fig. 4.2 as horizontal bars. Interestingly, responses of the Δ*mcpU* strain to these AAs slowly increased during observation time. This behavior suggests overlapping specificity of McpU with other chemoreceptors. Potential candidates are Cache-domain bearing receptors, such as McpX and McpV, or the hypothetical energy sensors IcpA and McpY (21).

Results from the thermal denaturation studies demonstrated direct interaction of the periplasmic region of McpU with all AAs except asp and glu. This finding is in agreement with the behavioral assays, which supports the hypothesis that McpU is a general AA sensor and that the chemotactic response is mediated through direct binding. The only exception is glu, which does not bind to McpU-PR *in vitro*, but elicits an McpU-dependent chemotaxis response. We hypothesize that chemotaxis towards glu is mediated through indirect binding to McpU, analogous to McpC of *B. subtilis*, which senses gln via binding of GlnH, an ABC transport-binding lipoprotein (24). *S. meliloti* possesses a general L-amino acid transporter system with broad specificity (Aap), and the solute binding protein AapJ is a potential candidate for mediating glu taxis (30). Alternatively, *S. meliloti* might have evolved a specialized periplasmic binding protein to mediate chemotaxis towards glu, especially in light of the increased number of solute-binding protein-dependent transporters in rhizobia compared to other bacteria (31).

Previous work identified two conserved residues, asp-155 and asp-182, in the amino-proximal PDC domain of McpU as critical for proline binding (18). Using DSF, we showed that only three of the AAs were able to exhibit weak interaction with the variant protein McpU-PR^{D182E} (Fig. 4.3). Therefore, AA sensing by McpU most likely occurs in the same ligand-binding pocket. The presence of two negatively charged amino acids within the binding pocket may also explain the lack of interaction of McpU-PR with the acidic AAs asp and glu. In addition, we excluded direct

binding of sugars and most organic acids, however, identified citric acid as a likely ligand for McpU (Table 1).

Using ITC, we confirmed the lack of asp and glu binding to McpU-PR. Therefore, McpU can be placed in the same sub-family of broad range AA receptors that possess a dual PDC domain structure, but do not sense negatively charged AAs directly, such as *B. subtilis* McpC and *P. syringae* PctA (23, 24). We also titrated McpU-PR with the two strongest attractants, arg and phe. Unfortunately, binding parameters with arg could not be determined due to erratic releases of heat during titration, which lowered the signal to noise ratio beyond resolution of a binding isotherm (data not shown). This behavior might be attributed to the positively charged guanidinium group in arg, which probably interacted non-specifically with McpU-PR (32). Phe bound with a K_d of 458 μM, which indicates weaker binding compared to pro with a K_d of 29 μM (Fig. 4.4). The chemotaxis response of *S. meliloti* to phe is about 50 % stronger than to pro (Fig. 4.1), but this difference is not necessarily reflected in the *in vitro* binding characteristics. A similar observation was made for the binding of ala and pro to *B. subtilis* McpC (24), which can be explained by different conformational changes of the receptor and consequently, signaling to the histidine kinase CheA. Interestingly, titration of McpU-PR with phe and pro resulted in opposite heat signals, which is often an indication of different binding sites (Fig. 4.4). However, the binding-site variant protein McpU-PR^{D182E} was unable to bind either ligand, which supports a one-binding site model (Fig. 4.3). Therefore, other factors, including temperature and buffer condition contributed to the sign of heat signal (33).

Our previous study identified McpU as the most important chemoreceptor for host sensing (20). Here, we classified McpU as broad-range AA sensor, which also directly interacts with citric acid. Individual AAs elicit a broad spectrum of response intensities and times, which aids in survival

and host sensing of *S. meliloti* in the soil.

MATERIALS AND METHODS

Media and growth conditions

S. meliloti RU11/001 (wild type) (34), RU11/828 (Δ*mcpU*) (21), and RU13/149 (*che*) (21) were grown in TYC (0.5% (w/v) tryptone, 0.3% (w/v) yeast extract, 0.13% $CaCl_2$ x 6 H_2O (w/v) [pH 7.0], streptomycin (600 μg/ml) at 30 °C (35). Motile cells for hydrogel capillary assays were grown for two days in TYC, diluted 1:1,000 in 3 ml TYC and grown overnight. Cultures were then diluted 1:1,000 in 10 ml Rhizobial Basal minimal medium (RB) (6.1 mM K_2HPO_4, 3.9 mM KH_2PO_4, 1 mM $MgSO_4$, 1 mM $(NH_4)_2SO_4$, 0.1 mM $CaCl_2$, 0.1 mM NaCl, 0.01 mM Na_2MoO_4, 0.001 mM $FeSO_4$, 20 μg/l biotin, 100 μg/l thiamine (29)), layered on Bromfield agar plates with no antibiotics (36), and incubated at 30°C for approximately 15 h to an optical density at 600 nm (OD_{600}) of 0.16 ± 0.02.

Hydrogel capillary assay

Prior to experiments, capillaries containing a cross-linked hydrogel were prepared according to Webb *et al.* (20). Amino acids (Fluka Analytical kit, 21 L-amino acids + glycine) were dissolved in RB to 1 mM, sterile filtered, and stored at -30 °C. Hydrogel capillaries were washed and equilibrated for four hours twice with RB. AA solutions were thawed to room temperature and briefly vortexed. For equilibration of the capillaries with AAs, capillaries were placed into 50 μl of AA solution per capillary and left overnight at 4 °C. Cells were prepared and harvested by centrifugation at 4,000 x g for 5 min at room temperature, suspended with RB to an OD_{600} of 0.12. One repetition of the hydrogel capillary assay was performed as described in Webb *et al.* (20).

Quantification of chemotaxis responses

Quantification of the responses were essentially performed according to Webb *et al*. (20) with minor modifications. Images from the hydrogel capillary assay were adjusted by rotation to align the capillaries in such a way that the capillaries rest precisely on top of one another when images were stacked. Rotated images were then imported to ImageJ (37) as an image sequence. A rectangular region of interest (ROI) spanning 424 pixels wide and 235 pixels high was placed in front of the mouth of the capillary to encapsulate the chemotactic response and the Time Series Analyzer V3 plugin (38) was utilized to attain the average intensity from this ROI ("Response ROI"). To account for background, an ROI with the same dimensions was placed at the top of each image, distant from the chemotactic response ("Background ROI"). The average intensities obtained from the background of each image were subtracted from their respective intensities of the Response ROIs. These intensity values were then normalized to the greatest average intensity value observed from the wild-type (wt) strain, which was the response to 1mM arginine at 16 min.

Expression and purification of the wild type and mutant variant periplasmic region of McpU (McpU-PR)

The recombinant ligand-binding, periplasmic region of McpU (McpU-PR, $McpU_{40-284}$) and its single amino acid substitution variant ($McpU\text{-}PR^{D182E}$) were overproduced from plasmid pBS373 and pBS390 (18) in *E. coli* M15/pREP4, providing N-terminal His_6 tagged proteins. Five L of each cell culture were grown to an OD_{600} of 0.8 at 37°C in LB containing 100 µg/ml ampicillin and 50 µg/ml kanamycin and gene expression was induced by the addition of 0.6 mM isopropyl-β-D-thiogalactopyranoside. Cultivation was continued for 4 h at 25°C until harvest. Cells were suspended in 50 ml column buffer (500 mM NaCl, 25 mM imidazole, 1 mM PMSF, 20 mM $NaPO_4$, pH 7.4) and lysed by three passages through a French pressure cell at 20,000 psi (SLM

Aminco, Silver Spring, MD) and the soluble fraction was loaded onto three stacked 5 ml NTA columns (GE Healthcare Life Sciences) charged with Ni^{2+}. Protein was eluted from the column with elution buffer (500 mM NaCl, 250 mM imidazole, 1 mM PMSF, 20 mM $NaPO_4$, pH 7.0) in a gradient fashion. Pooled fractions were further purified by Äktaprime™ Plus gel filtration HiPrep 26/60 Sephacryl S-300 HR (GE Healthcare). The column was equilibrated and developed in 100 mM NaCl, 50 mM HEPES, pH 7.0 at 0.5 ml/min, and protein containing fractions were pooled and concentrated by ultrafiltration using 10-kDa regenerated cellulose membranes in a 50 ml and 10 ml Amicon filter units (Millipore, Bedford, MA) and stored at 4°C.

Thermal denaturation studies

Differential scanning fluorimetry (DSF) experiments were performed essentially as described in Webb *et al.* (18) using a Bio-Rad CFX96 Realtime System, C1000™ Thermal Cycler in conjunction with Bio-Rad CFX Manager Software (Life Science Research 2000 Alfred Nobel Dr. Hercules, California 94547, USA). Compounds were dissolved in 100 mM NaCl, 50 mM HEPES, pH 7.0 and used at final concentrations of 10 mM unless otherwise stated. McpU-PR or McpU-PR_{D182E} and SYPRO® Orange (Invitrogen, Grand Island, NY) were diluted in the same buffer to final concentrations of 10 μM protein and a final SYPRO® Orange concentration of 0.7x (from 5,000x stock). Thirty-microliter reactions of all conditions were performed in duplicate. A temperature gradient was applied from 10–85 °C with a 30 sec equilibration at each 0.5 °C. Fluorescence was quantified using the preset parameters for FRET as the fluorophore and SYBR green as the target. Melting temperatures were recorded and averaged.

Isothermal titration calorimetry

McpU-PR and McpU-PR^{D182E} in 100 mM NaCl, 50 mM HEPES, pH 7.0 were concentrated to 601 μM using 10-kDa regenerated cellulose membranes as described above. Measurements were made on a VP-ITC Microcalorimeter (MicroCal, Northampton, MA) at 10 °C to maintain a folded protein population, because the McpU-PR begins to unfold around 20 °C during thermal denaturation (Webb et al. 2014). McpU-PR or McpU-PR^{D182E} were placed in the sample cell and titrated with 5 μl injections of 16.6 mM arginine, aspartate, glutamate, phenylalanine, and proline dissolved in protein dialysis buffer (100 mM NaCl, 50 mM HEPES, pH 7.0). Baselines produced using the compounds dissolved in dialysis buffer was subtracted from each protein titration. Data analysis was carried out using the "one binding sites" model of the MicroCal version of Origin 8.1 software (OriginLab, Northampton, MA).

ACKNOWLEDGMENTS

This study was supported by National Science Foundation grant MCB-1253234. We are indebted to Bahareh Behkam for sharing the Zeiss Axio Observer Research microscope and the Omnicure S1000 UV light source, to Florian Schubot for sharing the ABI7300 real-time PCR system, and to Timofey Arapov, Katherine Broadway, Keith Compton, and Rafael Castaneda Saldana for critical reading of the manuscript.

Table 4.1. Thermal shift of McpU-PR with various organic acids, inorganic salts, and sugars.

Compound	ΔT_m (°C)	Compound	ΔT_m (°C)
Organic acids		Sugars	
Citric acid	14	Arabinose	1.0
Fumaric acid	0	Fructose	0
Glutaronic acid	0	Galacturonic acid	1.5
Itaconic acid	0	Glucose	0
Malic acid	0	Maltose	0
Succinic acid	0	Mannose	0
	0	Rhamnose	0
Inorganic salts		Ribose	0
NaCl	0	Sucrose	0.5
$NaNO_3$	1.5	Xylose	0
KCl	0		

All compounds were tested at final concentrations of 10 and 100 mM, with the exception of citric acid, which was tested at 10 mM. The sugars are D-enantiomers, glutaronic acid is the D-enantiomer, and malic acid is the L-enantiomer. Only maximal temperature shifts are listed.

REFERENCES

1. **Jones KM, Kobayashi H, Davies BW, Taga ME, Walker GC.** 2007. How rhizobial symbionts invade plants: the *Sinorhizobium-Medicago* model. Nat. Rev. Microbiol. **5:**619-633.
2. **Cooper JE.** 2007. Early interactions between legumes and rhizobia: disclosing complexity in a molecular dialogue. J. Appl. Microbiol. **103:**1355-1365.
3. **Suzaki T, Yoro E, Kawaguchi M.** 2015. Leguminous plants: inventors of root nodules to accommodate symbiotic bacteria. Int. Rev. Cell Mol. Biol. **316:**111-158.
4. **Hirsch AM, Lum MR, Downie JA.** 2001. What makes the rhizobia-legume symbiosis so special? Plant Physiol. **127:**1484-1492.
5. **Ames P, Bergman K.** 1981. Competitive advantage provided by bacterial motility in the formation of nodules by *Rhizobium meliloti*. J. Bacteriol. **148:**728-908.
6. **Bergman K, Gulash-Hoffee M, Hovestadt RE, Larosiliere RC, Ronco PG, 2nd, Su L.** 1988. Physiology of behavioral mutants of *Rhizobium meliloti*: evidence for a dual chemotaxis pathway. J. Bacteriol. **170:**3249-3254.
7. **Caetano-Anolles G, Wall LG, De Micheli AT, Macchi EM, Bauer WD, Favelukes G.** 1988. Role of motility and chemotaxis in efficiency of nodulation by *Rhizobium meliloti*. Plant Physiol. **86:**1228-1235.
8. **Dharmatilake AJ, Bauer WD.** 1992. Chemotaxis of *Rhizobium meliloti* towards nodulation gene-inducing compounds from alfalfa roots. Appl. Environ. Microbiol. **58:**1153-1158.
9. **Malek W.** 1989. Chemotaxis in *Rhizobium meliloti* strain L5.30. Microbiology **152:**611-612.
10. **Soby S, Bergman K.** 1983. Motility and chemotaxis of *Rhizobium meliloti* in soil. Appl. Environ. Microbiol. **46:**995-998.
11. **Uren NC.** 2000. Types, amounts and possible functions of compounds released into the rhizosphere by soil-grown plants, p. 19-40. *In* Pinton R, Varanini Z, Nannipiero P (ed.), The Rhizosphere: Biochemistry and Organic Substances at the Soil-Plant Interface. CRC Press, New York.
12. **Scharf BE, Hynes MF, Alexandre GM.** 2016. Chemotaxis signaling systems in model beneficial plant-bacteria associations. Plant Mol. Biol.
13. **Mellor HY, Glenn AR, Arwas R, Dilworth MJ.** 1987. Symbiotic and competitive properties of motility mutants of *Rhizobium trifolii* Ta1. Arch. Microbiol. **148:**34-39.
14. **Miller LD, Yost CK, Hynes MF, Alexandre G.** 2007. The major chemotaxis gene cluster of *Rhizobium leguminosarum* bv. *viciae* is essential for competitive nodulation. Mol. Microbiol. **63:**348-362.
15. **Althabegoiti MJ, Lopez-Garcia SL, Piccinetti C, Mongiardini EJ, Perez-Gimenez J, Quelas JI, Perticari A, Lodeiro AR.** 2008. Strain selection for improvement of *Bradyrhizobium japonicum* competitiveness for nodulation of soybean. FEMS Microbiol. Lett. **282:**115-123.
16. **Nelson EB.** 2004. Microbial dynamics and interactions in the spermosphere. Annu. Rev. Phytopathol. **42:**271-309.
17. **Barbour WM, Hattermann DR, Stacey G.** 1991. Chemotaxis of *Bradyrhizobium japonicum* to soybean exudates. Appl. Environ. Microbiol. **57:**2635-2639.
18. **Webb BA, Hildreth S, Helm RF, Scharf BE.** 2014. *Sinorhizobium meliloti* chemoreceptor McpU mediates chemotaxis toward host plant exudates through direct proline sensing. Appl. Environ. Microbiol. **80:**3404-3415.

19. **Gaworzewska ET, Carlile MJ.** 1982. Positive chemotaxis of *Rhizobium leguminosarum* and other bacteria towards root exudates from legumes and other plants. J. of Gen. Microbiol. **128:**1179-1188.
20. **Webb BA, Helm RF, Scharf BE.** 2016. Contribution of individual chemoreceptors to *Sinorhizobium meliloti* chemotaxist towards amino acids of host and nonhost seed exudates. Mol. Plant Microbe Interact. **29:**231-239.
21. **Meier VM, Muschler P, Scharf BE.** 2007. Functional analysis of nine putative chemoreceptor proteins in *Sinorhizobium meliloti*. J. Bacteriol. **189:**1816-1826.
22. **Anantharaman V, Aravind L.** 2000. Cache - a signaling domain common to animal Ca(2^+)-channel subunits and a class of prokaryotic chemotaxis receptors. Trends Biochem. Sci. **25:**535-537.
23. **McKellar JL, Minnell JJ, Gerth ML.** 2015. A high-throughput screen for ligand binding reveals the specificities of three amino acid chemoreceptors from *Pseudomonas syringae* pv. *actinidiae*. Mol. Microbiol. **96:**694-707.
24. **Glekas GD, Mulhern BJ, Kroc A, Duelfer KA, Lei V, Rao CV, Ordal GW.** 2012. The *Bacillus subtilis* chemoreceptor McpC senses multiple ligands using two discrete mechanisms. J. Biol. Chem. **287:**39412-39418.
25. **Ulrich LE, Zhulin IB.** 2005. Four-helix bundle: a ubiquitous sensory module in prokaryotic signal transduction. Bioinformatics **21 Suppl 3:**iii45-iii48.
26. **Reyes-Darias JA, Yang Y, Sourjik V, Krell T.** 2015. Correlation between signal input and output in PctA and PctB amino acid chemoreceptor of *Pseudomonas aeruginosa*. Mol. Microbiol. **96:**513-525.
27. **Niesen FH, Berglund H, Vedadi M.** 2007. The use of differential scanning fluorimetry to detect ligand interactions that promote protein stability. Nat Protoc **2:**2212-2221.
28. **Mesibov R, Adler J.** 1972. Chemotaxis toward amino acids in *Escherichia coli*. J. Bacteriol. **112:**315-326.
29. **Götz R, Limmer N, Ober K, Schmitt R.** 1982. Motility and chemotaxis in two strains of *Rhizobium* with complex flagella. J. Gen. Microbiol. **128:**789-798.
30. **Dunn MF.** 2015. Key roles of microsymbiont amino acid metabolism in rhizobia-legume interactions. Crit. Rev. Microbiol. **41:**411-451.
31. **Mauchline TH, Fowler JE, East AK, Sartor AL, Zaheer R, Hosie AH, Poole PS, Finan TM.** 2006. Mapping the *Sinorhizobium meliloti* 1021 solute-binding protein-dependent transportome. Proc. Natl. Acad. Sci. U S A **103:**17933-17938.
32. **Makhatadze GI, Privalov PL.** 1992. Protein interactions with urea and guanidinium chloride. A calorimetric study. J. Mol. Biol. **226:**491-505.
33. **Du X, Li Y, Xia YL, Ai SM, Liang J, Sang P, Ji XL, Liu SQ.** 2016. Insights into Protein-Ligand Interactions: Mechanisms, Models, and Methods. Int. J. Mol. Sci. **17**.
34. **Pleier E, Schmitt R.** 1991. Expression of two *Rhizobium meliloti* flagellin genes and their contribution to the complex filament structure. J. Bacteriol. **173:**2077-2085.
35. **Platzer J, Sterr W, Hausmann M, Schmitt R.** 1997. Three genes of a motility operon and their role in flagellar rotary speed variation in *Rhizobium meliloti*. J. Bacteriol. **179:**6391-6399.
36. **Sourjik V, Schmitt R.** 1996. Different roles of CheY1 and CheY2 in the chemotaxis of *Rhizobium meliloti*. Mol. Microbiol. **22:**427-436.
37. **Rasband WS.** ImageJ, U. S. National Institutes of Health, Bethesda, Maryland, USA. http://imagej.nih.gov/ij/**:**1997-2014.

38. **Balaji J.** 2014. Time Series Analyzer Version 3.0. Dept. of Neurobiology, UCLA.

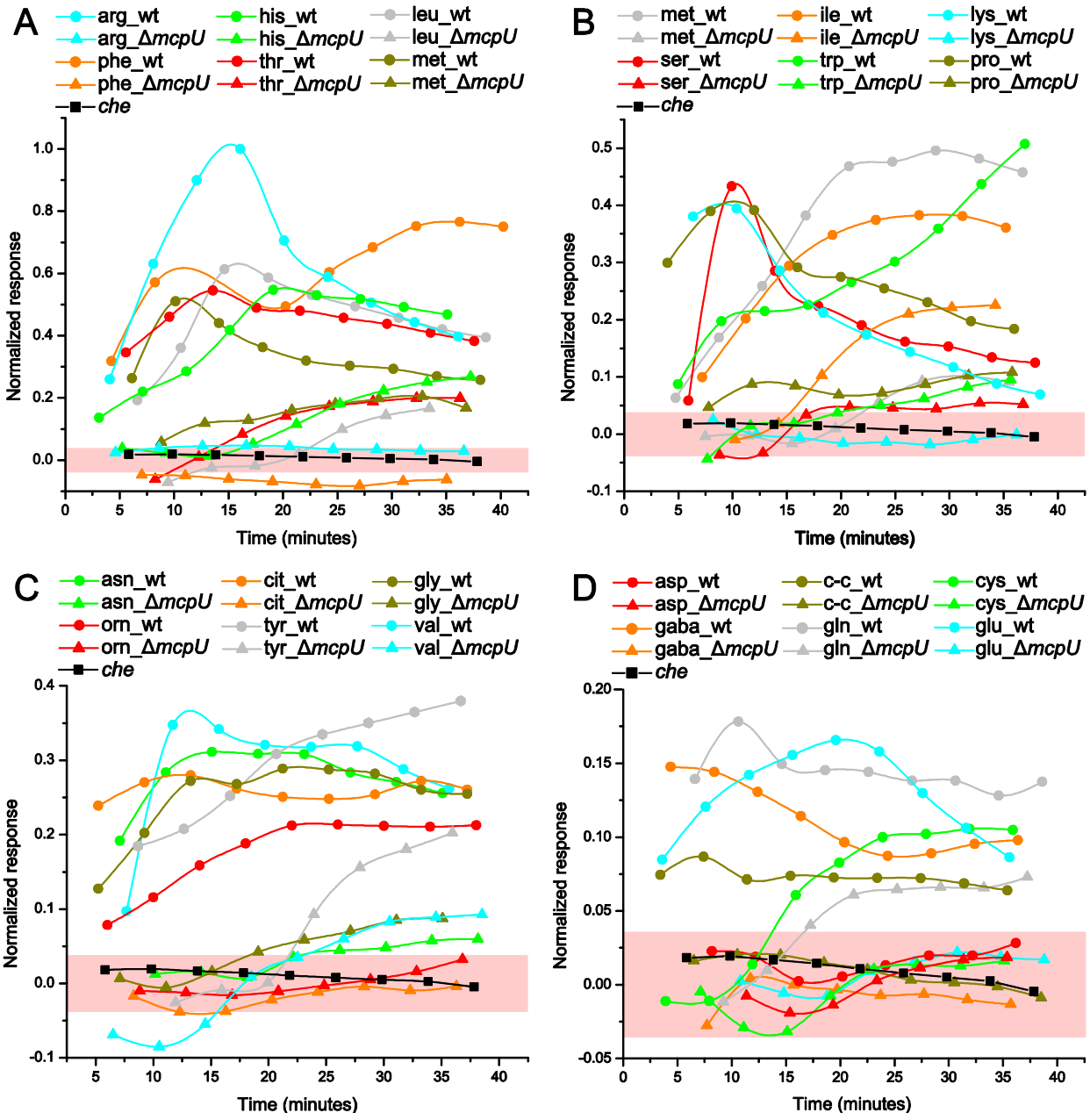

Fig. 4.1 Chemotaxis responses of *S. meliloti* wild type and the Δ*mcpU* strain to AAs at a concentration of 1 mM in the hydrogel capillary assay. Images were taken every four minutes and the pixel intensities at the mouth of the capillaries were quantified and normalized to the maximum response observed (wild-type response to arginine at 16 min). Wild-type (●) and Δ*mcpU* (■) responses to each AA are color-coded and grouped from the highest to the weakest response;

A. 0.51-1.00; **B.** 0.38-0.50; **C.** 0.21-0.38, and **D.** 0.09-0.18, respectively. The response of the *che* strain (black squares and lines in A - D) to arg is given for comparison. The pink box in each graph represents the region of no response as determined by fluctuations in background pixel intensity (± 0.036).

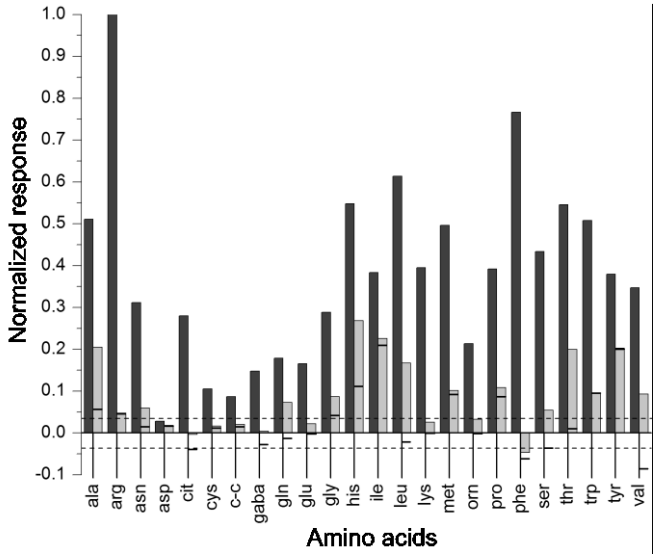

Fig. 4.2 Maximal peak responses of *S. meliloti* wild type (dark gray) and the Δ*mcpU* strain (light gray) to AAs normalized to the maximum response to arg at 16 min. The horizontal lines in columns of the Δ*mcpU* strain reflect its response at the time of wild-type peak response. The dotted lines depict the region of no response.

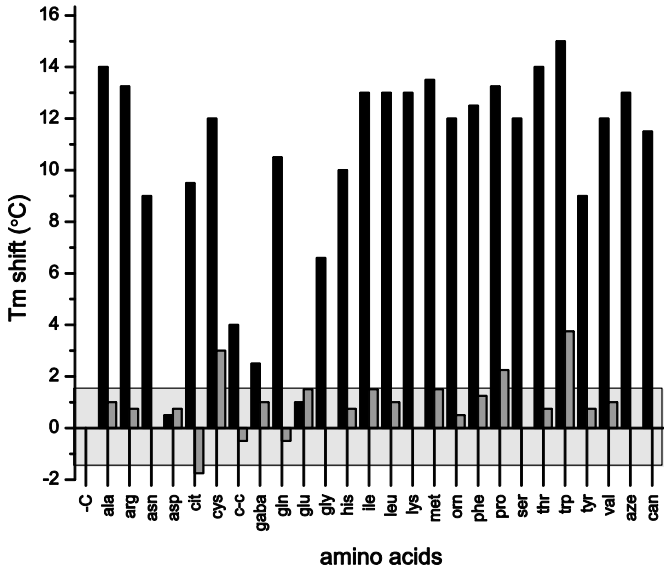

Fig. 4.3 Interaction of McpU-PR and McpU-PR^{D182E} with AAs determined by differential scanning fluorimetry. Protein stability was monitored as a function of fluorescence intensity and the T_m shift was recorded after subtraction of the negative control. McpU-PR (black) and McpU-PR^{D182E} (dark gray) were tested at a concentration of 10 μM with or without 10 mM of each AA with the following exceptions due to solubility limitations: asn, 9.4 mM; asp, 4.8 mM; c-c, 0.115 mM; glu, 4.3 mM; phe, 6 mM; trp, 5.8 mM; and tyr, 0.62 mM. Cit, citrulline; c-c, cystine; orn, ornithine. The horizontal box (light gray) represents the background (± 1.5 °C) encompassing the range in fluctuation of fluorescence from the negative control.

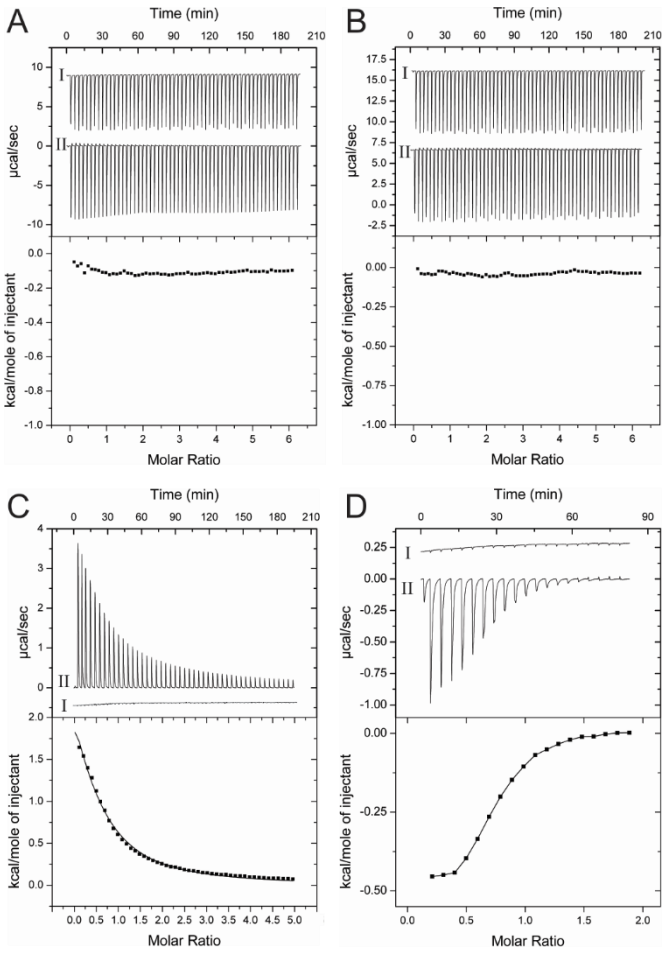

Fig. 4.4 Isothermal titration calorimetry with McpU-PR and AAs. The upper panels show raw titration data of protein (I) and buffer (II), the lower panels are the integrated and dilution corrected peak areas of the raw titration data. **A.** 601 µM McpU-PR with 16.6 mM asp; **B.** 601 µM McpU-PR with 16.6 mM glu; **C.** 601 µM McpU-PR with 16.6 mM phe; **D.** 601 µM McpU-PR with 16.6 mM pro. Data were fit with the One-set-of-sites model of the MicroCal version of Origin7 (Northampton, MA).

Chapter 5 - *Sinorhizobium meliloti* chemotaxis to quaternary ammonium compounds is mediated by the novel chemoreceptor McpX

BENJAMIN A. WEBB[1], K. KARL COMPTON[1], RAFAEL CASTAÑEDA SALDAÑA[1], TIMOFEY ARAPOV[1], W. KEITH RAY[2], RICHARD F. HELM[2], AND BIRGIT E. SCHARF[1]*

[1]Virginia Tech, Department of Biological Sciences, Life Sciences I, Blacksburg, VA 24061;

[2]Virginia Tech, Department of Biochemistry, Life Sciences I, Blacksburg, VA 24061

Key words: betaine, motility, osmoprotectant, plant host exudate, rhizosphere, symbiosis

* For correspondence:
E-mail bscharf@vt.edu
Tel (+1) 540 231 0757
Fax (+1) 540 231 4043
Biological Sciences, Life Sciences I
Virginia Tech
Blacksburg, VA 24061, USA

Submitted: Molecular Microbiology. Mol. Microbiol. July 11th, 2016. MMI-2016-16087 Manuscript is in revision.

Attribution: BAW created table 5.1. and has generated the data shown here in Fig. 5.2, 5.3b – 5.7. KKC generated the data for Table 5.2. RCS generated the data for Fig. 5.3a. TA created the image alignment script and helped with the method development for image organization, alignment, and analysis. Keith Ray helped with the generation of Supplementary Table 2. BAW, RFH, and BES drafted the final manuscript.

ABSTRACT

The bacterium *Sinorhizobium meliloti* is attracted to seed exudates of its host plant alfalfa (*Medicago sativa*). Since quaternary ammonium compounds (QACs) are exuded by germinating seeds, we assayed chemotaxis of *S. meliloti* towards betonicine, choline, glycine betaine, stachydrine, and trigonelline. The wild type displayed a positive response to all QACs. Using LC-MS, we determined that each germinating alfalfa seed exuded QACs in the nanogram range. Compared to the closely related non-host species, spotted medic (*Medicago arabica*), unique profiles were released. Further assessments of single chemoreceptor deletion strains revealed that an *mcpX* deletion strain displayed little to no response to these compounds. Differential scanning fluorimetry showed interaction of the isolated periplasmic region of McpX ($McpX^{PR}$, $McpX_{34\text{-}306}$) with QACs. Isothermal titration calorimetry experiments revealed tight binding to $McpX^{PR}$ with nanomolar dissociation constants (K_d) for choline and glycine betaine, micromolar K_d's for stachydrine and trigonelline, whereas titration with betonicine exhibited a K_d in the millimolar range. Our discovery of *S. meliloti* chemotaxis to plant-derived QACs adds another role to this group of compounds, which are known to serve as nutrient sources, osmoprotectants, and cell-to-cell signalling molecules. This is the first report of a bacterial chemoreceptor that mediates QACs taxis through direct binding.

INTRODUCTION

Bacteria of the *Rhizobiaceae* family have the ability to form a species-specific mutualism with plants of the *Leguminosae* family. This intimate relationship takes place inside of the legume root, specifically in a plant organ called the nodule (Jones *et al.*, 2007, Cooper, 2007, Suzaki *et al.*, 2015). During nodule formation, the rhizobia undergo metamorphosis into bacteroids, which then fix atmospheric nitrogen into ammonium. This form of nitrogen is utilised by the plant to aid in abundant growth (Jones *et al.*, 2007, Hirsch *et al.*, 2001). Bacterial chemotaxis precedes the mutualism and enables cells to actively swim through the soil by responding to host-released compounds and accumulate in the spermosphere and rhizosphere (Ames & Bergman, 1981, Bergman *et al.*, 1988, Caetano-Anolles *et al.*, 1988, Dharmatilake & Bauer, 1992, Malek, 1989, Soby & Bergman, 1983, Uren, 2000, Scharf *et al.*, 2016). Rhizobial motility and chemotaxis have been recognized to improve symbiotic interactions of *Bradyhizobium japonicum*, *Rhizobium leguminosarum*, *Rhizobium trifolii*, and *Sinorhizobium meliloti*, with soybean, pea, clover, and alfalfa, respectively (Ames & Bergman, 1981, Caetano-Anolles *et al.*, 1988, Mellor *et al.*, 1987, Miller *et al.*, 2007, Althabegoiti *et al.*, 2008).

Germinating seeds exude numerous compounds into the soil creating a species-specific spermosphere (Nelson, 2004). Seed exudates include a large variety of metabolites such as amino acids, organic acids, sugars, lipids, and flavonoids (Barbour *et al.*, 1991, Nelson, 2004, Webb *et al.*, 2014). Chemotaxis towards host seed exudates have been described for *B. japonicum*, *R. leguminosarum*, and *S. meliloti* (Barbour *et al.*, 1991, Gaworzewska & Carlile, 1982, Webb *et al.*, 2014, Webb *et al.*, 2016). However, the complex composition of exudates hampers the identification of individual molecules shaping the chemotactic response.

Attractants for flagellar-mediated bacterial chemotaxis are generally perceived by Methyl

accepting Chemotaxis Proteins (MCPs). *S. meliloti* uses eight chemoreceptors, namely seven methyl-accepting chemotaxis proteins (McpT to McpZ) and one internal chemotaxis protein (IcpA) (Meier *et al.*, 2007). Each chemoreceptor is composed of a distinctive sensing domain and a highly conserved signalling domain. Six of the MCPs are localized to the cytoplasmic membrane via two transmembrane-spanning regions, whereas McpY and IcpA lack such transmembrane domains (Meier *et al.*, 2007). A variety of molecules have been recognized to serve as chemoattractants, including amino acids, organic acids, and sugars, but the cognate chemoreceptors are mostly unidentified (Meier *et al.*, 2007). Through behavioural and *in vitro* binding assays, we recently discovered that *S. meliloti* McpU mediates proline chemotaxis via direct binding (Webb *et al.*, 2014). McpU was also found to be an important sensor for exudates from germinating alfalfa seeds and for the amino acid portion of exudates (Webb *et al.*, 2016). The periplasmic region of McpU ($McpU^{PR}$) contains two Cache_1 domains. In general, Cache domains bind small molecules, such as amino acids (Anantharaman & Aravind, 2000, Anantharaman *et al.*, 2001, Zhulin *et al.*, 2003). Mutational analyses and molecular modeling showed that ligands bind to the proximal McpU Cache domain (Webb *et al.*, 2014). A second *S. meliloti* chemoreceptor with a Cache_1 domain is McpX. However, cognate ligands for McpX or any of the remaining six chemoreceptors are unidentified.

One group of metabolites exuded by plant seeds and roots are quaternary ammonium compounds (QACs) (Phillips *et al.*, 1995). This compound class includes betaines, which possess a positively charged ammonium cation that bears no hydrogen atom and a negatively charged carboxylate and are therefore zwitterionic, and the positively charged choline, which is a precursor of glycine betaine. Many QACs are prevalent in organisms and serve as nutrient sources, osmoprotectants, and cell-to-cell signalling molecules (Chambers & Kunin, 1987, Kunin *et al.*, 1992, Lever *et al.*,

1994, Phillips *et al.*, 1992, Phillips *et al.*, 1998). Examples of betaines detected in plant tissues include betonicine (hydroxyproline betaine), glycine betaine, stachydrine (proline betaine), and trigonelline (Fig. 5.1). Stachydrine and trigonelline have been shown to be released from alfalfa seeds in quantities of 1.1 and 2.3 nmoles per seed, respectively (Phillips *et al.*, 1992). Like flavonoids, stachydrine and trigonelline have been described to induce *S. meliloti nodD2* gene activity, which is important for the initiation process of nodulation (Phillips *et al.*, 1992). In *S. meliloti*, QACs can serve as nutrient sources as well as osmoprotectants (Boncompagni *et al.*, 1999, Barra *et al.*, 2006, Gouffi *et al.*, 2000, Boivin *et al.*, 1990). Moreover, chemoattraction of phytoplankton and marine bacterial species to glycine betaine has been reported to play a role in the marine microbial food web (Seymour *et al.*, 2010). Finally, the archaeon *Halobacterium salinarum* is attracted to glycine betaine, choline, and carnitine (Kokoeva *et al.*, 2002). The study implicated an indirect sensing mechanism via a periplasmic binding protein forming a complex with these quaternary amines, which then binds to a transmembrane MCP (Kokoeva *et al.*, 2002). In this study, we quantified QACs (Fig. 5.1) exuded from germinating host and non-host seeds, analysed the chemotactic behaviour of *S. meliloti* toward individual QACs, identified the cognate chemoreceptor, McpX, and its *in vitro* binding characteristics to QACs. This is the first report of a bacterial chemoreceptor that mediates chemotaxis to QACs through direct binding.

RESULTS

Quaternary ammonium compound (QAC) quantification in seed exudates

We previously found the attractant proline and other amino acids to be exuded by host seeds and identified the chemoreceptor McpU as a universal amino acid sensor (Webb *et al.*, 2014, Webb *et al.*, 2016). Expanding upon this work, we performed a general LC-MS screen using hydrophilic interaction chromatography (HILIC) in positive ion mode, evaluating the seed exudates of *S. meliloti* host alfalfa (*Medicago sativa*) and closely related non-host spotted medic (*Medicago arabica*). This work led to the identification of several quaternary ammonium compounds (QACs) in alfalfa and spotted medic seed exudates including betonicine, choline, glycine betaine, stachydrine, and trigonelline. Stachydrine and trigonelline were already known to be exuded by alfalfa seeds (Phillips *et al.*, 1992, Phillips *et al.*, 1995). A preliminary chemotaxis screen revealed a positive response to several QACs for *S. meliloti* wild type (data not shown), prompting the development of a method to quantify the amounts of QACs exuded by germinating seeds of alfalfa and spotted medic by LC-MS/MS (Table 1).

The QAC profiles for alfalfa and spotted medic seed exudates were different, with a total amount of 241 nmol (249 ng) and 225 nmol (221 ng) QACs, respectively. To obtain the concentration of QACs at the seed surface, and therefore a value meaningful for chemotaxis experiments, exuded amounts per seed were converted using experimentally acquired seed volumes of 2.17 μl and 1.84 μl for alfalfa and spotted medic, respectively (Webb *et al.*, 2016). Compounds will diffuse from the seed into the spermosphere, where they are detected by *S. meliloti*. Concentrations at the seed surface are depicted in Figure 5.2 and range from approximately 4 to 400 μM, which are relevant concentrations for bacterial chemotaxis (Webb *et al.*, 2014, Meier *et al.*, 2007, Mello & Tu, 2007). Choline was exuded at the highest concentration and in similar amounts by both legume seeds.

Stachydrine was exuded at a similar concentration by alfalfa seeds, but 4-fold less by spotted medic seeds. Trigonelline was released at about half of the concentration determined for choline. Glycine betaine was exuded at 10-fold higher concentrations by spotted medic than alfalfa, but about 4-fold less than choline. Finally, betonicine release was much lower than the other measured compounds for alfalfa and not detectable for spotted medic. In comparison, glycine and proline, which are structurally similar to glycine betaine and stachydrine, are exuded at approximately 5-fold and 2.5-fold higher concentrations from alfalfa and spotted medic, respectively, when compared to choline (Webb *et al.*, 2016). Therefore, QACs are exuded from host and non-host seeds in chemotactically relevant concentrations and with unique profiles.

Chemotaxis of S. meliloti *wild type toward QACs*

Since QACs are exuded at concentrations relevant to bacterial chemotaxis, we investigated their chemotactic potency using the Adler capillary assay. We determined concentration-response curves for the five QACs in comparison with proline. The wild-type strain RU11/001 was attracted to all QACs with a maximal response at 1 mM choline and 100 mM for the remaining four QACs (Fig. 5.3). Responses were highest for stachydrine, followed by glycine betaine, trigonelline, and betonicine. Maximal response to choline was 4-fold lower than that to stachydrine. Compared to the wild-type response to proline with a maximal response at 10 mM, stachydrine and glycine betaine elicited a stronger response, while responses to trigonelline and betonicine were comparable. No response of the chemotaxis-negative strain (RU13/149; *che* strain) to stachydrine was observed (Fig. 5.3), and the same result was obtained for betonicine (data not shown). Altogether, the QACs elicit positive chemotactic responses from *S. meliloti* wild type. Choline is a weaker attractant, but elicits a response at lower concentrations than the other QACs tested.

Identification of chemoreceptors involved in QAC sensing

To identify the chemoreceptor(s) involved in QAC sensing, we used the semi-quantitative chemotaxis drop assay to screen *S. meliloti* wild type, eight single chemoreceptor deletion mutants, and a non-chemotactic *che* strain. In this assay, the accumulation of bacteria around the site of an attractant drop is observed as the formation of a denser cloud or ring, and responses were semi-quantified by comparison of pixel intensity using ImageJ. Two amino acids, glycine and proline were also included in the assay due to their structural similarities to glycine betaine and stachydrine. While the *che* strain showed no chemotactic response to any of the compounds (Table 2), the wild type displayed a strong positive response to all QACs except for betonicine, which elicited a moderate response. The majority of the strains showed a behaviour similar to wild type. Most profoundly, the Δ*mcpX* strain exhibited no response to any of the QACs and only a weak response to choline. It should be noted that the Δ*icpA* strain displayed weaker responses to all QACs and both amino acids as compared to wild type, but that responses were still more pronounced than those of the Δ*mcpX* strain. In conclusion, this screen clearly identified McpX as a chemoreceptor for QACs and indicated some involvement of IcpA. Since IcpA is assumed to be an energy sensor that senses intracellular metabolites, and therefore is thought to mediate chemotaxis indirectly, we focused our studies on McpX.

QACs and proline interact with the periplasmic region of McpX (McpX^{PR})

Chemoattractants can interact directly with the periplasmic region of chemoreceptors or they bind to a periplasmic binding protein, which then interacts with the chemoreceptor to elicit a response (Zhang *et al.*, 1999). To test whether the QACs bind to the isolated sensing domain *in vitro*, we overexpressed and purified the periplasmic region of McpX (McpX^{PR}, McpX$_{34\text{-}306}$) fused N-

terminally with a His_6 tag by affinity and size exclusion chromatography. Next, we performed differential scanning fluorimetry, which allows the identification of ligands that bind and stabilize purified proteins (Niesen *et al.*, 2007). The transition midpoint, T_m, during thermal unfolding of proteins shifts to higher temperatures upon binding of a low-molecular weight ligand. The T_m of $McpX^{PR}$ was determined to be 45.0 ± 0.0 °C in the absence of a ligand and increased in the presence of all QACs (Fig. 5.4A), indicating that they stabilize $McpX^{PR}$ through direct interaction. Betonicine caused the smallest shift (1 °C), while the addition of choline and glycine betaine resulted in larger shifts of 10 °C. Furthermore, we observed a dose response effect of $McpX^{PR}$ stability at 10-fold lower concentrations of QACs, in particular, T_m shifts were reduced by 0.5 to 3.5 °C (data not shown). We also analysed the binding of all proteinogenic amino acids and found that only proline caused a significant shift in T_m. Large negative shifts were observed for the acidic amino acids aspartate and glutamate. However, destabilisation is not typically observed upon ligand binding, and we attribute the reduction of T_m to unspecific protein destabilization. In summary, QACs and proline directly interact with the sensing domain of McpX.

Quantification of QAC chemotaxis in S. meliloti *wild type and the* mcpX *deletion strain*

The semi-quantitative drop assay and the DSF analysis identified McpX as a chemoreceptor for QACs (Table 2, Fig. 5.4). To quantify the importance of McpX for QAC chemotaxis, the responses of wild type and the Δ*mcpX* strain were compared in the high-throughput quantitative hydrogel capillary assay, which monitors responses in real-time under pseudo dark field microscopy. In this assay, a hydrogel capillary containing attractant is submersed in a bacterial pond, the region around the mouth of the capillary is imaged as cells accumulate at the source of attractant, and the increase in pixel intensity caused by the accumulation of cells is quantified. Capillaries were observed over

a period of 60 minutes allowing for the observation of cell accumulation due to attraction as well as cell dissipation most likely due to depletion of the attractants from the capillary into the bacterial pond. The wild type displayed a peak in response for betonicine, choline, glycine betaine, stachydrine, and trigonelline at 30, 50, 35, 20, and 19 minutes, respectively (Fig. 5.5A-E). The Δ*mcpX* strain showed no response when exposed to choline, glycine betaine, or trigonelline. However, positive responses were observed for betonicine and stachydrine albeit the peak responses were approximately 60% and 40% of the wild-type peak responses (Fig. 5.5F). This assay confirmed McpX as QAC receptor and revealed its indispensability for *S. meliloti* chemotaxis to choline, glycine betaine, and trigonelline, and its important contribution to betonicine and stachydrine chemotaxis.

QACs bind directly to McpX^{PR}

To determine binding parameters of McpX^{PR} with the QACs and proline, we performed isothermal calorimetry at 15 °C using a MicroCal VP-ITC. Titrations with all compounds produced exothermic heat signals until saturation confirming direct binding (Fig. 5.6). Data was fit with a one binding site model for titrations with betonicine, proline, stachydrine, and trigonelline. Upon fitting the data from choline and glycine betaine titration, we found that a model for two binding sites provided the best fits. The dissociation constants (K_d) for compounds fit with the "one binding site" model were calculated to be 2.3 mM with betonicine, 45.2 μM for proline, 3.8 μM with stachydrine, and 88.5 μM with trigonelline. The dissociation constants for compounds fit with the "two binding sites" model were calculated to be 123 nM and 2.1 μM with glycine betaine; 366 nM and 6 nM for choline. Therefore, choline and glycine betaine exhibit the strongest affinity to McpX^{PR}, followed by stachydrine, proline, trigonelline, and betonicine. Together, the ITC data

confirmed results gained from the DSF experiments and allowed ranking of compounds by affinity.

Analysis of a second binding site for QACs in McpX^{PR}

Choline and glycine betaine titrations of McpX^{PR} were best fit with the "two binding site" model. This observation led us to investigate closer whether McpX^{PR} has indeed two different ligand binding sites. If McpX^{PR} has only one binding site, then titration of protein previously saturated with a weaker ligand should produce a change in enthalpy (ΔH) due to displacement of the weaker ligand, and the apparent K_d ($K_{d\ app}$) should be weaker for the ligand with a higher affinity. If McpX^{PR} has two ligand binding sites, then titration of the protein previously saturated with a weaker ligand should yield the same change in enthalpy and $K_{d\ app}$ since the stronger ligand would bind to an empty site.

To aid in predicting the outcome of displacing the weaker ligand trigonelline with the strong ligand glycine betaine, the displacement titration was modeled *in silico* with ITCSim (MicroCal) using the experimentally acquired binding parameters for each ligand to McpX^{PR}. Upon displacement of trigonelline by glycine betaine, a predicted positive ΔH of about 7,600 calories/mol and a $K_{d\ app}$ of 1.0 μM for a one-binding site model was obtained (Fig. 5.7A). Upon actual experimentation, a negative enthalpy (-6,990 ± 337 calories/mol), similar to the direct titration with glycine betaine was measured (-6,151 ± 76 calories/mol), and the $K_{d\ app}$ was closer to the K_d calculated from the direct titration with glycine betaine (105 nM). These results indicate that glycine betaine binds to a site separate from trigonelline.

DISCUSSION

Plant root exudates mediate root-rhizosphere signalling and therefore shape soil microbial communities (Badri & Vivanco, 2009). The interaction of legumes with their bacterial symbiont is initiated by the release of attractants from host-plant germinating seeds and roots, followed by directed movement of the rhizobacterium towards the plant-borne attractants. We aim to classify host plant-derived attractants and their cognate chemoreceptors in the model organism *S. meliloti* to enhance our knowledge of this important symbiotic relationship. Previously, we established that the chemoreceptor McpU mediates chemotaxis to proline and other plant-borne amino acids (Webb *et al.*, 2016, Webb *et al.*, 2014). Here, we analysed the release of quaternary ammonium compounds (QACs) by legume seeds and characterised chemotaxis of *S. meliloti* towards QACs through behavioural and *in vitro* binding assays.

Our findings demonstrate that the QACs betonicine, choline, glycine betaine, stachydrine, and trigonelline are exuded by germinating seeds of alfalfa and spotted medic. We also identified homostachydrine in the seed exudates of alfalfa and spotted medic (data not shown). However, it was not quantified in this study due to the lack of a molecular standard. While stachydrine and trigonelline release from alfalfa seeds has been reported previously (Phillips *et al.*, 1992, Phillips *et al.*, 1995), the release of betonicine, choline, and glycine betaine is a new finding. We determined that a single seed of either species exudes a total of over 2 nmol QACs, which results in concentrations of individual compounds on the seed surface of up to 400 μM. The structurally similar amino acids, proline and glycine, yield seed surface concentrations of 1 and 2 mM, respectively (Webb *et al.*, 2016). Choline, a precursor of glycine betaine, is released in highest concentration and similar amounts from both legume seeds. The other four QACs, which are all betaines, exhibit more unique profiles. Stachydrine is the betaine exuded in the highest

concentration from alfalfa seeds and has been known to be the most abundant betaine in alfalfa tissues (Trinchant *et al.*, 2004). It can be speculated that differences in release profiles between host and non-host seeds contribute to a specific attraction of *S. meliloti* to the alfalfa rhizosphere. The amounts of betaines in legume tissues differ between species. While alfalfa tissues have been shown to contain betonicine, homostachydrine (pipecolate betaine), and stachydrine, the closely related red clover (*Trifolium pratense*) lacks homostachydrine and stachydrine, but contains higher levels of glycine betaine and trigonelline (Wood *et al.*, 1991).

As microbes adjust to the changes in osmolarity and salinity of an environment, they accumulate compatible solutes (Wood, 1999). Betaines, choline and certain amino acids such as proline are compatible solutes that protect bacterial cellular components and contribute to osmotic homeostasis and growth, thus serving as osmoprotectants (Gouffi *et al.*, 2000, McNeil *et al.*, 1999, Moe, 2013). Compatible solutes are utilised to various extents by different bacterial species. In *S. meliloti*, betaines are the best osmoprotectants, proline serves as an intermediate osmoprotectant, while choline is not used (Barra *et al.*, 2006, Boncompagni *et al.*, 1999, Alloing *et al.*, 2006, Smith *et al.*, 1988). Interestingly, there appears to be a positive correlation between the qualities as osmoprotectant and chemoattractant in *S. meliloti*. In the Adler capillary assay (Fig. 5.3), betaines attracted a larger number of *S. meliloti* cells as compared to proline and even more so to choline, although higher concentrations of betaines were required to elicit that response. The dose-response curves for betonicine, stachydrine, and trigonelline increased steeply to their peak at 100 mM, whereas response curves elicited by choline and glycine betaine were rather broad. This behaviour correlates with the optimal attractant concentrations used in the hydrogel assay, with the latter two QACs being assayed at 1 mM, compared to 50 mM for the remaining QACs (Fig. 5.5). The Δ*mcpX* strain lacked a response to choline, glycine betaine, and trigonelline, but only diminished its

response to betonicine and stachydrine by 40 and 60%, respectively, indicating that other receptors contribute to QAC sensing. A strong candidate for the second QAC receptor is IcpA, because the *icpA* deletion strain was the only other strain that displayed a reduced response to all QACs in the drop assay (Table 2). We are currently testing this notion by creating a Δ*icpA* Δ*mcpX* strain and assaying for QAC chemotaxis. In addition, the Δ*icpA* strain showed a reduced response to glycine and proline. The broad attractant spectrum of IcpA supports our hypothesis that IcpA serves as energy sensor, measuring the metabolic state of the cell (Meier *et al.*, 2007). In fact, metabolism by *S. meliloti* has been shown for several QACs (Burnet *et al.*, 2000, Goldmann *et al.*, 1991, Boncompagni *et al.*, 1999).

It would be interesting to investigate whether the *S. meliloti*-alfalfa symbiosis could be enhanced by QAC overproduction in the host plant and subsequent increased attraction of the symbiont to the rhizosphere of its host. Elevated glycine betaine levels have been generated in tomato plants by transformation with a bacterial *codA* gene that encodes choline oxidase to catalyze the conversion of choline to glycine betaine. This procedure yielded accumulation of glycine betaine resulting in greater tolerance to high temperatures and chilling stress during seed germination and plant growth (Li *et al.*, 2011, Park *et al.*, 2004). Furthermore, transgenic *Arabidopsis thaliana* expressing *codA* or two cyanobacterial glycine N-methyltransferases exhibited elevated levels of glycine betaine leading to improved abiotic stress tolerance (Huang *et al.*, 2008, Waditee *et al.*, 2005). In addition, traditional plant breeding yielded corn plants with an approximately 400-fold increase of glycine betaine in leaves (Rhodes *et al.*, 1989). Much work has been done to selectively breed alfalfa for growth in high saline soils, especially to generate seeds that tolerate high salinity during germination (Bhardwaj *et al.*, 2010, Anower *et al.*, 2013). It would be interesting to explore whether high-salinity resistance alfalfa breeds are expressing higher QAC levels and

simultaneously attracting a higher number of *S. meliloti* cells to their rhizosphere. In conclusion, enhanced production and release of compatible solutes by alfalfa can mediate high-salinity resistance to host and microsymbiont, attracts the symbiont to its host, protects it from high salt conditions, and propagates symbiosis.

Results from both *in vitro* binding assays, DSF and ITC, demonstrated direct binding of the periplasmic region of McpX ($MxpX^{PR}$) to all QACs as well as to proline. These findings are in agreement with the behavioural assays, supporting the conclusion that McpX is a QAC chemoreceptor mediating response through direct binding. The binding affinities obtained from the ITC studies correlate well with the size of the thermal shifts observed in DSF assays. In particular, choline (K_d = 6.0 nM) produced the largest shift in DSF, while addition of betonicine (K_d = 2.3 mM) resulted in the smallest significant shift (Fig. 5.5). There appears to be a correlation between QACs binding strength (Figs. 5.4 & 5.7), *S. meliloti* chemotaxis response (Figs. 5.3 & 5.5), and amounts released from germinating seeds (Table 5.1, Fig. 5.2). Choline, which yielded the highest concentrations on the seed surface, displayed the lowest K_d in the ITC assay, and elicited a chemotaxis response at concentrations as low as 0.1 and 1.0 mM. In contrast, betonicine, which produced a nearly 100-fold lower concentration on the seed surface, has a 10^6 lower affinity to $MxpX^{PR}$ and elicited a maximal chemotaxis response at 100-fold higher concentration as compared to choline. Thus, it is conceivable to speculate that McpX has evolved to display higher affinities for the more abundant QACs released by its host plant.

Titrations of $McpX^{PR}$ with betonicine, stachydrine, and trigonelline resulted in isotherms that fit well with the one-binding site model resulting in dissociation constants of 2.3 mM, 3.8 μM and 88.5 μM, respectively (Fig. 5.7). However, titrations with choline and glycine betaine yielded isotherms with two observable transitions and were fitted with the one-binding site model at low

confidence. Instead, the two-binding sites model provided the best fit for these curves, each generating two dissociation constants (Fig. 5.7). This result indicates that choline and glycine betaine either bind at two distinct sites with different affinities, or that they bind at one site, yet cause conformational changes that are detected as change in enthalpy.

Simulation of a competition experiment between McpX^{PR} saturated with trigonelline (weak ligand), titrated with glycine betaine (strong ligand) for the one-binding site model predicted a positive enthalpy (endothermic reaction). Experimentally, an exothermic reaction occurred that appears to disprove the one-binding site model (Fig. 5.7). However, data was best fitted with the one-binding site model, yielding an apparent K_d similar to K_d observed during a direct titration (Figs. 5.6 & 5.7). This result could be interpreted in two ways: (i) glycine betaine binds only to one site, but this site is distinct from the trigonelline binding site, or (ii) preceding saturation with trigonelline causes a conformational change that prevents the observation of a second transition. In search for potential residues that form the ligand-binding pocket, homology models of McpX^{PR} were constructed but only yielded low confidence models. We are currently attempting to analyse the binding mechanism by crystallisation and X-ray diffraction data collection of McpX^{PR} complexed with ligands.

This study characterised the first bacterial chemoreceptor that senses QACs. *S. meliloti* McpX mediates chemotaxis to QACs released during host-plant germination into the soil via direct binding. In addition to their function as nutrient sources, osmoprotectants, and cell-to-cell signals, we thus revealed a new function of QACs as chemoattractants.

EXPERIMENTAL PROCEDURES

Bacterial strains and plasmids

E. coli strains and derivatives of *S. meliloti* MV II-1 (Kamberger, 1979) and the plasmids used are listed in Table S1.

Medicago *spp.*

Medicago sativa cultivar 'Guardsman II' (Registration number CV-203, PI 639220; (Althabegoiti *et al.*, 2008) and *Medicago arabica* (L.) Huds. (accession SA7746) seeds were used in this study.

Chemicals

Stachydrine (L-proline betaine) and betonicine (L-hydroxyproline betaine) were purchased from Extrasynthese (Toulouse, France), and choline, glycine betaine and, trigonelline were from Sigma-Fluka (St. Louis, MO, USA). Amino acids were from a Fluka Analytical kit, 21 L-amino acids + glycine). Compounds were dissolved in RB and titrated to pH 7.0 with KOH for behavioural assays. For *in vitro* assays, compounds were dissolved in 100mM NaCl, 50 mM HEPES pH 7.0, and titrated with KOH when necessary.

Media and growth conditions

E. coli strains were grown in lysogeny broth (LB) (Bertani, 1951) at 37°C. *S. meliloti* strains were grown in TYC (0.5% (w/v) tryptone, 0.3% (w/v) yeast extract, 0.087% $CaCl_2$ x 2 H_2O (w/v) [pH 7.0]) at 30°C (Platzer *et al.*, 1997). Motile cells for Adler capillary assays and hydrogel capillary assays were prepared essentially as described in Webb *et al.* 2016 (Webb *et al.*, 2016)with minor modifications. Briefly, overnight were diluted 1:1,000 in 10 ml Rhizobial Basal minimal medium

(RB) (6.1 mM K_2HPO_4, 3.9 mM KH_2PO_4, 1 mM $MgSO_4$, 1 mM $(NH_4)_2SO_4$, 0.1 mM $CaCl_2$, 0.1 mM NaCl, 0.01 mM Na_2MoO_4, 0.001 mM $FeSO_4$, 20 μg l^{-1} biotin, 1 mg l^{-1} thiamine (Götz *et al.*, 1982)) and layered on Bromfield agar plates (Sourjik & Schmitt, 1996). Cultures were harvested at an optical density of 600 nm (OD_{600}) of 0.16 ± 0.02. Motile cells for drop assays were prepared the same way on Bromfield-RB overlay plates, except they were grown to an OD_{600} of 0.33 ± 0.01.

Quantification of quaternary ammonium compounds (QACs) in seed exudates

Seed exudates from seeds (0.1 g) were prepared in triplicate for each *Medicago spp*. as described previously (Webb *et al.*, 2016). A multiple reaction monitoring (MRM) method using authentic standards was developed for the identification and quantification of each QAC essentially as described previously (Servillo *et al.*, 2016, Sánchez-Hernández *et al.*, 2012, Naresh Chary *et al.*, 2012, Li *et al.*, 2010) using the direct infusion method on a 3200 QTrap (ABSciex, see Supporting Information for details). All samples and standards were dissolved in RB and diluted to working concentrations in 90% Buffer A (ACN:50 mM ammonium formate, pH 3.2 (9:1)) and 10% Buffer B (ACN:50 mM ammonium formate, pH 3.2:water (5:4:1)), sonicated for 5 min, and centrifuged at 14,000 x g for 5 min. The sample queue was arranged in a random fashion with RB blank samples on each end and one in the middle. All biological samples were tested in biological triplicates and technical triplicates and standards were tested in technical triplicates. Using an Agilent 1100 series auto sampler, 5 μl of each sample was injected onto a 2.6 μm HILIC 100A HPLC column 100 x 2.1 mm (Kinetex) equipped with a KrudKatcher Ultra (Phenomenex) guard system. The column was equilibrated with 90% Buffer A and 10% Buffer B for 13 min at a flow rate of 200 μl min^{-1}, followed by sample injection and 2 min wash step. Compounds were eluted in a 9-min gradient to 100% Buffer B, followed by 2 min wash of 100% Buffer B. Ion suppression

or enhancement was evident for the detection of all QACs except for stachdyrine in alfalfa exudate. Ion suppression was accounted for by using the standard addition method (Furey *et al.*, 2013). LC-MS data was processed and analysed with Analyst (AB Sciex, Version 1.6).

Chemotaxis drop assay

Hydroxypropyl methylcellulose (HPMC) was added to a final concentration of 0.2% to each *S. meliloti* culture and 1 ml was pipetted into a 35 mm petri plate. One µl of a 100 mM compound solution in RB was spotted in the center, and plates were imaged every two min for 30 min in a Bio-Rad Universal Hood II with standardized camera zoom and constant exposure of 0.65 sec. For each data set, images were imported into ImageJ as an image stack and analysed by setting a 25 pixel diameter circle as 'Region Of Interest (ROI)' around the center of the plate. The z-axis profile of each ROI was plotted for the stack and the average pixel intensity of the first image was subtracted from the average pixel intensity of the image with the highest intensity. The resulting change in average pixel intensity was used to determine the chemotactic response. Responses with a change in pixel intensity of less than 1 were binned into no response (-), changes of 1 to 4 were binned as moderate chemotactic response (+), and changes greater than 4 were categorized as strong chemotactic response (++). The *che* strain served as the negative control.

Traditional Adler capillary assay

Capillary assays were performed essentially as described by Adler (Adler, 1973), with minor modifications (Götz & Schmitt, 1987, Meier *et al.*, 2007). Cells were harvested by centrifugation at 3,000 x g for 5 min at room temperature and suspended in RB to OD_{600} of 0.17. Closed U-shaped tubes (bent from 65 mm micropipettes, Drummond Scientific Co., Broomall, Pennsylvania,

USA) were placed between two glass plates. For each capillary, 375 µl of bacterial suspension were used to make a bacterial pond. Capillary tubes (1 µl disposable micropipettes, Drummond Microcaps) were sealed at one end and filled with QAC solution. The capillaries were inserted open end first into the bacterial pond and incubated for two h at 22.5°C. Capillaries were removed, the sealed end was cut off and the complete contents were transferred into 999 µl RB using a Drummond bulb dispenser. Dilutions were plated in duplicates on TYC plates containing streptomycin. After incubation for three days at 30°C, colonies were counted. Compounds were tested in technical triplicate and the experiments were carried out in biological triplicate.

Hydrogel capillary assay

Capillaries containing a cross-linked hydrogel were prepared according to Webb *et al.* (Webb *et al.*, 2016). Prior to experiments, hydrogel capillaries were equilibrated for eight h with RB with one buffer exchange after the first 4 h. For equilibration of the capillaries with QACs, capillaries were placed into 50 µl of QAC solution per capillary and incubated overnight at 4°C. Motile cells were prepared and harvested by centrifugation at 4,000 x g for 5 min at room temperature and suspended in RB to an OD_{600} of 0.12. Three repetitions of the hydrogel capillary assay were performed as described (Webb *et al.*, 2016). Dose responses for each QAC were performed with wild type and the Δ*mcpX* strain to determine the concentration for optimal imaging of the chemotactic responses. Requirements were an increase in pixel intensity above background, pixel intensity values below the pixel saturation value of 255, and responses that could be completely encapsulated by a drawn 'Region Of Interest (ROI)' across the observed image. The optimal concentrations were determined to be 1 mM for choline and glycine betaine, and 50mM for betonicine, stachydrine, and trigonelline.

Quantification of the responses were essentially performed according to Webb et al. (Webb *et al.*, 2016) with minor modifications. Images from the hydrogel capillary assay were imported to MATLAB (MathWorks) and an Enhanced Correlation Coefficient (ECC) algorithm from the Image Alignment Toolbox (IAT) was utilised to perform a Euclidean transformation of images to align the capillaries in such a way that they rest precisely on top of one another when images were stacked (Evangelidis & Psarakis, 2008, Evangelidis, 2013). Rotated images were then imported to ImageJ (Rasband) as an image sequence. A rectangular region of interest (ROI) spanning 448 pixels wide and 270 pixels high was placed in front of the mouth of the capillary to encapsulate the chemotactic response and the Time Series Analyzer V3 plugin (Balaji, 2014) was utilised to attain the total intensity from this ROI (Response ROI) for each image. To account for background, an ROI with the same dimensions was placed at the top of each image, distant from the chemotactic response (Background ROI). The total intensities obtained from the background of each image were subtracted from their respective intensities of the Response ROIs. These intensity values were then normalized to the greatest total intensity value observed in the comparisons of wild type versus the Δ*mcpX* strain.

Construction of McpX^{PR} overexpressing plasmid

The *mcpX* 100-919 bps fragment was PCR amplified with Phusion DNA polymerase (NEBiolabs) using chromosomal DNA at template and cloned into Qiagen expression vector pQE30 using *Bam*HI and *Hin*dIII sites. Confirmation was obtained by pQE30 specific oligonucleotides and DNA sequencing.

Expression and purification of the periplasmic region of McpX

The recombinant ligand-binding, periplasmic region of McpX ($McpX^{PR}$, $McpX_{34-306}$) was overproduced from plasmid pBS455 in *E. coli* M15/pREP4, providing N-terminal His_6-tagged protein. Four liter of cell culture were grown to an OD_{600} of 0.7 at 37°C in LB containing 100 µg ml^{-1} ampicillin and 50 µg ml^{-1} kanamycin and gene expression was induced by the addition of 0.6 mM isopropyl-β-D-thiogalactopyranoside. Cultivation was continued for 4 h at 25°C and cells were harvested and stored at -30°C. Cells were suspended in 70 ml column buffer (500 mM NaCl, 25 mM imidazole, 20 mM $NaPO_4$, pH 7.4, 2 mM tri(2-carboxyethyl)phosphine (TCEP), 1 mM phenylmethylsulfonyl fluoride (PMSF)) with 1 µg/ml of DNase and lysed by three passages through a French pressure cell at 20,000 psi (SLM Aminco, Silver Spring, MD). The soluble fraction was loaded onto three stacked 5 ml NTA columns (GE Healthcare Life Sciences) charged with Ni^{2+}. Protein was eluted from the column a linear gradient of elution buffer (500 mM NaCl, 350 mM imidazole, 20 mM $NaPO_4$, pH 7.0, 2 mM TCEP, 1 mM PMSF). Protein-containing fractions were pooled and further purified by Äktaprime™ Plus gel filtration on HiPrep 26/60 Sephacryl S-300 HR (GE Healthcare). The column was equilibrated and developed in 100 mM NaCl, 50 mM HEPES, pH 7.0 at 0.5 ml min^{-1}. Protein-containing fractions were pooled, concentrated by ultrafiltration using 10-kDa regenerated cellulose membranes in a 50 ml Amicon filter unit (Millipore, Bedford, MA) and stored at 4°C.

Thermal denaturation studies

Differential scanning fluorimetry (DSF) experiments were performed essentially as described in Webb *et al.* (Webb *et al.*, 2014) using a Bio-Rad CFX96 Realtime System, C1000™ Thermal Cycler in conjunction with Bio-Rad CFX Manager Software (Life Science Research 2000 Alfred Nobel Dr. Hercules, California 94547, USA). Compounds were dissolved in 100 mM NaCl, 50

mM HEPES, pH 7.0 and used at final concentrations of 10 mM unless otherwise stated. McpX^{PR} and SYPRO® Orange (Invitrogen, Grand Island, NY) were diluted in the same buffer to final concentrations of 10 μM protein and 0.7 x SYPRO® Orange (from 5,000 x stock). QACs were tested at 1 mM and 10 mM final concentrations, while amino acids were tested at a final concentration of 10 mM with the following exceptions due to solubility limitations: asn, 9.4 mM; asp, 4.8 mM; c-c, 0.115 mM; glu, 4.3 mM; phe, 6.0 mM; trp, 5.8 mM; and tyr, 0.62 mM. Abbreviations are as follows, cit, citrulline; c-c, cystine; gaba, gamma aminobutyric acid; orn, ornithine. Thirty-microliter reactions of all conditions were performed in duplicate. A temperature gradient was applied from 10 to 85 °C with a 30-s equilibration at each 0.5 °C step. Fluorescence was quantified using the preset FRET parameters (excitation, 490 nm; emission, 530 nm). Melting temperatures were recorded and averaged.

Isothermal titration calorimetry

McpX^{PR} in 100 mM NaCl, 50 mM HEPES, pH 7.0 was used at 183 μM for testing with glycine betaine, 142 μM for testing with proline, 91.5 μM for testing with choline and trigonelline, 80 μM for testing with stachydrine, 75.7 μM for testing with betonicine, and 80 μM for the competition titration with trigonelline and glycine betaine. Ligands were dissolved in spent dialysis buffer (100 mM NaCl, 50 mM HEPES, pH 7.0). Measurements were made on a VP-ITC Microcalorimeter (MicroCal, Northampton, MA) at 15°C. McpX^{PR} was placed in the sample cell and titrated with ligand. Final QAC concentrations were as follows: choline and stachydrine at 1.5 mM; betonicine at 20 mM; proline at 6 mM; glycine betaine at 5.1 mM for the direct titration and 2.22 mM for the competition titration; trigonelline at 4.4 mM for the direct titration and 446 μM for the competition titration. Baselines were produced using the compounds dissolved in dialysis buffer and were

subtracted from each protein titration. For the baseline titration accompanying the competition titration, the cell was filled with trigonelline dissolved in buffer and titrated with glycine betaine. Data analysis was carried with the MicroCal version of Origin 8.1 software using the "one binding sites" model for titration with proline, stachydrine, and trigonelline; the "two-sites" model for choline and glycine betaine; and the "competitive binding" model for the titration of trigonelline-saturated $McpX^{PR}$ with glycine betaine (OriginLab, Northampton, MA). Binding parameters were evaluated *in silico* using ITCSim (MicroCal, Northampton MA).

ACKNOWLEDGMENTS

This study was supported by National Science Foundation grant MCB-1253234. We are grateful to Jody Jervis for sample preparation, Sherry Hildreth for LC-MS analysis, and Madeline Blake for help with drop assays. We are indebted to Bahareh Behkam for sharing the Zeiss Axio Observer Research microscope and the Omnicure S1000 UV light source, to Florian Schubot for sharing the ABI7300 real-time PCR system, and to Pecetti Luciano for *Medicago arabica* (L.) Huds. seeds.

AUTHOR CONTRIBUTION

B.A.W., K.K.C., and R.C.S. conducted the experimental studies and analysed data; B.A.W., W.K.R., and R.F.H. developed the multiple reaction monitoring (MRM) method for the proper QAC identification; T.A. developed the script for hydrogel capillary image analysis, B.A.W. and B.E.S. designed the experiments, interpreted the results and wrote the paper.

Table 5.1. **Amount of QACs exuded per seed of alfalfa and spotted medic**

Compound	ng/seed		pmol/seed	
	alfalfa	spotted medic	alfalfa	spotted medic
betonicine	1.5 ± 0.1	N.D.*	10 ± 0.6	N.D.*
choline	86.2 ± 4.7	91.3 ± 1.5	779 ± 45	893 ± 15
glycine betaine	3.6 ± 0.7	35.2 ± 5.9	31 ± 6	298 ± 50
stachydrine	108.5 ± 4.4	25.6 ± 1.3	758 ± 31	179 ± 9
trigonelline	49.2 ± 6.9	68.7 ± 3.0	827 ± 50	876 ± 22

All compounds were measured in ng/ml of exudate and converted to ng/seed or pmol/seed based on the number seeds in 0.1 g for each species. Each value is the mean of three experiments and standard deviation of the mean.
* Below the limit of detection.

Table 5.2. Chemotactic responses of *S. meliloti* strains with QACs and amino acids.

	betonicine	choline	glycine betaine	stachydrine	trigonelline	glycine	proline
wt	+	++	++	++	++	++	++
Δ*icpA*	-	+	+	+	+	+	+
Δ*mcpT*	+	+	++	++	++	++	++
Δ*mcpU*	++	-	++	++	++	-	++
Δ*mcpV*	+	++	++	++	++	++	++
Δ*mcpW*	+	+	++	+	++	+	++
Δ*mcpX*	-	+	-	-	-	++	+
Δ*mcpY*	++	++	++	++	++	++	++
Δ*mcpZ*	+	++	++	++	++	++	++
che	-	-	-	-	-	-	-

One µl of 100 mM attractant solution was spotted into the center of a culture containing 0.2% hydroxypropyl methylcellulose. Chemotaxis responses were observed as accumulation of bacteria around the site of attractant drop. Images were taken after 25-30 min and change in pixel intensities was determined. - denotes no chemotactic response (changes <1), + denotes moderate chemotactic response (changes 1-4), and ++ denotes strong chemotactic response (changes >4).

REFERENCES

1. **Jones KM, Kobayashi H, Davies BW, Taga ME, Walker GC.** 2007. How rhizobial symbionts invade plants: the *Sinorhizobium-Medicago* model. Nat. Rev. Microbiol. **5:**619-633.
2. **Cooper JE.** 2007. Early interactions between legumes and rhizobia: disclosing complexity in a molecular dialogue. J. Appl. Microbiol. **103:**1355-1365.
3. **Suzaki T, Yoro E, Kawaguchi M.** 2015. Leguminous plants: inventors of root nodules to accommodate symbiotic bacteria. Int. Rev. Cell Mol. Biol. **316:**111-158.
4. **Hirsch AM, Lum MR, Downie JA.** 2001. What makes the rhizobia-legume symbiosis so special? Plant Physiol. **127:**1484-1492.
5. **Ames P, Bergman K.** 1981. Competitive advantage provided by bacterial motility in the formation of nodules by *Rhizobium meliloti*. J. Bacteriol. **148:**728-908.
6. **Bergman K, Gulash-Hoffee M, Hovestadt RE, Larosiliere RC, Ronco PG, 2nd, Su L.** 1988. Physiology of behavioral mutants of *Rhizobium meliloti*: evidence for a dual chemotaxis pathway. J. Bacteriol. **170:**3249-3254.
7. **Caetano-Anolles G, Wall LG, De Micheli AT, Macchi EM, Bauer WD, Favelukes G.** 1988. Role of motility and chemotaxis in efficiency of nodulation by *Rhizobium meliloti*. Plant Physiol. **86:**1228-1235.
8. **Dharmatilake AJ, Bauer WD.** 1992. Chemotaxis of *Rhizobium meliloti* towards nodulation gene-inducing compounds from alfalfa roots. Appl. Environ. Microbiol. **58:**1153-1158.
9. **Malek W.** 1989. Chemotaxis in *Rhizobium meliloti* strain L5.30. Microbiology **152:**611-612.
10. **Soby S, Bergman K.** 1983. Motility and chemotaxis of *Rhizobium meliloti* in soil. Appl. Environ. Microbiol. **46:**995-998.
11. **Uren NC.** 2000. Types, amounts and possible functions of compounds released into the rhizosphere by soil-grown plants, p. 19-40. *In* Pinton R, Varanini Z, Nannipiero P (ed.), The Rhizosphere: Biochemistry and Organic Substances at the Soil-Plant Interface. CRC Press, New York.
12. **Scharf BE, Hynes MF, Alexandre GM.** 2016. Chemotaxis signaling systems in model beneficial plant-bacteria associations. Plant Mol. Biol.
13. **Mellor HY, Glenn AR, Arwas R, Dilworth MJ.** 1987. Symbiotic and competitive properties of motility mutants of *Rhizobium trifolii* Ta1. Arch. Microbiol. **148:**34-39.
14. **Miller LD, Yost CK, Hynes MF, Alexandre G.** 2007. The major chemotaxis gene cluster of *Rhizobium leguminosarum* bv. *viciae* is essential for competitive nodulation. Mol. Microbiol. **63:**348-362.
15. **Althabegoiti MJ, Lopez-Garcia SL, Piccinetti C, Mongiardini EJ, Perez-Gimenez J, Quelas JI, Perticari A, Lodeiro AR.** 2008. Strain selection for improvement of *Bradyrhizobium japonicum* competitiveness for nodulation of soybean. FEMS Microbiol. Lett. **282:**115-123.
16. **Nelson EB.** 2004. Microbial dynamics and interactions in the spermosphere. Annu. Rev. Phytopathol. **42:**271-309.
17. **Barbour WM, Hattermann DR, Stacey G.** 1991. Chemotaxis of *Bradyrhizobium japonicum* to soybean exudates. Appl. Environ. Microbiol. **57:**2635-2639.
18. **Webb BA, Hildreth S, Helm RF, Scharf BE.** 2014. *Sinorhizobium meliloti* chemoreceptor McpU mediates chemotaxis toward host plant exudates through direct proline sensing. Appl. Environ. Microbiol. **80:**3404-3415.

19. **Gaworzewska ET, Carlile MJ.** 1982. Positive chemotaxis of *Rhizobium leguminosarum* and other bacteria towards root exudates from legumes and other plants. J. Gen. Microbiol. **128:**1179-1188.
20. **Webb BA, Helm RF, Scharf BE.** 2016. Contribution of individual chemoreceptors to *Sinorhizobium meliloti* chemotaxist towards amino acids of host and nonhost seed exudates. Mol. Plant Microbe Interact. **29:**231-239.
21. **Meier VM, Muschler P, Scharf BE.** 2007. Functional analysis of nine putative chemoreceptor proteins in *Sinorhizobium meliloti*. J. Bacteriol. **189:**1816-1826.
22. **Anantharaman V, Aravind L.** 2000. Cache - a signaling domain common to animal Ca(2^+)-channel subunits and a class of prokaryotic chemotaxis receptors. Trends Biochem. Sci. **25:**535-537.
23. **Anantharaman V, Koonin EV, Aravind L.** 2001. Regulatory potential, phyletic distribution and evolution of ancient, intracellular small-molecule-binding domains. J. Mol. Biol. **307:**1271-1292.
24. **Zhulin IB, Nikolskaya AN, Galperin MY.** 2003. Common extracellular sensory domains in transmembrane receptors for diverse signal transduction pathways in bacteria and archaea. J. Bacteriol. **185:**285-294.
25. **Phillips DA, Wery J, Joseph CM, Jones AD, Teuber LR.** 1995. Release of flavonoids and betaines from seeds of seven *Medicago* species. Crop Sci. **35:**805-808.
26. **Chambers ST, Kunin CM.** 1987. Isolation of glycine betaine and proline betaine from human urine. Assessment of their role as osmoprotective agents for bacteria and the kidney. J. Clin. Invest. **79:**731-737.
27. **Kunin CM, Hua TH, Van Arsdale White L, Villarejo M.** 1992. Growth of *Escherichia coli* in human urine: role of salt tolerance and accumulation of glycine betaine. J. Infect. Dis. **166:**1311-1315.
28. **Lever M, Sizeland PC, Bason LM, Hayman CM, Chambers ST.** 1994. Glycine betaine and proline betaine in human blood and urine. Biochim. Biophys. Acta **1200:**259-264.
29. **Phillips DA, Joseph CM, Maxwell CA.** 1992. Trigonelline and stachydrine released from alfalfa seeds activate NodD2 protein in *Rhizobium meliloti*. Plant. Physiol. **99:**1526-1531.
30. **Phillips DA, Sande ES, Vriezen JAC, de Bruijn FJ, Le Rudulier D, Joseph CM.** 1998. A new genetic locus in *Sinorhizobium melilot*i is involved in stachydrine utilization. Appl. Environ. Microbiol. **64:**3954-3960.
31. **Boncompagni E, Osteras M, Poggi MC, le Rudulier D.** 1999. Occurrence of choline and glycine betaine uptake and metabolism in the family *Rhizobiaceae* and their roles in osmoprotection. Appl. Environ. Microbiol. **65:**2072-2077.
32. **Barra L, Fontenelle C, Ermel G, Trautwetter A, Walker GC, Blanco C.** 2006. Interrelations between glycine betaine catabolism and methionine biosynthesis in *Sinorhizobium meliloti* strain 102F34. J. Bacteriol. **188:**7195-7204.
33. **Gouffi K, Bernard T, Blanco C.** 2000. Osmoprotection by pipecolic acid in *Sinorhizobium meliloti*: Specific effects of D and L isomers. Appl. Environ. Microbiol. **66:**2358-2364.
34. **Boivin C, Camut S, Malpica CA, Truchet G, Rosenberg C.** 1990. Rhizobium meliloti Genes Encoding Catabolism of Trigonelline Are Induced under Symbiotic Conditions. Plant Cell **2:**1157-1170.
35. **Seymour JR, Simo R, Ahmed T, Stocker R.** 2010. Chemoattraction to dimethylsulfoniopropionate throughout the marine microbial food web. Science **329:**342-345.

36. **Kokoeva MV, Storch KF, Klein C, Oesterhelt D.** 2002. A novel mode of sensory transduction in archaea: binding protein- mediated chemotaxis towards osmoprotectants and amino acids. EMBO J. **21:**2312-2322.
37. **Mello BA, Tu Y.** 2007. Effects of adaptation in maintaining high sensitivity over a wide range of backgrounds for *Escherichia coli* chemotaxis. Biophys J. **92:**2329-2337.
38. **Zhang Y, Gardina PJ, Kuebler AS, Kang HS, Christopher JA, Manson MD.** 1999. Model of maltose-binding protein/chemoreceptor complex supports intrasubunit signaling mechanism. Proc. Natl. Acad. Sci. U S A **96:**939-944.
39. **Niesen FH, Berglund H, Vedadi M.** 2007. The use of differential scanning fluorimetry to detect ligand interactions that promote protein stability. Nat. Protoc. **2:**2212-2221.
40. **Badri DV, Vivanco JM.** 2009. Regulation and function of root exudates. Plant Cell Environ. **32:**666-681.
41. **Trinchant JC, Boscari A, Spennato G, Van de Sype G, Le Rudulier D.** 2004. Proline betaine accumulation and metabolism in alfalfa plants under sodium chloride stress. Exploring its compartmentalization in nodules. Plant Physiol. **135:**1583-1594.
42. **Wood KV, Stringham KJ, Smith DL, Volenec JJ, Hendershot KL, Jackson KA, Rich PJ, Yang WJ, Rhodes D.** 1991. Betaines of alfalfa : characterization by fast atom bombardment and desorption chemical ionization mass spectrometry. Plant Physiol **96:**892-897.
43. **Wood JM.** 1999. Osmosensing by bacteria: signals and membrane-based sensors. Microbiol. Mol. Biol. Rev. **63:**230-262.
44. **McNeil SD, Nuccio ML, Hanson AD.** 1999. Betaines and related osmoprotectants. Targets for metabolic engineering of stress resistance. Plant Physiol. **120:**945-950.
45. **Moe LA.** 2013. Amino acids in the rhizosphere: from plants to microbes. Am. J. Bot. **100:**1692-1705.
46. **Alloing G, Travers I, Sagot B, Le Rudulier D, Dupont L.** 2006. Proline betaine uptake in *Sinorhizobium meliloti:* Characterization of Prb, an opp-like ABC transporter regulated by both proline betaine and salinity stress. J. Bacteriol. **188:**6308-6317.
47. **Smith LT, Pocard JA, Bernard T, Le Rudulier D.** 1988. Osmotic control of glycine betaine biosynthesis and degradation in *Rhizobium meliloti*. J. Bacteriol. **170:**3142-3149.
48. **Burnet MW, Goldmann A, Message B, Drong R, El Amrani A, Loreau O, Slightom J, Tepfer D.** 2000. The stachydrine catabolism region in *Sinorhizobium meliloti* encodes a multi-enzyme complex similar to the xenobiotic degrading systems in other bacteria. Gene **244:**151-161.
49. **Goldmann A, Boivin C, Fleury V, Message B, Lecoeur L, Maille M, Tepfer D.** 1991. Betaine use by rhizosphere bacteria: genes essential for trigonelline, stachydrine, and carnitine catabolism in *Rhizobium meliloti* are located on pSym in the symbiotic region. Mol. Plant Microbe Interact. **4:**571-578.
50. **Li S, Li F, Wang J, Zhang W, Meng Q, Chen TH, Murata N, Yang X.** 2011. Glycinebetaine enhances the tolerance of tomato plants to high temperature during germination of seeds and growth of seedlings. Plant, cell & environment **34:**1931-1943.
51. **Park EJ, Jeknic Z, Sakamoto A, DeNoma J, Yuwansiri R, Murata N, Chen TH.** 2004. Genetic engineering of glycinebetaine synthesis in tomato protects seeds, plants, and flowers from chilling damage. The Plant journal : for cell and molecular biology **40:**474-487.
52. **Huang J, Rozwadowski K, Bhinu VS, Schafer U, Hannoufa A.** 2008. Manipulation of sinapine, choline and betaine accumulation in *Arabidopsis* seed: towards improving the

nutritional value of the meal and enhancing the seedling performance under environmental stresses in oilseed crops. Plant Physiol. and biochemistry : PPB / Societe francaise de physiologie vegetale **46:**647-654.
53. **Waditee R, Bhuiyan MN, Rai V, Aoki K, Tanaka Y, Hibino T, Suzuki S, Takano J, Jagendorf AT, Takabe T, Takabe T.** 2005. Genes for direct methylation of glycine provide high levels of glycinebetaine and abiotic-stress tolerance in *Synechococcus* and *Arabidopsis*. Proc. Natl. Acad. Sci. U S A **102:**1318-1323.
54. **Rhodes D, Rich PJ, Brunk DG, Ju GC, Rhodes JC, Pauly MH, Hansen LA.** 1989. Development of two isogenic sweet corn hybrids differing for glycinebetaine content. Plant Physiol. **91:**1112-1121.
55. **Bhardwaj S, Sharma NK, Srivastava PK, Shukla G.** 2010. Salt tolerance assessment in alfalfa (*Medicago sativa* L.) ecotypes. Botany Research Journal **3:**1-6.
56. **Anower MR, Mott IW, Peel MD, Wu Y.** 2013. Characterization of physiological responses of two alfalfa half-sib families with improved salt tolerance. Plant Physiol. and biochemistry : PPB / Societe francaise de physiologie vegetale **71:**103-111.
57. **Kamberger W.** 1979. An Ouchterlony double diffusion study on the interaction between legume lectins and rhizobial cell surface antigens. Arch. Microbiol. **121:**83-90.
58. **Bertani G.** 1951. Studies on lysogenesis. I. The mode of phage liberation by lysogenic *Escherichia coli*. J. Bacteriol. **62:**293-300.
59. **Platzer J, Sterr W, Hausmann M, Schmitt R.** 1997. Three genes of a motility operon and their role in flagellar rotary speed variation in *Rhizobium meliloti*. J. Bacteriol. **179:**6391-6399.
60. **Götz R, Limmer N, Ober K, Schmitt R.** 1982. Motility and chemotaxis in two strains of *Rhizobium* with complex flagella. J. Gen. Microbiol. **128:**789-798.
61. **Sourjik V, Schmitt R.** 1996. Different roles of CheY1 and CheY2 in the chemotaxis of *Rhizobium meliloti*. Mol. Microbiol. **22:**427-436.
62. **Servillo L, Giovane A, Casale R, Balestrieri ML, Cautela D, Paolucci M, Siano F, Volpe MG, Castaldo D.** 2016. Betaines and related ammonium compounds in chestnut (*Castanea sativa* Mill.). Food chemistry **196:**1301-1309.
63. **Sánchez-Hernández L, Nozal L, Marina ML, Crego AL.** 2012. Determination of nonprotein amino acids and betaines in vegetable oils by flow injection triple-quadrupole tandem mass spectrometry: a screening method for the detection of adulterations of olive oils. J. Agric. Food Chem. **60:**896-903.
64. **Naresh Chary V, Dinesh Kumar C, Vairamani M, Prabhakar S.** 2012. Characterization of amino acid-derived betaines by electrospray ionization tandem mass spectrometry. Journal of mass spectrometry : JMS **47:**79-88.
65. **Li C, Hill RW, Jones AD.** 2010. Determination of betaine metabolites and dimethylsulfoniopropionate in coral tissues using liquid chromatography-time-of-flight mass spectrometry and stable isotope-labeled internal standards. Journal of chromatography. B, Analytical technologies in the biomedical and life sciences **878:**1809-1816.
66. **Furey A, Moriarty M, Bane V, Kinsella B, Lehane M.** 2013. Ion suppression; a critical review on causes, evaluation, prevention and applications. Talanta **115:**104-122.
67. **Adler J.** 1973. A method for measuring chemotaxis and use of the method to determine optimum conditions for chemotaxis by *Escherichia coli*. J. Gen. Microbiol. **74:**77-91.
68. **Götz R, Schmitt R.** 1987. *Rhizobium meliloti* swims by unidirectional, intermittent rotation of right-handed flagellar helices. J. Bacteriol. **169:**3146-3150.

69. **Evangelidis GD, Psarakis EZ.** 2008. Parametric image alignment using enhanced correlation coefficient maximization. IEEE transactions on pattern analysis and machine intelligence **30:**1858-1865.
70. **Evangelidis GD.** 2013. IAT: A Matlab toolbox for image alignment. http://www.iatool.net.
71. **Balaji J.** 2014. Time Series Analyzer Version 3.0. Dept. of Neurobiology, UCLA.

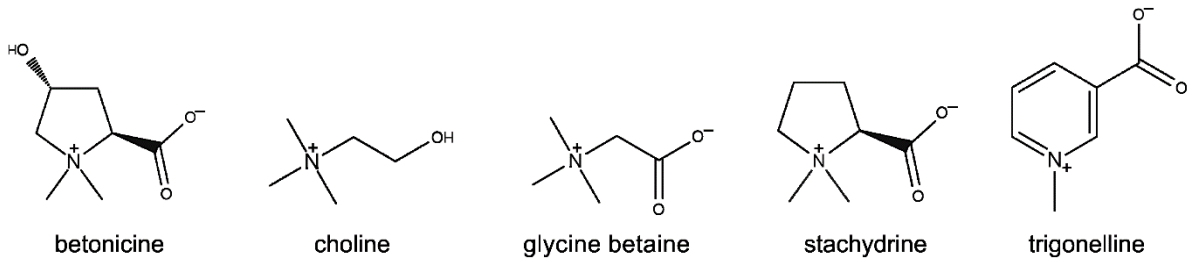

Fig. 5.1. Structures of Quaternary ammonium compounds (QACs) analysed in this study. Betonicine and stachydrine are also known as hydroxyproline betaine and proline betaine, respectively. Of the QACs, betonicine, glycine betaine, stachydrine, and trigonelline are sub-classified as betaines.

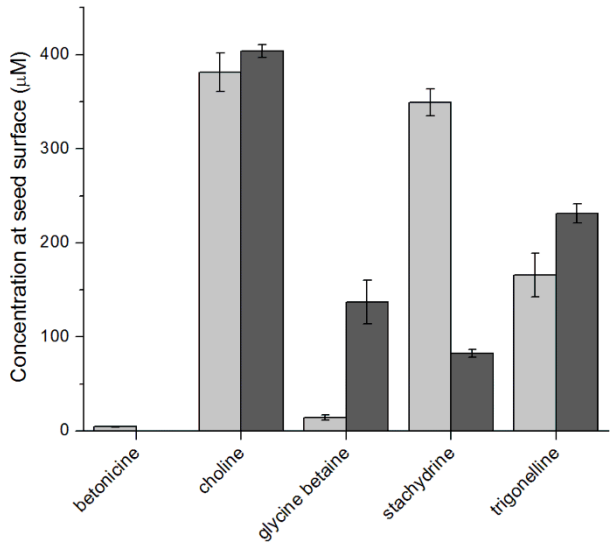

Fig. 5.2. QAC concentrations residing at the surface of a germinating seed. QAC quantities in seed exudates were measured with liquid chromatography-mass spectrometry. Exuded amounts and seed volumes, 2.17 μl for alfalfa and 1.84 μl for spotted medic, were used to calculate a concentration at the seed surface (Webb *et al.*, 2016). Light grey bars are for an *M. sativa* seed and dark grey bars are for an *M. arabica* seed. Values are means and standard deviations of three biological replicates.

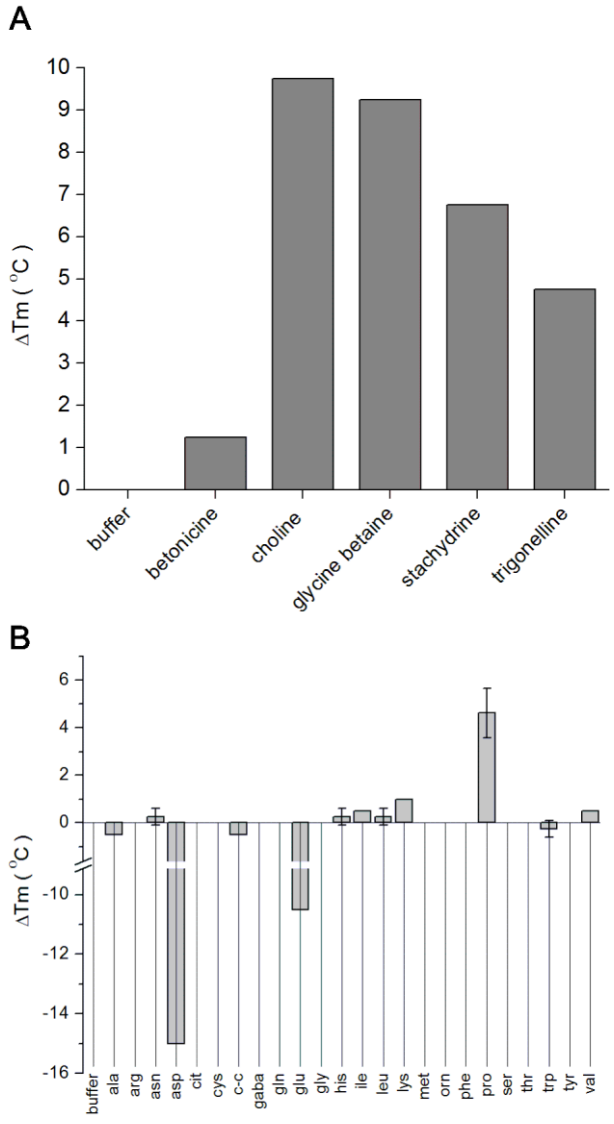

Fig. 5.3. Interaction of McpXPR with QACs (A) and amino acids (B) measured with differential scanning fluorimetry. Protein stability was monitored as a function of fluorescence intensity and the T_m shift was recorded after subtraction of the negative control (protein alone in buffer). No standard deviations were recorded for (A), because duplicate samples displayed no variation in T_m.

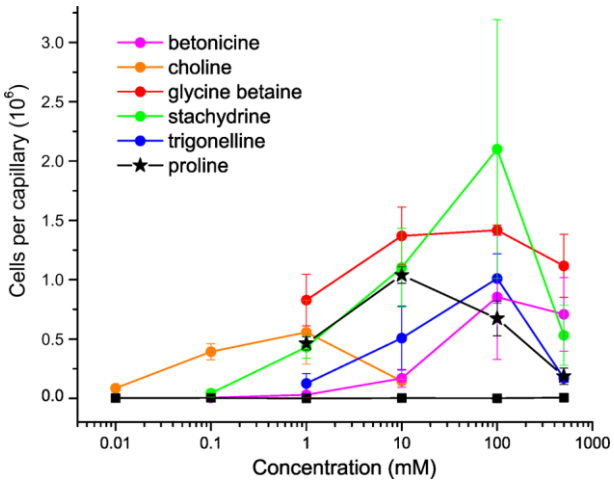

Fig. 5.4. Chemotaxis responses of S. meliloti wild type to QACs and proline in the Adler capillary assay. Graphs with circles denote the wild-type responses to QACs; the black graph with asterisks as symbol denote the wild-type responses to proline; the black graph with squares as symbol denote the average responses of the chemotaxis null strain (*che*) to stachydrine. The standard deviations for the *che* strain are smaller than the symbols. Values are the means and standard deviations of three biological replicates.

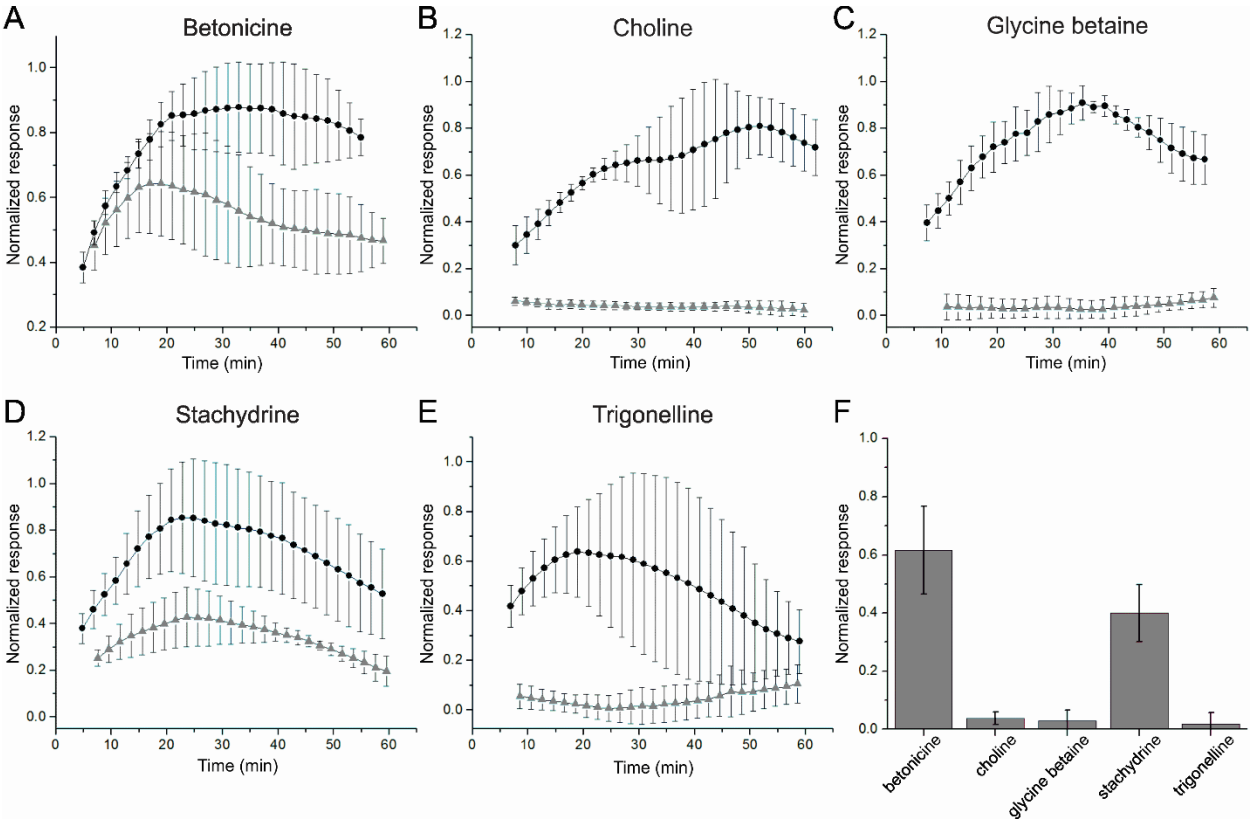

Fig. 5.5. Chemotaxis responses of *S. meliloti* wild type and the *mcpX* deletion strain to QACs in the hydrogel capillary assay. Images were taken under pseudo dark field, encapsulating the mouth of the capillary, and pixel intensities caused by cell accumulation were analysed. Black circles denote the wild type and gray triangles denote the *mcpX* deletion strain. Responses to (A) 50 mM betonicine; (B) 1 mM choline; (C) 1 mM glycine betaine; (D) 50 mM stachydrine; (E) 50 mM trigonelline. (F) Responses of the *mcpX* deletion strain were normalized to the corresponding peak responses of the wild type. Briefly, the response values from five time points enveloping the peak response of the wild type were compared to the values of the same time points of the *mcpX* deletion strain. For each QAC, responses were normalized to the highest observed response of the wild type.

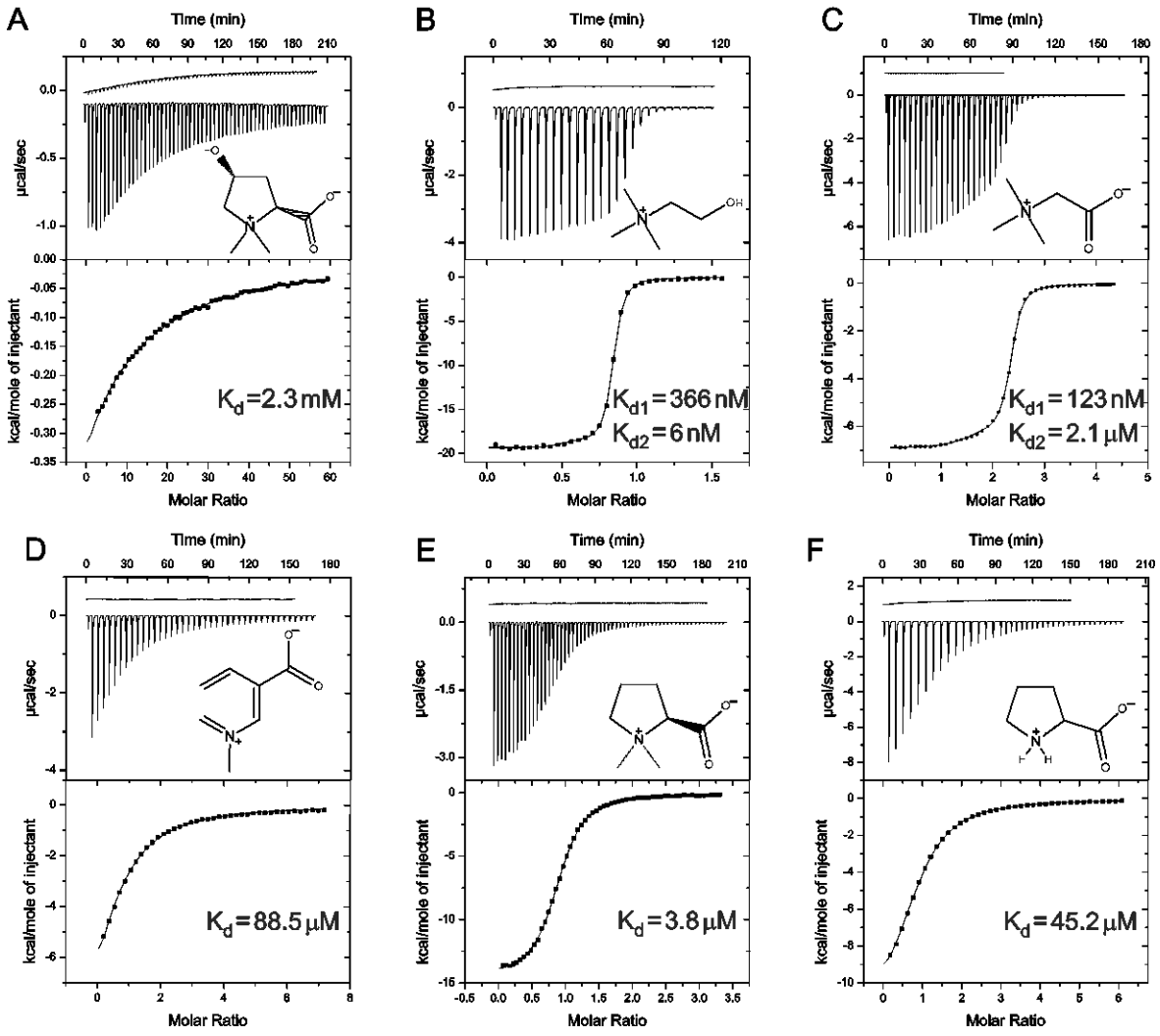

Fig. 5.6. Isothermal titration calorimetry of McpX^{PR} with QACs and proline. Upper panels show the raw titration data, and lower panels show the normalized and dilution corrected integrated peak areas of the raw titration data. (A) 75.7 µM McpX^{PR} with 20 mM betonicine; (B) 91.5 µM McpX^{PR} with 1.5 mM choline; (C) 183 µM McpX^{PR} with 5.1 mM glycine betaine; (D) 91.5 µM McpX^{PR} with 4.44 mM trigonelline; (E) 80 µM McpX^{PR} with 1.5 mM stachydrine; (F) 142 µM McpX^{PR} with 6 mM proline. Data were fit with the one-set-of-sites model of the MicroCal version of Origin7 (Northampton, MA) for A, D, E, and F. The two-set-of-sites model was used to fit B and C. Chemical structures represent the ligand. K_d was calculated from the reported K_a.

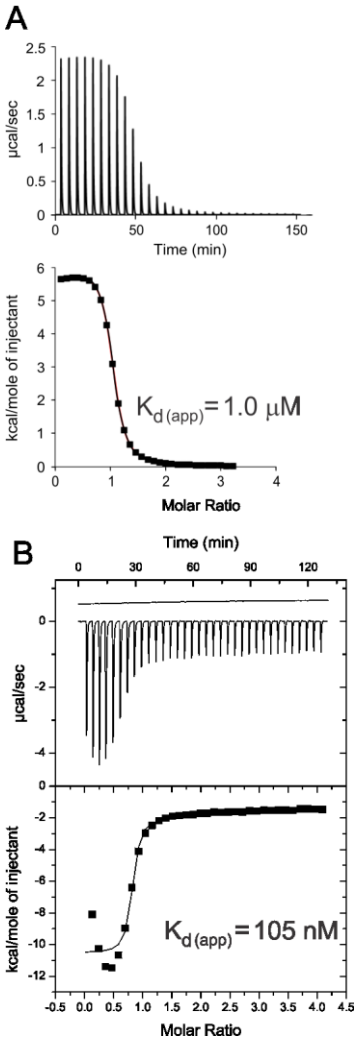

Fig. 5.7. Competition experiment with a McpX^{PR}/trigonelline complex and glycine betaine. The upper panels show raw titration data of protein and buffer with the specific compound. The lower panels are the integrated and dilution corrected peak areas of the raw titration data. (A) Simulation of a theoretical competition between a McpX^{PR}/trigonelline complex and glycine betaine, where McpX^{PR} is saturated with trigonelline in the sample cell and titrated with glycine betaine. The parameters for the simulated titration are 80 µM McpX^{PR} and 446 µM trigonelline in the sample cell, 5 µl injections of 2.22 mM glycine betaine. Experimentally determined binding parameters for glycine betaine and trigonelline with McpX^{PR} were obtained from the direct

injection experiments in Fig. 5.5 and used for the simulation. (B) 80 μM $McpX^{PR}$ saturated with 446 μM trigonelline in the sample cell, titrated with 2.22 mM glycine betaine.

Chapter 6 - Final Discussion

In Chapters 2, 3, and 4 we show how McpU interacts with and mediates chemotaxis to 19 of 20 proteinogenic AAs and interacts directly with 19 of 20 AAs and likely interacts with glutamate in an indirect manner.

The mechanism of direct binding of McpU to amino acids most likely involves hydrogen bonding between the amino group of the ligand and the carboxyl group of two conserved aspartates, Asp155, Asp182. As well, based on homology modeling, it is predicted that hydrogen bonds are formed with the carboxylate group by Tyr91 and Arg96. These characteristics of binding the amino and carboxylate groups are also predicted to be accurate for the characterized chemoreceptors Tlp3 (*C. jejuni*), McpC (*B. subtilis*), Mlp24 and Mlp37 (*V. cholera*) (1-3), which also have or are predicted to have tandem PAS domains.

The variation in ligand profiles amongst these MCPs can be explained by the AA residue side chains that protrude into the binding pocket from the opposite side of the residues that bind the AA main chain. For example, in Tlp3 of *C. jejuni* the residues Val126, Leu128, Leu144 and Val171 are short and hydrophobic and allow for binding of large AA ligands (1), whereas in McpC of *B. subtilis* these residues are substituted with larger, polar side chains (Tyr121, Gln123, Tyr133 and Ser161) and allow for binding of AAs with polar and relatively smaller side chains (2). Liu et al 2015 noted that Val126 and Leu128 of Tlp3 are substituted by Met110 and Trp112 in McpU of *S. meliloti* and argued that McpU likely only binds to small ligands due to the bulky nature of Met and Trp (1). Regardless of the prediction by Liu et al 2015, our results from the thermal denaturation and ITC studies indicate that $McpU^{PR}$ directly interacts with 18 of 20 AAs (Figs. 2.7

& 3.4) including the biggest and bulkiest of AAs. A clear picture of how McpU binds to these ligands can be elucidated through crystallographic studies with and without AAs.

Aspartate was the only AA that did not elicit a chemotactic response nor bound to $McpU^{PR}$, however the chemically related AA, glutamate elicits a response yet does not appear to directly interact with $McpU^{PR}$. Aspartate and glutamate have in common a negatively charged carboxyl group in the sidechain. This negative charge could be what prevents direct binding to McpU. Periplasmic binding proteins (PBP) used for indirect binding to MCPs with tandem PAS domains have been described before, e.g. aspartate indirectly binds to Tlp1 of *C. jejuni*; arginine, lysine, and methionine indirectly bind McpC of *B. subtilis* (2, 4). Therefore, we hypothesize that glutamate indirectly binds $McpU^{PR}$ with the aid of a periplasmic binding protein (PBP).

In chapter 4 we show that the chemotactic potency of seed exudates from host (alfalfa) and non-host (spotted medic) is the same, but single *mcp* deletion strains displayed distinct various responses revealing a hierarchy in importance for chemotaxis to the exudates. The Δ*mcpZ* strain was the only one that responded differently towards the two exudates indicating that the exudate compositions are different. The amino acid profiles (20 proteinogenic AAs plus citrulline, cystine, and ornithine) almost match each other in regards to quantities, with spotted medic exuding slightly higher amounts. Synthetic AA mixtures mimicking the amounts from the exudates elicit different chemotactic responses, i.e. 23% of the response to alfalfa exudate and 37% the response to spotted medic exudate, which means there are more unidentified attractants and/or repellents in the alfalfa exudate compared to the spotted medic exudate. The single *mcp* deletion strains have various responses to the synthetic mixtures revealing another hierarchy of importance for mediating chemotaxis to the AA mixtures. McpU is the most important followed by IcpA, McpX, and McpY. Interestingly, the strain lacking *mcpY* displayed a response approximately 20% greater than the

wild type. McpY is an internal receptor and is predicted to mediate chemotaxis to redox materials inside the cell, such as oxygen. After deleting *mcpY* one would expect the response to be less than that of the wild type, especially since the deletion strain showed a decrease in response to the whole exudate. Given the predicted role of McpY, a correlation with the increase in response to the synthetic AA mixture cannot be made; however, a different role as a sensor for attractants *and* repellents could explain these observations. For example, McpY may sense an AA as a repellent, thus an *mcpY* deletion strain would exhibit a stronger response to the synthetic AA mixture than the wild type. In this scenario, McpY may sense other repellents in the whole exudate, but a relatively large amount of attractants overwhelms a potential repellent response in an *mcpY* deletion mutant.

In Chapter 5, five quaternary ammonium compounds (QACs) are quantified in host and non-host exudates where it is revealed that the two different species exude different amounts of each. This is contrary to the AA exudate profiles of the two species and finally opens the door for designing systems where *S. meliloti* exhibits preferential chemotaxis toward the host. The QACs were shown to be strong attractants for *S. meliloti*, and McpX is characterized as a novel bacterial chemoreceptor for direct binding of the QACs. We also show evidence that IcpA may also be involved in mediating chemotaxis to the QACs. However, IcpA likely indirectly senses most attractants since it is predicted to sense energy flux involved with the electron transport chain. Indeed, some of the QACs have been documented as energy sources for *S. meliloti* (5-7). Crystallographic studies of $McpX^{PR}$ with and without QACs will reveal the mechanism of binding and allow for further design of a preferential chemotaxis system.

Soils typically contain indigenous *Sinorhizobium* strains that have lower symbiotic efficiency and/or weaker nitrogen fixing abilities than the seed inoculum strains on the market (8-

13). These indigenous strains are generally better adapted to the soils and are able to outcompete the newly introduced inoculum strains for nodule residence, in effect reducing crop yields (13-18). The establishment of the first nodules induces a feedback mechanism in which alfalfa greatly reduces further nodulation (19). Therefore, early nodulation by indigenous strains is to be avoided in order to propagate symbiosis with the inoculum strain during the first year of growth. The adaptation(s) that the indigenous populations utilize to outcompete inoculum strains is not known, however, chemotaxis could very well be a contributing factor. A strain of *Bradyrhizobium japonicum*, which forms the same symbiosis with soybean, was selected for enhanced chemotaxis in a laboratory setting and was shown to have a greater nodulation efficiency than its parent strain (20). This experiment with *B. japonicum* indicates that a similar scenario could be accomplished with *S. meliloti* and alfalfa.

Microscopic analysis of an indigenous *S. meliloti* field isolate, (Sm11) (21), indicated that it had a greater chemotactic ability toward the attractant proline than the common seed inoculum strain, Sm1021. Interestingly, the lab strain RU11/001 (of which all studies in this dissertation were performed with) displayed the strongest response out of the three strains (Fig. 6.1). A potential explanation for this occurrence is that the immediate ancestor of RU11/001 (RU10/406) was originally selected for greater motility on swim plates in a laboratory setting (22). Unfortunately, the nitrogen fixing abilities of RU11/001 appear to be less than that of the inoculum strain, Sm1021 (lab observations, unpublished). The nitrogen fixing ability of the Sm11 strain relative to the other two strains is not known. This experiment showing proline-taxis was only performed once, thus would need to be repeated to show statistical significance. Nevertheless, this result indicates that chemotaxis to an attractant exuded by alfalfa could be enhanced beyond that of indigenous field isolates. Evidently, the chemotactically enhanced strain would also need to

maintain a high proficiency in fixing nitrogen. Our new understandings of how the *Sinorhizobium meliloti-Medicago sativa* symbiosis is propagated through chemotaxis could help to outcompete indigenous strains and increase crop yields in a resource conserving manner.

Throughout the lifespan of the crop (typically 4-5 yr), alfalfa will form nodules each year (23). At this point in the plants life, root exudate is the main source of attractant compounds. During these later stages of growth, little is known about the persistence of the inoculum strains, however it is known that indigenous strains typically maintain their populations throughout the years (24). To outcompete indigenous strains for nodulation during these later stages, research would need to be done to 1) determine how to maintain inoculum strain in the soil for years, and 2) identify the attractants coming from the new roots that form nodules. Knowing these factors could aid in maintaining nodulation with an inoculum strain. If maintenance of the inoculum strain is not achievable, then perhaps a periodic soil treatment with inoculum near the alfalfa roots could aid in maintaining inoculum populations.

Enhancement of *S. meliloti* chemotaxis toward the host is one avenue towards increasing crop yields, and the knowledge we have acquired from this work can aid in the optimization of *S. meliloti* chemotaxis. Two ways of optimizing would include 1) targeted mutagenesis of residues involved in ligand binding based on structural predictions, and 2) random mutagenesis of the PR and selection of mutants exhibiting enhanced chemotaxis. AA residue changes could cause an increased affinity for an attractant ligand, class of ligands, or broaden the ligand spectrum. For example, a change in the binding pocket of $McpU^{PR}$ could alter it in a way that it senses betaines instead. These types of mutagenesis studies have been performed with the Tar receptor of *E. coli* (25, 26), where the ligand specificity of Tar was changed based on the amino acid residue substitutions. As well, affinities for particular ligands of the chemoreceptor were altered. In these

studies, the DNA encoding for the PR was randomly mutagenized and resulting mutants were then screened in swim plates, Adler capillary assays, and a kinase (CheA) activation assay.

It is more likely that mutagenesis of a PR results in diminished chemotaxis to attractants as compared to enhanced chemotaxis. If random mutagenesis does not result in chemotaxis enhancement of *S. meliloti*, then another method may be used to expand the ligand profile of the organism by creating a chimeric MCP. Chimeric MCPs (specifically Tar chimeras) have been created to study this possibility of expanding ligand profiles in *E. coli* (27) by swapping the PR of Tar with the sensing domains of other chemoreceptors. For instance, Tar of *E. coli* does not sense citrate, but when the periplasmic region of Tar was replaced with the sensing region of CitA, this chimeric MCP could directly bind citrate and mediate chemotaxis towards it. Interestingly, by cloning the sensing region of *citA* into a different part of the periplasmic region, this new chimeric receptor mediated a repellent response to citrate. The repellent response indicated that the periplasmic region had adopted a different structural conformation that induces an opposing cytoplasmic signal. Now that we know specific ligands and their affinities to $McpU^{PR}$ and $McpX^{PR}$, both the mutagenesis and the PR swapping techniques can be employed in studies with *S. meliloti* to either enhance chemotaxis to the known ligands, and/or broaden their ligand specificities. Another point to keep in mind when broadening the ligand specificity of an *S. meliloti* chemoreceptor is the chance of sensing non-host specific chemicals. Therefore, one would need to focus on a search for chemoreceptors from other organisms with the ability to sense host derived chemicals.

Germinating alfalfa seeds release the Nod factor inducing flavonoids, chrysoeriol and luteolin, which prime *S. meliloti* for root nodulation (28-30). The relatively strong attractants trigonelline and stachydrine are also released from germinating seeds and induce Nod factor

production (31), therefore, defining the seed derived attractants is of importance in this study because chemotaxis to the spermosphere is crucial for the establishment and subsequent nodulation (32). Once *S. meliloti* is established in the relatively short-lived spermosphere, *S. meliloti* would be proximal to an emerging root as it grows through the spermosphere, thus allowing the rhizobium to colonize the growing root. Young seedlings such as these are primed for nodulation, and a large population of rhizobia would enhance the efficacy of nodulation and the number of nodules formed (33), therefore, knowing the attractants and MCPs that perceive them could aid in developing strains with enhanced chemotaxis to the spermosphere to ultimately lead toward greater nodulation by an inoculum strain.

Coating the seed with an attractant of choice sounds like a reasonable solution, but changes to the inoculum strain would still need to be made, so that the attractant only elicits chemotaxis from the inoculum strain, or else indigenous strains would have an equal opportunity to be attracted to the seedling. Also, due watering, substances from the seed coatings diffuse into the soil and may or may not form an undisturbed gradient with higher concentrations of attractant closer to the seedlings, thus an inoculum strain may be led in the wrong direction. While coating a seed with an attractant may not be ideal, engineering an alfalfa line that secretes more attractant during early growth stages would likely maintain a gradient leading to accumulation of rhizobium on the root.

While chemotaxis plays a role in propagating the mutualism with alfalfa, other non-plant derived factors affect the process, such as abiotic factors like soil chemistry, exogenous fertilization, temperature, and moisture, and biotic factors like predation, quorum sensing, hitchhiking on nematodes, and plant growth promoting microbes (34-42). While chemotaxis can be tuned for optimal encounters with host plants, the aforementioned factors likely need to be

optimal for *S. meliloti*, thus soils must be taken care of prior, during, and after seed inoculation with a chemotactically enhanced strain of *S. meliloti*.

Most plant families lack the ability to form such a beneficial mutualism. Our acquired knowledge could aid in non-legume/rhizobia studies that seek to establish a similar mutualism in order to take advantage of a natural nitrogen source. For instance, the diazotroph *Azospirillum brasilense* forms an associative symbiosis with corn (the most cultivated crop in the United States (43)) by utilizing chemotaxis to find host roots (44). Like alfalfa, corn roots exude attractants, therefore, it is conceivable that chemotaxis of *A. brasilense* to corn roots could be enhanced with a chemoreceptor that has been optimized for sensing corn root derived attractants, thus propagating the symbiosis more efficiently and increasing corn yields.

Taken together, the results of matching host-derived attractants with the corresponding bacterial chemoreceptors presented in this study enhances our understanding of how the symbiosis is propagated prior to the exchange of species specific signals, i.e. flavonoids and Nod factors. These facts will aid in future studies aimed at further elucidation of the specificity of the remaining chemoreceptors and host attractants, as well as constructing *S. meliloti* strains with enhanced chemotaxis to the host.

REFERENCES

1. **Liu YC, Machuca MA, Beckham SA, Gunzburg MJ, Roujeinikova A.** 2015. Structural basis for amino-acid recognition and transmembrane signalling by tandem Per-Arnt-Sim (tandem PAS) chemoreceptor sensory domains. Acta Crystallogr D **71:**2127-2136.
2. **Glekas GD, Mulhern BJ, Kroc A, Duelfer KA, Lei V, Rao CV, Ordal GW.** 2012. The *Bacillus subtilis* chemoreceptor McpC senses multiple ligands using two discrete mechanisms. J Biol Chem **287**.
3. **Nishiyama S, Suzuki D, Itoh Y, Suzuki K, Tajima H, Hyakutake A, Homma M, Butler-Wu SM, Camilli A, Kawagishi I.** 2012. Mlp24 (McpX) of *Vibrio cholerae* implicated in pathogenicity functions as a chemoreceptor for multiple amino acids. Infect Immun **80:**3170-3178.
4. **Machuca MA, Liu YC, Beckham SA, Gunzburg MJ, Roujeinikova A.** 2016. The crystal structure of the tandem-PAS sensing domain of *Campylobacter jejuni* chemoreceptor Tlp1 suggests indirect mechanism of ligand recognition. J Struct Biol **194:**205-213.
5. **Alloing G, Travers I, Sagot B, Le Rudulier D, Dupont L.** 2006. Proline betaine uptake in *Sinorhizobium meliloti*: Characterization of Prb, an Opp-like ABC transporter regulated by both proline betaine and salinity stress. J Bacteriol **188:**6308-6317.
6. **Boncompagni E, Osteras M, Poggi MC, Le Rudulier D.** 1999. Occurrence of choline and glycine betaine uptake and metabolism in the family *Rhizobiaceae* and their roles in osmoprotection. Appl Environ Microbiol **65:**2072-2077.
7. **Boivin C, Camut S, Malpica CA, Truchet G, Rosenberg C.** 1990. *Rhizobium meliloti* genes encoding catabolism of trigonelline are induced under symbiotic conditions. Plant Cell **2:**1157-1170.
8. **Torres Tejerizo G, Del Papa MF, Soria-Diaz ME, Draghi W, Lozano M, Giusti Mde L, Manyani H, Megias M, Gil Serrano A, Puhler A, Niehaus K, Lagares A, Pistorio M.** 2011. The nodulation of alfalfa by the acid-tolerant Rhizobium sp. strain LPU83 does not require sulfated forms of lipochitooligosaccharide nodulation signals. J Bacteriol **193:**30-39.
9. **Singleton PW, Tavares JW.** 1986. Inoculation Response of Legumes in Relation to the Number and Effectiveness of Indigenous Rhizobium Populations. Appl Environ Microbiol **51:**1013-1018.
10. **Eardly BD, Hannaway DB, Bottomley PJ.** 1985. Characterization of Rhizobia from Ineffective Alfalfa Nodules: Ability to Nodulate Bean Plants [Phaseolus vulgaris (L.) Savi.]. Appl Environ Microbiol **50:**1422-1427.
11. **Del Papa MF, Pistorio M, Draghi WO, Lozano MJ, Giusti MA, Medina C, van Dillewijn P, Martinez-Abarca F, Moron Flores B, Ruiz-Sainz JE, Megias M, Puhler A, Niehaus K, Toro N, Lagares A.** 2007. Identification and characterization of a nodH ortholog from the alfalfa-nodulating Or191-like rhizobia. Molecular plant-microbe interactions : MPMI **20:**138-145.
12. **Catroux G, Hartmann A, Revellin C.** 2001. Trends in rhizobial inoculant production and use. Plant and Soil **230:**21-30.
13. **Yates RJ, Howieson JG, Reeve WG, O'Hara GW.** 2011. A re-appraisal of the biology and terminology describing rhizobial strain success in nodule occupancy of legumes in agriculture. Plant and Soil **348:**255-267.
14. **Jordan DC.** 1952. Studies on the legume root nodule bacteria .3. Growth factor requirements for effective, ineffective, and parasitic strains. Can J Bot **30:**693-700.

15. **Streeter JG.** 1994. Failure of inoculant Rhizobia to overcome the dominance of indigenous strains for nodule formation. Can J Microbiol **40:**513-522.
16. **Zeng ZH, Chen WX, Hu YG, Sui XH, Chen DM.** 2007. Screening of highly effective *Sinorhizobium meliloti* strains for 'Vector' alfalfa and testing of its competitive nodulation ability in the field. Pedosphere **17:**219-228.
17. **Thies JE, Singleton PW, Bohlool BB.** 1991. Modeling symbiotic performance of introduced rhizobia in the field by use of indexes of indigenous population-size and nitrogen status of the soil. Appl Environ Microbiol **57:**29-37.
18. **Dowling DN, Broughton WJ.** 1986. Competition for Nodulation of Legumes. Ann Rev Microbiol **40:**131-157.
19. **Caetanoanolles G, Bauer WD.** 1988. Feedback-Regulation of Nodule Formation in Alfalfa. Planta **175:**546-557.
20. **Althabegoiti MJ, Lopez-Garcia SL, Piccinetti C, Mongiardini EJ, Perez-Gimenez J, Quelas JI, Perticari A, Lodeiro AR.** 2008. Strain selection for improvement of Bradyrhizobium japonicum competitiveness for nodulation of soybean. Fems Microbiol Lett **282:**115-123.
21. **Schneiker-Bekel S, Wibberg D, Bekel T, Blom J, Linke B, Neuweger H, Stiens M, Vorholter FJ, Weidner S, Goesmann A, Puhler A, Schluter A.** 2011. The complete genome sequence of the dominant *Sinorhizobium meliloti* field isolate SM11 extends the *S. meliloti* pan-genome. J Biotechnol **155:**20-33.
22. **Krupski G, Gotz R, Ober K, Pleier E, Schmitt R.** 1985. Structure of complex flagellar filaments in *Rhizobium meliloti*. J Bacteriol **162:**361-366.
23. **Georgieva N.** 2015. NODULATION DYNAMICS IN ALFALFA VARIETIES (Medicago sativa L.). Banats J Biotechnol **6:**83-89.
24. **Samac D.** 2016. Persistence & Diversity of Rhizobial Bacteria Nodulating Alfalfa. USDA ARS Forage Focus.
25. **Derr P, Boder E, Goulian M.** 2006. Changing the specificity of a bacterial chemoreceptor. J Mol Biol **355:**923-932.
26. **Bi SY, Yu DQ, Si GW, Luo CX, Li TQ, Ouyang Q, Jakovljevic V, Sourjik V, Tu YH, Lai LH.** 2013. Discovery of novel chemoeffectors and rational design of *Escherichia coli* chemoreceptor specificity. Proc Natl Acad Sci USA **110:**16814-16819.
27. **Bi S, Pollard AM, Yang Y, Jin F, Sourjik V.** 2016. Engineering hybrid chemotaxis receptors in bacteria. ACS Synth Biol.
28. **Hartwig UA, Phillips DA.** 1991. Release and Modification of nod-Gene-Inducing Flavonoids from Alfalfa Seeds. Plant Phys **95:**804-807.
29. **Hartwig UA, Maxwell CA, Joseph CM, Phillips DA.** 1989. Interactions among Flavonoid nod Gene Inducers Released from Alfalfa Seeds and Roots. Plant Phys **91:**1138-1142.
30. **Hartwig UA, Maxwell CA, Joseph CM, Phillips DA.** 1990. Chrysoeriol and luteolin released from alfalfa seeds induce *nod* genes in *Rhizobium meliloti*. Plant Phys **92:**116-122.
31. **Phillips DA, Wery J, Joseph CM, Jones AD, Teuber LR.** 1995. Release of Flavonoids and Betaines from Seeds of 7 Medicago Species. Crop Sci **35:**805-808.
32. **Nelson EB.** 2004. Microbial dynamics and interactions in the spermosphere. Annu Rev Phytopathol **42:**271-309.
33. **DA Phillips CM, UA Hartwig, CM Joseph, J Wery.** 1991. Rhizosphere flavonoids released by alfalfa. The rhizosphere and Plant growth **14:**149-154.

34. **de Oliveira WS, Oliveira PPA, Corsi M, Duarte FRS, Tsai SM.** 2004. Alfalfa yield and quality as function of nitrogen fertilization and symbiosis with *Sinorhizobium meliloti*. Sci Agric **61:**433-438.
35. **Gurich N, Gonzalez JE.** 2009. Role of quorum sensing in *Sinorhizobium meliloti*-alfalfa symbiosis. J Bacteriol **191:**4372-4382.
36. **Thies JE, Woomer PL, Singleton PW.** 1995. Enrichment of *Bradyrhizobium Spp* populations in soil due to cropping of the homologous host legume. Soil Biol Biochem **27:**633-636.
37. **Peoples MB, Ladha JK, Herridge DF.** 1995. Enhancing legume N-2 fixation through plant and soil-management. Plant and Soil **174:**83-101.
38. **Brockwell J, Bottomley PJ, Thies JE.** 1995. Manipulation of rhizobia microflora for improving legume productivity and soil fertility - a critical assessment. Plant and Soil **174:**143-180.
39. **Bais HP, Weir TL, Perry LG, Gilroy S, Vivanco JM.** 2006. The role of root exudates in rhizosphere interations with plants and other organisms. Ann Rev Plant Biol **57:**233-266.
40. **Garau G, Reeve WG, Brau L, Deiana P, Yates RJ, James D, Tiwari R, O'Hara GW, Howieson JG.** 2005. The symbiotic requirements of different Medicago spp. suggest the evolution of Sinorhizobium meliloti and S-Medicae with hosts differentially adapted to soil pH. Plant and Soil **276:**263-277.
41. **Zahran HH.** 1999. Rhizobium-legume symbiosis and nitrogen fixation under severe conditions and in an arid climate. Microbiol Mol Biol R **63:**968-+.
42. **Horiuchi J, Prithiviraj B, Bais HP, Kimball BA, Vivanco JM.** 2005. Soil nematodes mediate positive interactions between legume plants and rhizobium bacteria. Planta **222:**848-857.
43. **USDA.** 2016. Crop values, 2015 summary.
44. **Scharf BE, Hynes MF, Alexandre GM.** 2016. Chemotaxis signaling systems in model beneficial plant-bacteria associations. Plant Mol Biol.

1. **Liu YC, Machuca MA, Beckham SA, Gunzburg MJ, Roujeinikova A.** 2015. Structural basis for amino-acid recognition and transmembrane signalling by tandem Per-Arnt-Sim (tandem PAS) chemoreceptor sensory domains. Acta Crystallogr D **71:**2127-2136.
2. **Glekas GD, Mulhern BJ, Kroc A, Duelfer KA, Lei V, Rao CV, Ordal GW.** 2012. The Bacillus subtilis Chemoreceptor McpC Senses Multiple Ligands Using Two Discrete Mechanisms. Journal of Biological Chemistry **287**.
3. **Nishiyama S, Suzuki D, Itoh Y, Suzuki K, Tajima H, Hyakutake A, Homma M, Butler-Wu SM, Camilli A, Kawagishi I.** 2012. Mlp24 (McpX) of Vibrio cholerae Implicated in Pathogenicity Functions as a Chemoreceptor for Multiple Amino Acids. Infect Immun **80:**3170-3178.
4. **Machuca MA, Liu YC, Beckham SA, Gunzburg MJ, Roujeinikova A.** 2016. The crystal structure of the tandem-PAS sensing domain of Campylobacter jejuni chemoreceptor Tlp1 suggests indirect mechanism of ligand recognition. J Struct Biol **194:**205-213.

5. **Alloing G, Travers I, Sagot B, Le Rudulier D, Dupont L.** 2006. Proline betaine uptake in Sinorhizobium meliloti: Characterization of Prb, an Opp-like ABC transporter regulated by both proline betaine and salinity stress. Journal of bacteriology **188:**6308-6317.
6. **Boncompagni E, Osteras M, Poggi MC, Le Rudulier D.** 1999. Occurrence of choline and glycine betaine uptake and metabolism in the family Rhizobiaceae and their roles in osmoprotection. Applied and environmental microbiology **65:**2072-2077.
7. **Boivin C, Camut S, Malpica CA, Truchet G, Rosenberg C.** 1990. Rhizobium meliloti Genes Encoding Catabolism of Trigonelline Are Induced under Symbiotic Conditions. Plant Cell **2:**1157-1170.
8. **Jordan DC.** 1952. Studies on the Legume Root Nodule Bacteria .3. Growth Factor Requirements for Effective, Ineffective, and Parasitic Strains. Can J Bot **30:**693-700.
9. **Streeter JG.** 1994. Failure of Inoculant Rhizobia to Overcome the Dominance of Indigenous Strains for Nodule Formation. Canadian journal of microbiology **40:**513-522.
10. **Zeng ZH, Chen WX, Hu YG, Sui XH, Chen DM.** 2007. Screening of highly effective Sinorhizobium meliloti strains for 'Vector' alfalfa and testing of its competitive nodulation ability in the field. Pedosphere **17:**219-228.
11. **Schneiker-Bekel S, Wibberg D, Bekel T, Blom J, Linke B, Neuweger H, Stiens M, Vorholter FJ, Weidner S, Goesmann A, Puhler A, Schluter A.** 2011. The complete genome sequence of the dominant Sinorhizobium meliloti field isolate SM11 extends the S. meliloti pan-genome. J Biotechnol **155:**20-33.
12. **Krupski G, Gotz R, Ober K, Pleier E, Schmitt R.** 1985. Structure of Complex Flagellar Filaments in Rhizobium-Meliloti. Journal of bacteriology **162:**361-366.
13. **Derr P, Boder E, Goulian M.** 2006. Changing the specificity of a bacterial chemoreceptor. J Mol Biol **355:**923-932.
14. **Bi SY, Yu DQ, Si GW, Luo CX, Li TQ, Ouyang Q, Jakovljevic V, Sourjik V, Tu YH, Lai LH.** 2013. Discovery of novel chemoeffectors and rational design of Escherichia coli chemoreceptor specificity. Proceedings of the National Academy of Sciences of the United States of America **110:**16814-16819.
15. **Bi S, Pollard AM, Yang Y, Jin F, Sourjik V.** 2016. Engineering Hybrid Chemotaxis Receptors in Bacteria. ACS Synth Biol.
16. **de Oliveira WS, Oliveira PPA, Corsi M, Duarte FRS, Tsai SM.** 2004. Alfalfa yield and quality as function of nitrogen fertilization and symbiosis with Sinorhizobium meliloti. Sci Agric **61:**433-438.
17. **Gurich N, Gonzalez JE.** 2009. Role of Quorum Sensing in Sinorhizobium meliloti-Alfalfa Symbiosis. Journal of bacteriology **191:**4372-4382.
18. **Thies JE, Woomer PL, Singleton PW.** 1995. Enrichment of Bradyrhizobium Spp Populations in Soil Due to Cropping of the Homologous Host Legume. Soil Biol Biochem **27:**633-636.
19. **Peoples MB, Ladha JK, Herridge DF.** 1995. Enhancing Legume N-2 Fixation through Plant and Soil-Management. Plant and Soil **174:**83-101.
20. **Brockwell J, Bottomley PJ, Thies JE.** 1995. Manipulation of Rhizobia Microflora for Improving Legume Productivity and Soil Fertility - a Critical-Assessment. Plant and Soil **174:**143-180.
21. **Bais HP, Weir TL, Perry LG, Gilroy S, Vivanco JM.** 2006. The role of root exudates in rhizosphere interations with plants and other organisms. Annual Review of Plant Biology **57:**233-266.

22. **Garau G, Reeve WG, Brau L, Deiana P, Yates RJ, James D, Tiwari R, O'Hara GW, Howieson JG.** 2005. The symbiotic requirements of different Medicago spp. suggest the evolution of Sinorhizobium meliloti and S-Medicae with hosts differentially adapted to soil pH. Plant and Soil **276:**263-277.
23. **Zahran HH.** 1999. Rhizobium-legume symbiosis and nitrogen fixation under severe conditions and in an arid climate. Microbiol Mol Biol R **63:**968-+.
24. **Horiuchi J, Prithiviraj B, Bais HP, Kimball BA, Vivanco JM.** 2005. Soil nematodes mediate positive interactions between legume plants and rhizobium bacteria. Planta **222:**848-857.
25. **USDA.** 2016. Crop values, 2015 summary.
26. **Scharf BE, Hynes MF, Alexandre GM.** 2016. Chemotaxis signaling systems in model beneficial plant-bacteria associations. Plant Mol Biol.

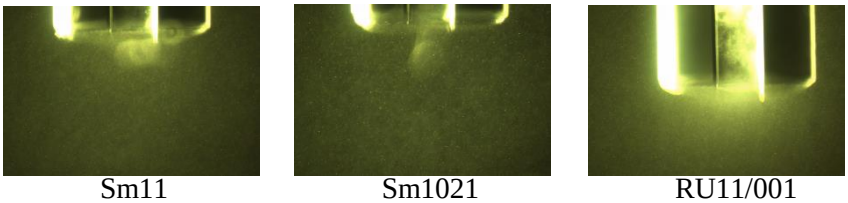

Sm11 Sm1021 RU11/001

Fig. 6.1. Chemotaxis response of three different *S. meliloti* strains to proline in the agarose capillary assay. Strains were cultured for motility using RB/overlays. Cultures were harvested and suspended in RB. Cultures were placed in a chemotaxis chamber in which a 1% agarose capillary filled with 10 mM L-proline was placed. The area around the mouth of the capillary was monitored for 1 h. Images shown are from 30 min after the initial placement of the capillary into the cultures and represent the time of peak responses. Sm11 is an indigenous field isolate, Sm1021 is a common seed inoculum strain, and RU11/001 is a lab strain selected originally selected from a field isolate for greater motility on swim plates.